

https://dspace.org/

The design and synthesis of mycobacterium tuberculosis caseinolytic protease inhibitors

Shuro, Pious

2019
https://hdl.handle.net/10539/28862

Downloaded from a DSpace repository. https://dspace.org/

The design and synthesis of Mycobacterium tuberculosis caseinolytic protease inhibitors

By

Pious Shuro

A dissertation submitted to the Faculty of Science, University of the Witwatersrand, Johannesburg

In fulfilment of the requirements for the Degree of Master of Science

Supervised by Dr. Maya Mellisa Makatini

May, 2019



DECLARATION

I declare that the work presented in this dissertation was carried out exclusively by me under the supervision of Dr M.M. Makatini. It is being submitted for the degree of Master of Science at the University of the Witwatersrand, Johannesburg, and has not been submitted before for any degree or examination in any other university.

_____

Pious Shuro

ABSTRACT

Tuberculosis (TB) is the main cause of death from a single infectious agent, ranking above HIV/AIDS. Approximately 2.0 billion people worldwide are infected with *Mycobacterium tuberculosis (M.tb)* but only a fraction of 5-15% develop the TB disease and 1.5 million deaths were also estimated (worldwide). The emergence of Multi-drug resistant (MDR), Extensive –drug resistant (XDR) and Total- drug resistant (TDR) TB infections has increased the need or demand for researchers to discover and develop novel anti-TB drugs with a new and effective mode of action against drug resistant TB strains, with safe and short treatment time. This project was aimed at designing and synthesizing novel ecumicin derivatives as caseinolytic protease inhibitors with anti-tb activity

This work describes the synthesis of ecumicin natural amino acids derivatives, cationic with lassomcyin residues derivatives, lysine cationic derivatives and *N*-methylated and peptoid derivatives. Previous studies propose that ecumicin binds to the acidic region of the (ATPase) or the ClpP proteolytic system or the allosteric site of ClpC. The designed peptides were synthesized using solid phase peptide synthesis and using various coupling conditions. Coupling conditions and amino acid sequences impacted the success of the synthesis of the derivatives with highly cationic peptides showing better results compared to *N*- methylated peptides and OxymaPure yielding better results compared to HATU coupling reagents. Successfully synthesized and purified peptides were tested for activity against *Mycobacterium tuberculosis* strain. For the tested compounds, non-showed any activity against *Mycobacterium tuberculosis* strain.

ACKNOWEDGEMENTS

I would like to express my heartfelt gratitude to my **Maker** and my **Source of life**, my **God** for affording me with precious life, strength and protection and enablement to carry out this project.

I want to thank my supervisor, **Dr M.M. Makatini** for guidance, support, patience and encouragement throughout the project.

Peptide group: Ntombi, Khanani, Thabo and Phatu: This is the team that complemented my project.

Much appreciation to the **Mass Spectrometry Team**, Eric, Thapelo and Refilwe;

The **NMR team**, Dr Hendrik and Dr Izak Kotzé

Organic group particular mention to Memory, Dr Charles, and Donald

Glass blower: Mr. Dzara

My **family** for their moral support; special mention to Mr. and Mrs. Dzingirai

I am grateful to The **University of the Witwatersrand** for the privilege to use their facilities to do the research and the **South African Medical Research Council** and **National Research Foundation for funding this project.**

LIST OF ABBREVIATIONS

Acids

AcOH	Acetic acid
HBF_4	tetrafluoroboric acid
HCL	Hydrochloric acid
PTSA	*p*-Toluene sulphonic acid
TFA	Trifluoroacetic acid
TFMSA	trifluoromethanesulfonic acid

Coupling reagents

COMU	1-Cyano-2-ethoxy-2-oxoethylidenaminooxy) dimethylamino-morpholino-carbenium hexafluorophosphate
DBU	1, 8-Diazabicyclo [5.4.0] undec-7-ene
DIC	N, N′-Diisopropylcarbodiimide
DIPEA	Diisopropylethylamine
HATU	O-(7-Azabenzotriazole-1-yl)-N, N, N'N'-tetramethyluronium hexafluorophosphate
HBTU	(2-(1H-benzotriazol-1-yl)-1,1,3,3-tetramethyluronium hexafluorophosphate, Hexafluorophosphate Benzotriazole TetramethylUronium)
HOAt	1-Hydroxy-7-azabenzotriazole
HOBt	Hydroxybenzotriazole

Linkers

BAL	4-(4-Formyl-3,5-dimethoxyphenoxy) butyric acid
DVB	Divinylbenzene
HMBA	Hydroxymethylbenzoic acid
HMPA	4-Hydroxymethyl-3-methoxyphenoxyacetic acid)

NBP	*N*-butylpyrrolidinone
PEG	polyethylene glycol
PEGA	Poly (ethylene glycol)-poly (*N, N*-dimethylarcralyamide)-copolymer
PHB	Polyhydroxybutyrate
PS	Polystyrene
SASRIN	3-methoxy-4-hydroxymethyl phenol

Protecting groups

Acm	acetamidomethyl
Boc	ter-butyloxycarbonly
Fmoc	9-fluaronlymethlyoxycarbonyl
Fmoc-OSu	Fluorenylmethoxycarbonyloxy) succinimide
Mbh	- 4,4'-Dimethoxybenzhydryl
Mtr	4-Methoxy-2,3,6-trimethylbenzenesulfonyl
Pbf	2,2,4,6,7-Pentamethyldihydrobenzofuran-5-sulfonyl
Pmc	2,2,5,7,8-pentamethylchroman-6-sulfonyl
tBu	tertbutyl
tButhio	tertbutylthio
trt	triphenylmethyl

Solvents

ACN	Acetonitrile
DCM	Dichloromethane
DCU	Dicyclohexylurea
DFM	dimethyl formaamide
DMSO	Dimethylsuphoxide
IPA	Isopropanol

MeOH	Methanol
MeTHF	Methyltetrahydrofuran
NMP	N-Methyl-2-pyrrolidone
THF	Tetrahydrofuran
TMU	Tetramethylurea

Other reagents

EDT	ethanedithiol
$MgSO_4$	Anhydrous magnesium sulphate
MTT	3-(4,5-Dimethylthiazol-2-yl)-2,5-diphenyltetrazoliumbromide
$NaHCO_3$	Sodiumhydrogencarbonate
TES	Triethylsilane
TIS	Triisopropylsilane

Miscellaneous

AA	Amino acid
AIDS	Acquired Immune Deficiency Syndrome
AMP	Antimicrobial Peptides
ATPase	Adenosine triphosphatase
Clp	caseinolytic protease
ClpP	caseinolytic protease subunit P
DNA	Deoxyribonucleic acid
EDR	Extensive-Drug Resistant
EPTB	Extra-Pulmonary Tuberculosis
HIV	Human Immune Virus
HRMS	High Resolution Mass Spectrometer
LCMS	Liquid Chromatography- Mass Spectrometer

LPS	Liquid Phase Synthesis
MD	Molecular Dynamics
MDR	Multi-Drug Resistant
MIC	Minimum Inhibition Concentration
MM	Molecular Mechanics
NMR	Nuclear Magnetic Resonance
NRPS	Non-Ribosomal Peptide Synthetase
NTD	N- Terminus Domain
PTB	Pulmonary Tuberculosis
QM	Quantum Mechanics
RNA	Ribonucleic acid
SPPS	Solid Phase Peptide Synthesis
TB	Tuberculosis
TDR	Total –Drug Resistant
TLC	Thin Layer Chromatography

TABLE OF FIGURES

Figure 1: Pathogenic life cycle of *M.tb*[8] 1
Figure 2: Mechanism of action of current TB drugs[18] 3
Figure 3: Structure of Ecumicin.[19] 3
Figure 4: Ecumicin binding mechanism on NTD of *M.tb* ClpC1.[11] 5
Figure 5: Normal functioning of the Clp complex. (B) Peptide promotes ATP hydrolysis but prevent protein degradation.[20] 6
Figure 6: Multifunctional properties of AMPs[31]. 7
Figure 7: Various functions of AMPs.[31] MN: polymorphonuclear neutrophils; ADP adinoside diphosphate; ATP adenos. 8
Figure 8: Mechanism of action of AMPs.[35] 9
Figure 9: Amino acid sequence and recently proposed structure of lassomycin.[13,43,44] 10
Figure 10: Structure and topology of four different lasso peptides. The ring residues are shown in green, amino acids belonging to the loop in blue, and the amino acids in the tail in red. Disulphide bridges are shown in yellow.[41] 10
Figure 11: Unthreaded lassomycin structure previous reported.[13] 11
Figure 12: Structure of Cyclomarin A.[27,47] 12
Figure 13: Binding sites of ecumicin, cyclomarin A, and lassomycin on ClpC1.[11] 12
Figure 14: Effects of microwave energy on synthesis of difficult peptide sequences.[61] 16
Figure 15: Covalent side-chain to side-chain cyclization a) Disulphide; b) Lactam; c) Ether/thioether/lactone; d) Disiloxane; P-Peptide.[88] 26
Figure 16: Ecumicin[19] and Ecumicin derivative, PS01. 32
Figure 17: Molecular ion peak of the 5 amino acids which were successfully coupled during the synthesis of PS01. 33
Figure 18: Molecular ion peak of the 5 amino acids which were successfully coupled during the synthesis of PS01. 35
Figure 19: Molecular peak of the 14 amino acids which were successfully coupled during the synthesis of PS01. 36
Figure 20: Molecular peaks of the 15 amino acids which were successfully coupled during the synthesis of PS01 using OxymaPure. 37
Figure 21: PS06 amino acid sequence. 38
Figure 22: Molecular peaks of the 5th amino acids which were successfully coupled during the synthesis of PS06 39

Figure 23: Molecular peaks 1-2 of the 6th amino acids which were successfully coupled during the synthesis of PS06. 39
Figure 24: Molecular peaks 3-5 of the 6th amino acids which were successfully coupled during the synthesis of PS0 40
Figure 25: Molecular peaks of the 7th amino acids which were successfully coupled during the synthesis of PS06. 40
Figure 26: Molecular peaks of the 8th amino acids which were successfully coupled during the synthesis of PS06. 41
Figure 27: Molecular peaks of the 9 amino acids which were successfully coupled during the synthesis of PS06. 42
Figure 28: Molecular peaks of the 15 amino acids which were successfully coupled during the synthesis of PS06. 43
Figure 29: PS07 amino acid sequence. 45
Figure 30: PS09 amino acid sequence. 45
Figure 31: PS10 amino acid sequence. 45
Figure 32: PS08 amino acid sequence. 47
Figure 33: Molecular peak of the 19 amino acids which were successfully coupled during the synthesis of PS08 47
Figure 34: Parallel β-sheet in peptides and proteins.[116,117] 49
Figure 35: Interactions among Valine and Threonine pairing β-sheets.[19] 50
Figure 36: Lysine cationic derivatives 50
Figure 37: PS15 LC-MS Spectrum. 52
Figure 38: PS16 LC-MS Spectrum. 52
Figure 39: PS17 LC-MS Spectrum. 53
Figure 40: PS18 LC-MS Spectrum. 54
Figure 41: *N*-methylated amino acid and peptoids substituted peptide derivatives: *N*-methylated amino acid residues are in red and peptoid residue is in blue color. 56
Figure 42: PS19 structure. 58
Figure 43: PS19-7 amino acid sequence MS results. 58
Figure 44: PS19-8 amino acid sequence MS results. 59
Figure 45: PS19-9 amino acid sequence MS results. 59
Figure 46: PS19-10 amino acid sequence MS results. 60
Figure 47: PS19-11 amino acid sequence MS results. 61
Figure 48: PS19-12 amino acid sequence MS results. 61

Figure 49: PS19-13 amino acid sequence MS results. 62
Figure 50: PS19-14 amino acid sequence MS results. 62
Figure 51: PS20 amino acid sequence 63
Figure 52: PS20-8 amino acid sequence MS results. 63
Figure 53: PS20-9 amino acid sequence MS results. 64
Figure 54: PS20-10 amino acid sequence MS results. 65
Figure 55: PS20-11 amino acid sequence MS results. 65
Figure 56: PS20-12 amino acid sequence MS results. 66
Figure 57: PS20-13 amino acid sequence MS results. 66
Figure 58: PS20-14 amino acid sequence MS results. 67
Figure 59: PS21 amino acid sequence. 69
Figure 60: PS21-5 amino acid sequence MS results. 69
Figure 61: PS21-9 amino acid sequence MS results. 70
Figure 62: PS21-10 amino acid sequence MS results. 70
Figure 63: PS21-11 amino acid sequence MS results. 71
Figure 64: PS21-12 amino acid sequence MS results. 72
Figure 65: PS21-13 amino acid sequence MS results. 73
Figure 66: PS23 amino acid sequence. 78
Figure 67: Micro broth dilution results for PS17. 81
Figure 68: *N*- methylated valine structure 88
Figure 69: *N*- methylated leucine structure. 89
Figure 70: *N*-methylated isoleucine structure 89
Figure 71: MS results for PS01 using HBTU coupling reagent. ..... - 1 -
Figure 72: LC-MS results for PS01 sing OxymaPure coupling reagent. ..... - 2 -
Figure 73: LC-MS results for PS06. ..... - 3 -
Figure 74: LC-MS for PS08. ..... - 4 -
Figure 75: MS results for PS19-14 amino acid sequence. ..... - 5 -
Figure 76: MS results for PS20-14 amino acid sequence. ..... - 6 -
Figure 77: LCMS results for PS20-13 amino acid sequence. ..... - 7 -
Figure 78: LCMS for PS20-14 amino acid sequence 1. ..... - 8 -
Figure 79: PS20- LCMS PS20-14 amino acid sequence results 2. ..... - 9 -
Figure 80: MS results for PS21-13 amino acid sequence. ..... - 10 -
Figure 81: *N*-methylated valine LC-MS results. ..... - 11 -
Figure 82: *N*-methylated isoleucine LC-MS results. ..... - 12 -

Figure 83: *N*-methylated leucine LC-MS results. ..... - 13 -
Figure 84: MS results for Fmoc valine peptoid. ..... - 14 -
Figure 85: PS12 ^{1} H NMR Spectrum. ..... - 15 -
Figure 86: PS12 ^{13}C NMR Spectrum. ..... - 16 -
Figure 87: PS13 ^{1}H NMR Spectrum. ..... - 17 -
Figure 88: PS13 ^{13}C NMR Spectrum. ..... - 18 -
Figure 89: PS 14 ^{1}H NMR Spectrum. ..... - 19 -
Figure 90: PS14 ^{13}C NMR Spectrum. ..... - 20 -
Figure 91: PS22 ^{1}H NMR Spectrum. ..... - 21 -

LIST OF TABLES

Table 1: Anti-tuberculosis activity of cyclomarin A, lassomycin, and ecumicin.[1] 13
Table 2: Overview of the three subgroups of resins for Fmoc –based SPPS and their swelling properties. 19
Table 3: Shows types of resin linkers, commercial names, their *C*-terminal functionality and stability.[73] 20
Table 4: Chemical modifications of peptides.[86] 24
Table 5: PS01 LC-MS masses found after each coupling. 34
Table 6: Summary of peptide synthesis conditions 36
Table 7: PS06 LC-MS masses found for particular coupling. 43
Table 8: Summary of peptide synthesis conditions 51
Table 9: LCMS masses found for data cationic peptides. 54
Table 10: HRMS results for PS19, PS20 and PS21 the synthesized *N*-methylated peptides. 57
Table 11: Showing results for peptides antimicrobial activity 80
Table 12: MIC for PS08 results 81

LIST OF SCHEMES

Scheme 1: Activation of amino acid carboxylic group via different types of coupling reagents.[49,54] 14
Scheme 2: Formation of epimers in peptide synthesis.[53,55] 15
Scheme 3: The removal of Fmoc group by secondary amine for the formation of a free $–NH_2$ in SPPS. R = amino acid side chain; Y= side chain protecting group; Z=O, NH; X=CH_2, NH, and N(CH_3).[68] 17
Scheme 4: Boc deprotection mechanism[57] 21
Scheme 5: Carbocation formed during cleavage are quenched by nucleophiles.[77,78] 22
Scheme 6: Indole dimerization and side chain reaction after Boc deprotection.[83,84] 23
Scheme 7: Four different ways of peptide cyclization.[92] 25
Scheme 8: Peptide modification changes that increase enzymatic stability. X and Y are any chemical group or atom. R_1, R_2 and R_3 are amino acids side chain groups.[86] 27
Scheme 9: Showing the SPPS with the final cleaved and cyclized structures.[48,92,109,110] 31
Scheme 10: Side reactions when DIC is used.[49] 37
Scheme 11: i) Reagents and conditions: Fmoc amino acid, paraformaldehyde, *p*-TSOH, toluene, reflux, 15 hours. ii) Aluminum chloride, triethylsilane (TES), dry DCM, ambient temperature, 4 hours. 75
Scheme 12: Proposed mechanism for methylation of Fmoc-amino acid 76
Scheme 13: Peptoids synthesis procedure a) & d): DIPEA, dry DCM; b): Activated 2-chlorotrityl resin; c): Amine, DMF 77
Scheme 14: Proposed resin activation mechanism**.** 77
Scheme 15: Proposed peptoid synthesis mechanism[133,134] 77
Scheme 16: Proposed mechanism of Peptoid protection by Fmoc-Cl.[84] 78

TABLE OF CONTENTS

DECLARATION i

ABSTRACT ii

ACKNOWEDGEMENTS iii

LIST OF ABBREVIATIONS iv

TABLE OF FIGURES viii

LIST OF TABLES xii

LIST OF SCHEMES xiii

TABLE OF CONTENTS xiv

CHAPTER 1: Introduction 1

1.1 Tuberculosis Trend 1

1.2 Problems with the current drugs 2

1.3 Ecumicin promising anti-tuberculosis drugs 3

1.4 The Caseinolytic protease inhibition 5

1.5. Cyclic peptides as antimicrobial peptides (AMPs) 6

1.5.1 Lassomycin 9

1.5.2 Cyclomarin A 11

1.5.3 Comparison of binding sites and activities of aforementioned AMPs 12

1.6 Peptide synthesis 13

1.6.1 Peptide synthesis methods 15

1.6.2 Resins Support 18

1.6.3 Solvent type 19

1.6.4 Linkers 20

1.6.5 Cleavage mixture 21

1.7 Drug derivatization and modification 23

1.7.1 Enhancing peptide stability by chemical modification 24

1.8 Limitations of peptides drugs, Ecumicin 27

1.9 Aims and objectives of the project 28
1.9.1 Aim 28
1.9.2 Objectives 28
1.9.3 Hypotheses and Questions 28
CHAPTER 2: Ecumicin derivatives 30
2.1 Introduction 30
2.2 Purification 32
2.3 Biological studies 32
2.4 Results and discussion 32
2.4.1 Synthesis of PS01 32
2.4.2 Replacement of Tryptophan with Tyrosine 38
2.4.3 Lassomycin residue 44
2.5 Conclusion 46
CHAPTER 3: Ecumicin cationic derivatives 47
3.1 Synthesis of PS08 by manual SPPS using HATU as the coupling reagent 47
3.2 Synthesis of PS15-PS18 by manual SPPS using HATU as the coupling reagent 48
3.3 PS15 and PS16 results and discussion 51
3.4 PS17 and PS18 results and discussion 53
3.5 Conclusion 55
CHAPTER 4: *N*-Methylated peptides and Peptoid 56
4.1 Synthesis of *N*-methylated peptides 56
4.1.1 PS19 results and discussion 57
4.1.2 PS20 results and discussion 63
4.1.3 PS21 results and discussion 68
4.2 Synthesis of *N*- methylated amino acids 75
4.2.1 Results and discussion 75
4.2.2 Mechanism of *N*-methylation of Fmoc- amino acid 76

4.3 Synthesis of Valine peptoids 77
4.4 Synthesis of PS23 peptoid derivative 78
4.5 Conclusion 79
CHAPTER 5: Biological activity 80
5.1 *In-vitro* antimicrobial susceptibility 80
5.2 Broth dilution assay 80
CHAPTER 6: Conclusion 82
CHAPTER 7: Experimental 84
7.1 Materials and Methods 84
7.1.1 General procedure A: SPPS for both manual and automation[73] 85
7.1.2 General procedure B: Resin loading capacity determination 85
7.1.3 General procedure C: Disulphide peptide cyclization 86
7.1.4 General procedure D: Global cleavage 86
7.1.5 General procedure E: Synthesis of Fmoc- oxazolidinone from Fmoc amino acid[89] 86
7.1.6 General procedure F: Synthesis of Fmoc-*N*-methylated –α- amino acid from Fmoc-oxazolidinone 86
7.1.7 General procedure G: Synthesis of Fmoc-peptoid 86
7.2 Synthesis of PS12, PS13 and PS14 87
7.3 Synthesis of PS01 90
7.3.1 Synthesis of PS01a and PS01b 90
7.4 Synthesis of PS06, PS07, PS08, PS09 and PS10 91
7.5 Synthesis of PS15 and PS16 91
7.6 Synthesis of PS17 and PS18 93
7.7 Synthesis of PS19, PS20, PS21 and PS22 94
REFERENCES 96
APPENDIX ..... - 1 -

CHAPTER 1: Introduction

1.1 Tuberculosis Trend

Tuberculosis (TB) is a serious infectious epidemic disease caused by a gram-positive bacterial pathogen known as bacillus *Mycobacterium tuberculosis (M.tb)*.[1,2] Compared to HIV/AIDS, TB is the main cause of death from a single infectious agent.[3] Studies have shown that an estimate of 2 billion people in the world are infected with *M.tb* but only a fraction of 5-15% develops the TB disease and 1.5 million deaths were also estimated (worldwide).[3-6] Multi-drug resistant (MDR) TB prevalence of 490 000 were reported in 2016 and an additional 110 000 cases that were susceptible to isoniazid but resistant to rifampicin (RR-TB), the most effective first-line anti-TB drug.[3] TB can result in high mortality rates (>50%) if not treated properly.[3,4] TB is transmitted by patients with active Pulmonary Tuberculosis (PTB) infection through sneezing or coughing which results in the spread of *M.tb*- containing droplets through the air (Figure 1).[3,6,7] Patients with inactive or latent TB do not transmit the disease as most of the bacilli are killed or encapsulated by the immune system resulting in granuloma formation.

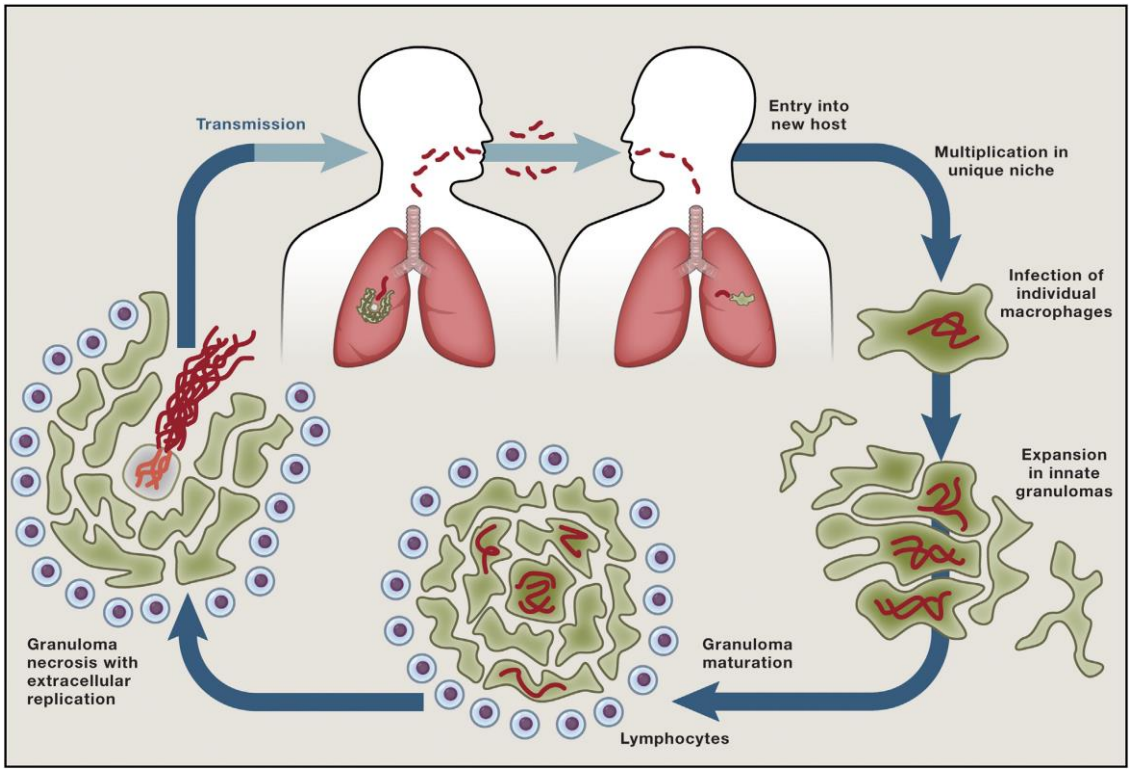


Figure 1: Pathogenic life cycle of *M.tb*[8]

TB disease is found in two different forms namely pulmonary tuberculosis (PTB) and extra-pulmonary tuberculosis (EPTB) with the most frequent form being pulmonary tuberculosis (PTB) representing between 75-80% of all TB cases.[3,9] Infection by *M.tb* of the pulmonary parenchyma or lungs is called PTB. EPTB is the infection by *M.tb* of other organs apart from the pulmonary parenchyma, for example lymph node, osteoarticular, gastrointestinal and peritoneal.[9]

M.tb is increasingly become resistant to available antibiotics making it difficult to treat the TB disease.[2,10,11] This has led to the emergence of multidrug resistant TB (MDR), extensively drug resistant TB (XDR) and total drug resistant TB (TDR).[12-14] MDR-TB strains are resistant to first-line TB drugs and XDR-TB strains are resistant to first and second-line TB drugs.[1,10,12] XDR-TB constitutes an estimate of 10% of MDR-TB case.[5] Drug sensitive-TB can be cured in 6-12 months, MDR-TB can take more than 20 months and XDR-TB is very difficult to treat.[5,10] Late diagnosis, wrong treatment, high treatment costs and failure to comply with the treatment course due to long treatment period and harsh side effects results in multiple resistance. Multiple resistance is best indicated by the increased cases of TDR-TB strains which cannot be treated with current TB drugs.[5] The emergence of MDR, XDR and TDR TB infections has increased the need or demand for researchers to discover and develop novel anti-TB drugs with a new and effective mode of action against drug resistant TB strains, with safe and short treatment time.

1.2 Problems with the current drugs

Currently available anti-TB drugs are not effective against MDR and XDR TB infections [1] and have failed to prevent the spread of TB.[15] Another problem with the current TB drugs is their co-morbidity with other treatments of various diseases. This is caused by drug-drug interaction which weakens the effectiveness of TB drugs and/or adverse reaction resulting in detrimental effects to the patient.[16] Such is the current challenge with diabetic patients who are also infected with active TB. There are possible dangers of relapse, prolonged treatment and possible increase chance of death.[17] The first line and second line drugs have similar mode of action which are inhibiting the synthesis of protein, Deoxyribonucleic acid (DNA), Ribonucleic acid (RNA) and cellular membrane components in *M.tb* (Figure 2).[1] Development of anti TB drugs with these mechanisms of action poses a concern or a threat of all drugs becoming simultaneously ineffective due to *M.tb* resistance to a single drug. Figure 2 shows the mechanism of action of current TB drugs.

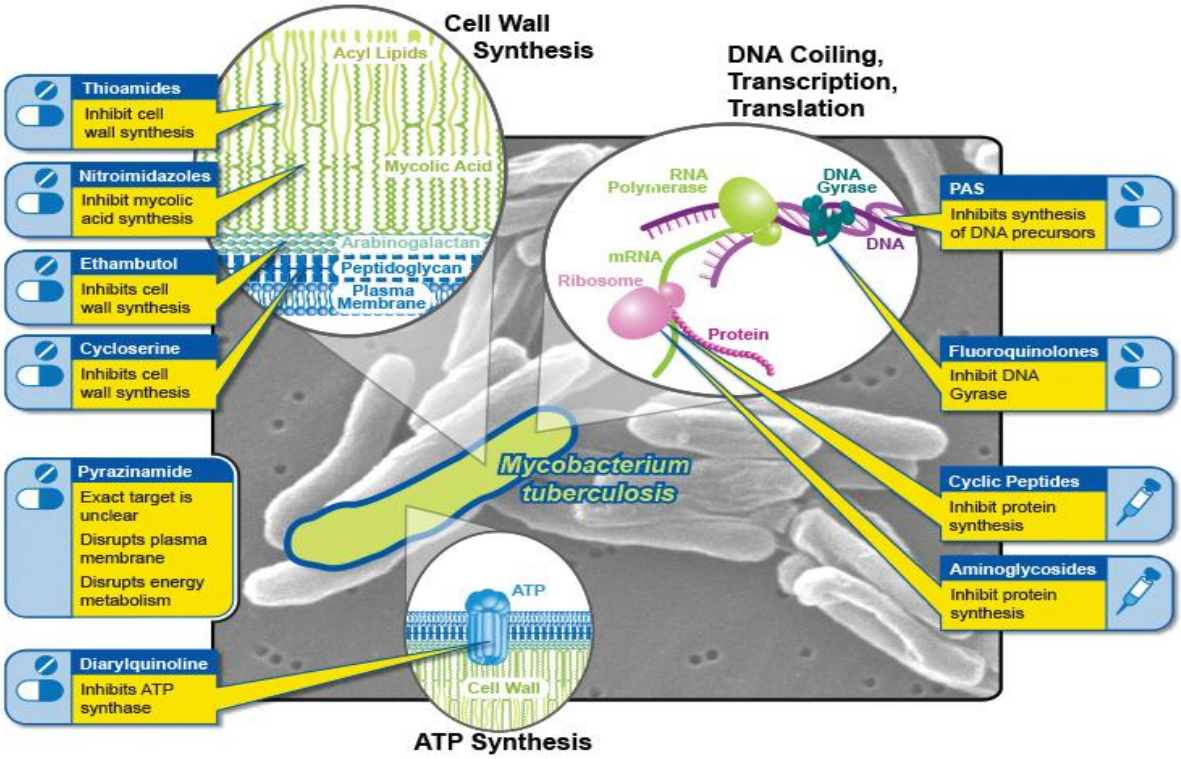


Figure 2: Mechanism of action of current TB drugs[18]

1.3 Ecumicin promising anti-tuberculosis drugs

Ecumicin is a macro cyclic tridecapeptide (Figure 3) produced by *Nonomuraea* spp. MJM5123.

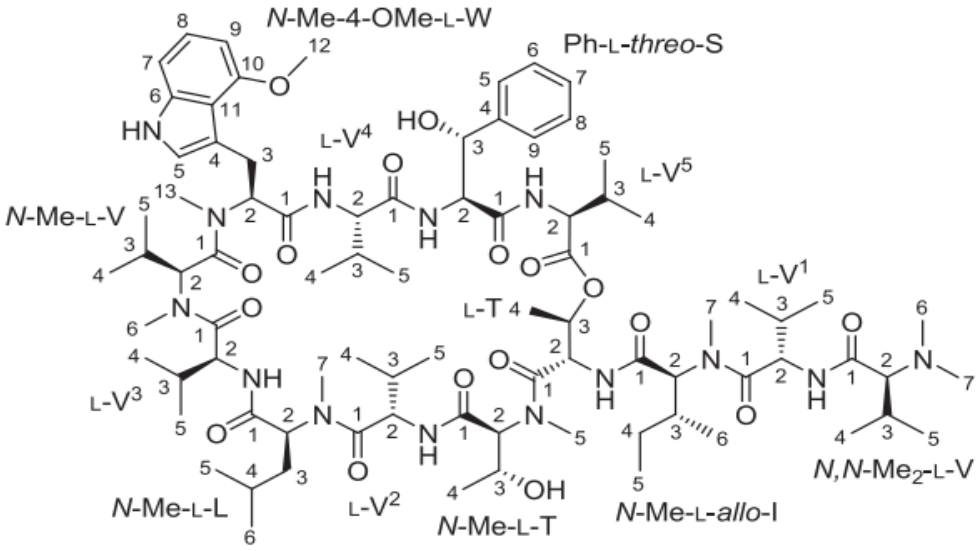


Figure 3: Structure of Ecumicin.[19]

It is a novel natural product with a specific and potent role against *M.tb* working via the caseinolytic protease (Clp).[1,20] It is a secondary metabolite produced by Non-Ribosomal

Peptide Synthetase (NRPS) and is comprised of 13 amino acids which are a combination of natural and highly methoxylated unnatural amino acids. High throughput screening of *Actinomycete* extracts against *M.tb* H37Rv lead to the discovery of ecumicin.[19]

Ecumicin displays both *in vitro* and *in vivo* activity against drug-susceptible, MDR and XDR with minimum inhibitory concentration (MIC) values ranging from 0.16 to 0.62 μM and minimal bactericidal concentration of 1.5 μM for non-replicating *M.tb*.[1,5] Compared to first-line TB drugs, ecumicin has a similar or higher activity profile.[21] However, its activity *in vivo* is low compared to rifampicin and the permeability coefficients suggest poor to modest intestinal absorption. Hence more studies need to be done to improve its pharmacokinetics although its cyclic structure and *N*-methylated pattern (Figure 3) likely contributed to the resistance to enzymatic digestion.[5,21]

Ecumicin has a different mode of action compared to the current available drugs. It targets the caseinolytic protease (Clp), an enzyme responsible for degrading proteins and maintaining cellular integrity while the current drugs target the cell wall, DNA and RNA.[1,20] By interfering with the Clp Adenosine triphosphatase (ATPase) or the ClpP proteolytic system, excessive decomposition of proteins and toxic accumulation of folded proteins aggregates is observed respectively. This leads to disrupted and uncontrolled proteolysis which results in cell death.[20-22] The binding mechanism of ecumicin is still under study although many suggestions have been reported. According to molecular docking studies, ecumicin binds to the 1 and 4-helix of the ClpC1 *N*-terminal domain specifically on P82, R83, K85, K86, E89 and E115 (Figure 4). Hydrogen bonding was observed with R83 and E89 although information on which ecumicin residue binds to these sites was not provided.[11]

Another study suggested that ecumicin binds to the allosteric site of ClpC1 instead of the protein's ATPase domain since ecumicin does not inhibit the ATPase activity. This reasoning then implied that the specific binding of ecumicin to the allosteric site of ClpC1 leads to conformational changes, stimulating the ATPase activity; hence changes the proteolytic activity of ClpC1/ClpP1/ClpP2.[1] The unique target and mechanism of ecumicin predict no cross- resistance with the existing TB drugs, hence it is selective and there is no co-morbidity.[21]

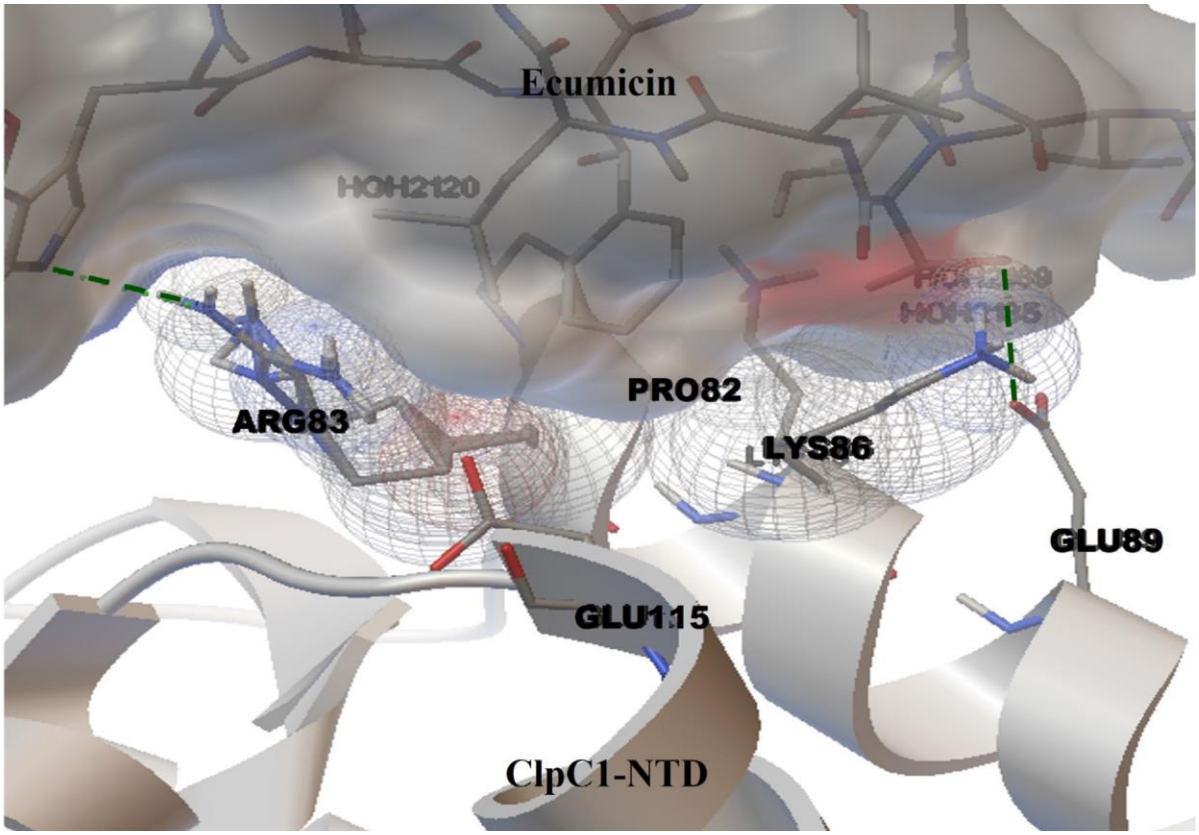


Figure 4: Ecumicin binding mechanism on NTD of *M.tb* ClpC1.[11]

1.4 The Caseinolytic protease inhibition

The Clp is an enzyme responsible for maintaining protein homeostasis and cellular integrity in many bacteria species, including mycobacteria.[1] Protein quality is controlled by breaking down misfolded, short-lived and damaged proteins resulting from thermal or chemical stress, intrinsic structural instability, and translational errors.[1,20] The caseinolytic complex is made up of two main subunits namely proteolytic subunit (ClpP) and the regulatory ATPase adapters, ClpX or ClpA in Gram-negative organisms and ClpX or ClpC in Gram-positive organisms (ClpC/X) or (ClpA/X) subunit (Figure 5).[20] ClpA and ClpX are members of the Clp/Heat shock protein (Hsp) 100 family of molecular chaperones that belongs to the AAA+ superfamily of ATPases associated with various cellular activities.[23,24] *M.tb.* possesses its orthologue ClpC instead of ClpA. Yet other gram- positive bacteria similarly have the orthologues ClpC or ClpE in place of ClpA.[23] Degradation of folded or unfolded proteins to short peptides and/or amino acids can either be ATP dependent or independent.[25]

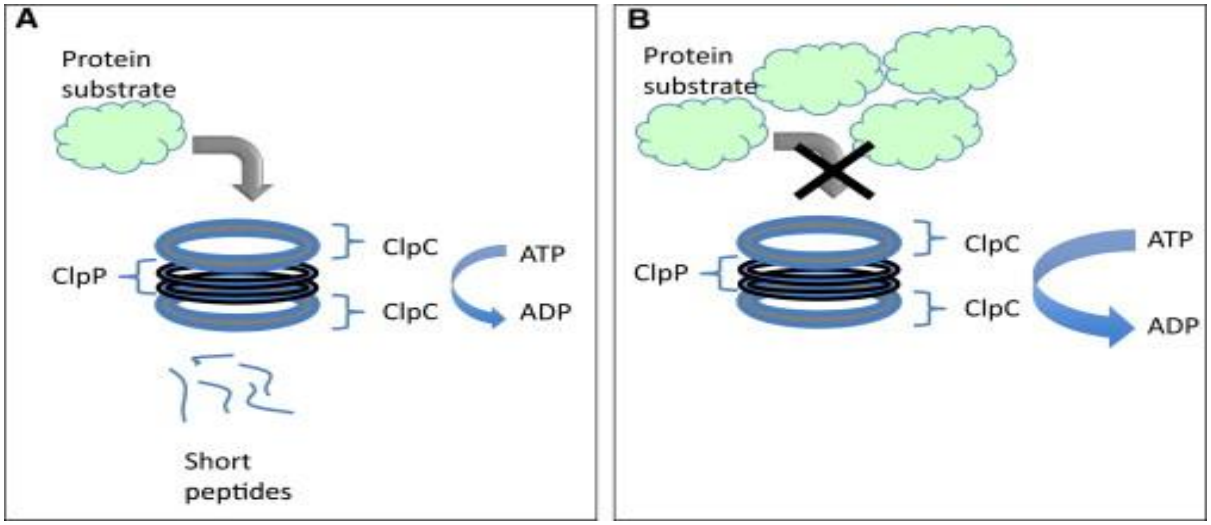


Figure 5: Normal functioning of the Clp complex. (B) Peptide promotes ATP hydrolysis but prevent protein degradation.[20]

Unfolded and short peptides are degraded directly by ClpP. Globular folded proteins are energy dependent and are degraded by ClpP-ClpC complex in mycobacterium. Protein substrates are recognized by regulatory subunits, translocated and directed into the proteolytic chamber (ClpP) where degradation takes place.[25] ATPases provide energy for the unfolding of proteins to be degraded and this energy comes from ATP hydrolysis.[20,26] Different from other site specific proteases, caseinolytic protease form a degradative Clp complex typically consisting of a sandwich of two heptameric rings of ClpP protease (ClpP1 and ClpP2) units flanked by two hexameric rings of Clp (ClpC and ClpX) ATPases, thus structurally and functionally resembling the eukaryotic proteasome.[27]

1.5. Cyclic peptides as antimicrobial peptides (AMPs)

Thus far three classes of naturally occurring peptides; (ecumicin, lassomycin and cyclomarin) have been isolated and reported to have the ability to bind to the caseinolytic protease complex and cause cell death.[11]

Antimicrobial peptides (AMPs) are endogenous polypeptides produced by multicellular organisms in order to protect a host from bacteria, viruses or fungi.[28,29] AMPs are sometimes defined as host defence peptides against pathogens and pests in diverse organisms ranging from microbes to animals and are found in all forms of life.[30,31] AMPs range from 8 to 50 amino acid sequences and are characterised by amphipathic and cationic properties due to the ionic arginine, lysine and histidine residues with an overall charge range of +2, to +9.[28,29,32,33] Properties of AMPs are summarized in Figure 6.

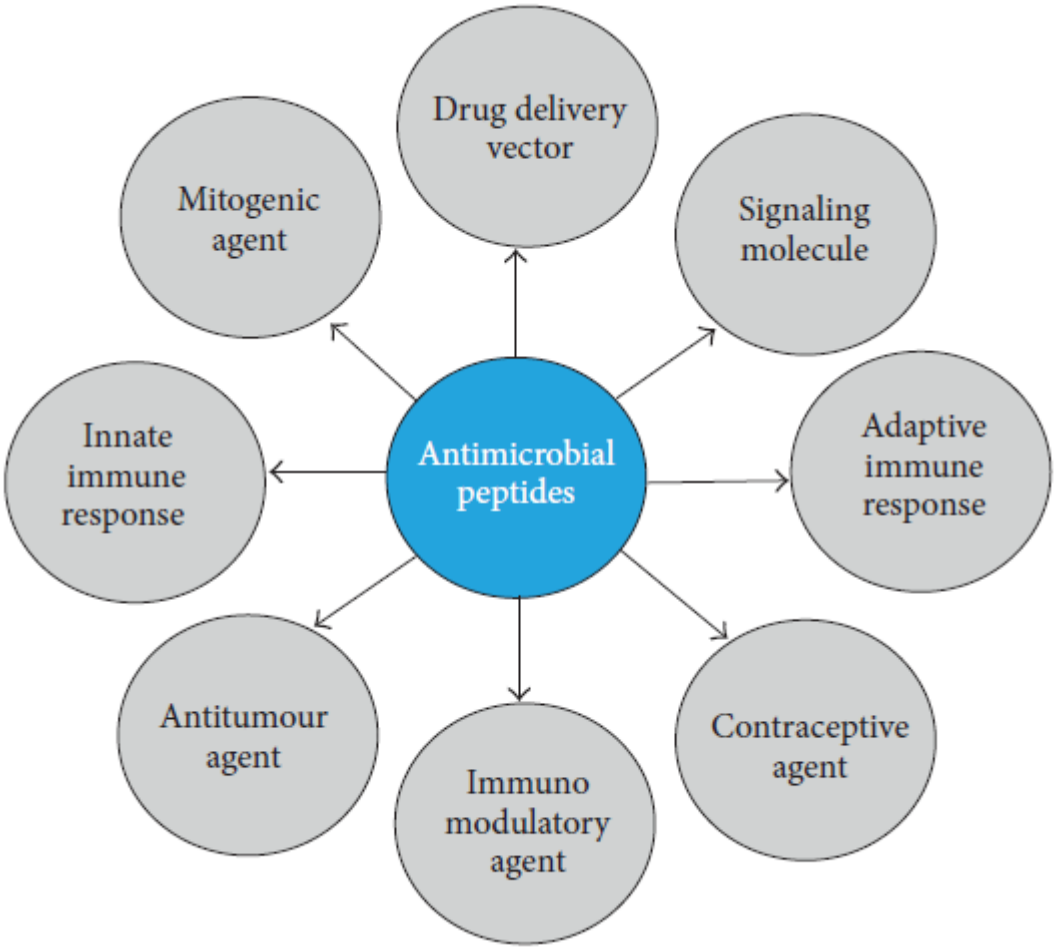


Figure 6: Multifunctional properties of AMPs[31].

AMPs primarily interact with the bacterial cell membrane by electrostatic force due to the cationic charge of the AMPs and anionic charge of the cell membrane surface.[28,34,35] Studies have shown that there is a strong linear relationship between cationic charge and biological activity because of a particular electrostatic interaction. Very strong bonding between the peptide and the membrane interface which is the phospholipid head group inhibit peptide translocation into the membrane's inner leaflet causing loss of antimicrobial activity.[31] Also there is correlation between concentration of peptide attached to the membrane interface and biological activity.[34]

AMPs are categorised in various ways, based on sequence, mechanism of action or structure.[31] AMPs exist in different molecular form structures such as α-helical and β-sheet loop although many of them are linear peptides from plants, insects and animals. Linear peptides can be helical with or without cysteine but with an over representation of one or two amino acids (proline-arginine and tryptophan-histidine). Cyclic or loop peptides have one or

more disulphide cyclic bond or lactone backbone.[28] Polycyclic peptides are produced by bacteria and loop peptides are produce by all major forms of life. These include lantibiotics and cyclotides.[29,30] Disulphide bonds or cyclization of peptide stabilises the AMPs such that AMPs maintain a particular structure in solution and consequently retain the same stable conformation when interacting with the membrane surface.[34] The existence of such versatile structural forms of AMPs is very significant for their wide spectrum antimicrobial activity.[33] In addition, properties such as size, charge, hydrophobicity, amphipathic stereo geometry, peptide self-association to the biological membrane add on to their wide range of antimicrobial activity[33]. Amphipathicity of a peptide is a measure of the spatial separation between hydrophilic and hydrophobic side chains.[36]

AMPs possess a range of functions which include immune modulation, killing bacteria be it gram- positive or gram-negative, antifungal as well as anti-cancer or anti-viral properties.[31] Many AMPs are effective against MDR and exhibits low probability for developing resistance mainly because of their mode of action which makes them lucrative potential novel drug candidates for diseases in which current drugs are increasingly becoming less effective due to drug resistance. Figure 7 shows the various functions of AMPs.

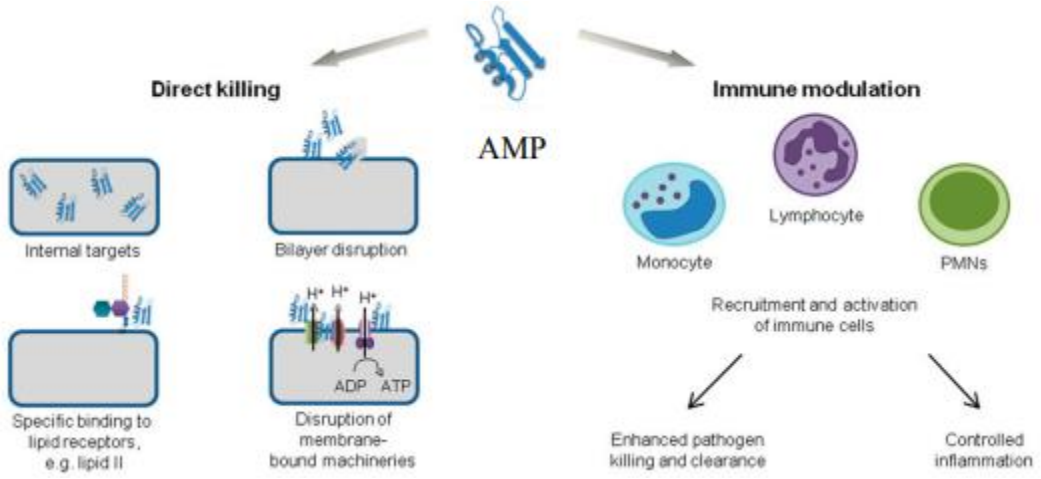


Figure 7: Various functions of AMPs.[31] MN: polymorphonuclear neutrophils; ADP adinoside diphosphate; ATP adenos.

AMPs kill bacteria by interacting with the bacterial cell membranes or cell walls. The positively charged residues of AMPs selectively bind to the negatively charged bacterial membrane allowing the hydrophobic component of AMPs to permeate the fatty layer of the membrane.[36] Binding of AMPs to the bacterial membrane leads to non-enzymatic disruption

and consequently cell death. AMPs are selective to specific species because of the differences in the membrane composition for microbes and cell types.[31,37] For example positively charged AMPs hardly binds to mammalian cell membrane which are enriched in the zwitterionic phospholipids neutral in net charge.[28,38] Four mechanisms that describe the cell membrane disruption by AMPs have been widely suggested which are namely the carpet model, the toroidal model, the aggregate channel model and the barrel-stave model (Figure 8).[28,39]

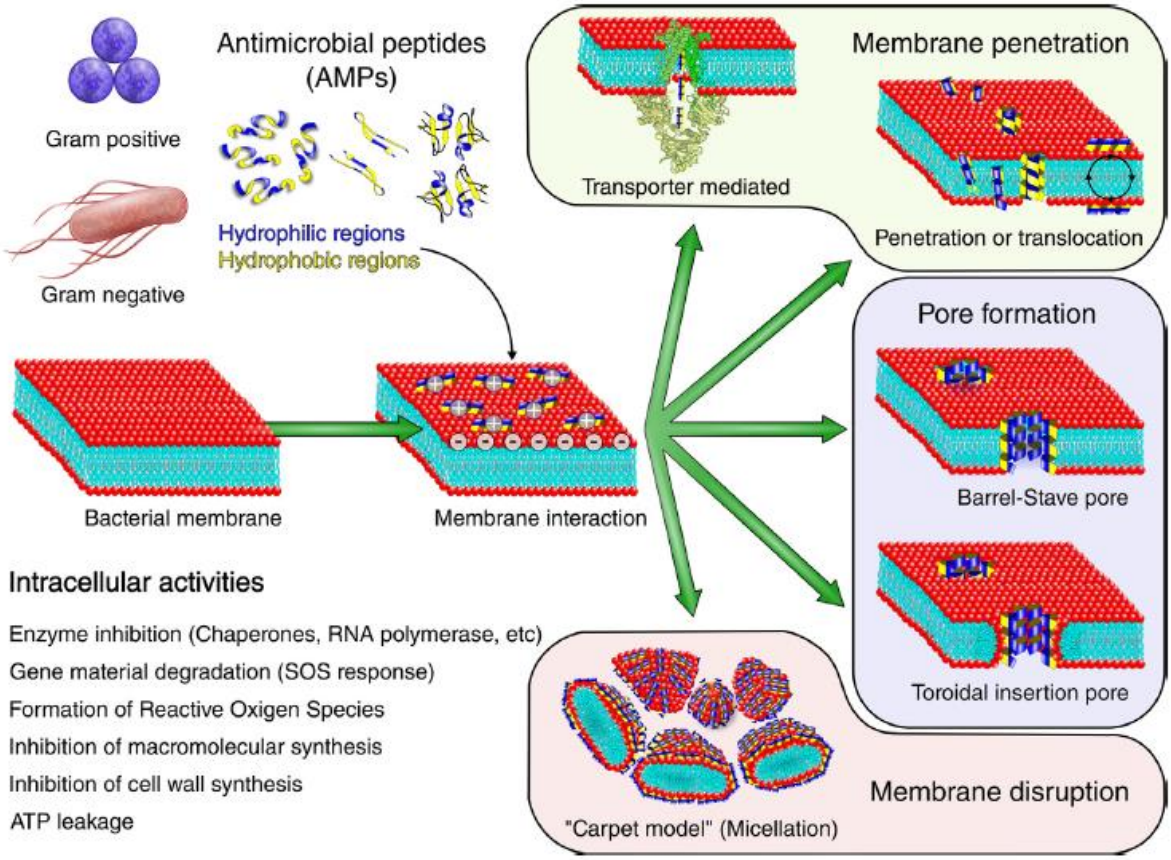


Figure 8: Mechanism of action of AMPs.[35]

1.5.1 Lassomycin

Lassomycin is a cyclic natural product that belongs to the "lasso" peptides. Lassomycin was isolated from an actinomycete (*Lentzea kentuckyensis sp.*) in a screen of a library of previously uncultured soil bacteria.[13,40] Lasso peptides are a group of bio active short peptides with different structures, and the *C* -terminus of 16-21 amino acids threads through an *N*-terminal macrolactam ring adopting an interleaving topological loop resembling a lasso or a slipknot (Figures 9 & 10).[41,42] Figure 9 shows the amino acid sequence of lassomycin and its recently proposed structure.

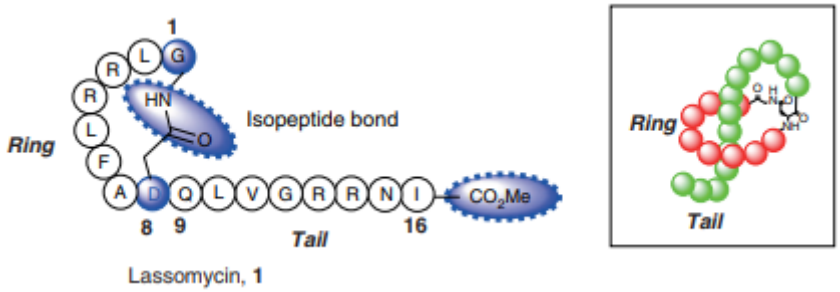
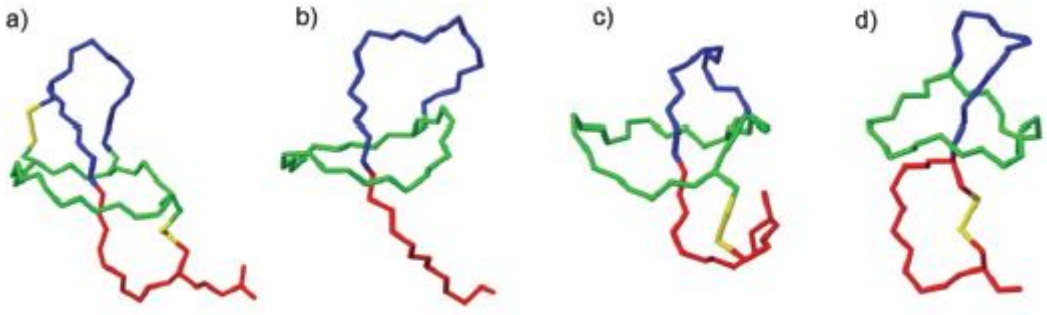


Figure 9: Amino acid sequence and recently proposed structure of lassomycin.[13,43,44]

Lasso peptides are ribosomally synthesized and post translationally modified. Lasso compounds are grouped into four classes based on the number of disulphide bonds (Figure 10). Class I has two disulphide bond formed between Cys 1/Cys 13 and Cys 7/Cys19 respectively. Class II has no disulphide bonds; it depends on large amino acids which are sterically hindered called "steric lock" to hold the lasso structure intact and to keep the tail of the lasso peptide from slipping out of the ring. Class III and 1V have one disulphide bond that connects the ring to the tail in one case or the other.[41,42,45]



Class I Class II Class III Class IV

Figure 10: Structure and topology of four different lasso peptides. The ring residues are shown in green, amino acids belonging to the loop in blue, and the amino acids in the tail in red. Disulphide bridges are shown in yellow.[41]

Lassomycin showed anti-TB activity against MDR and XDR *M.tb* as well as drug sensitive strains.[1] It has an MIC range from 0.41 to 1.65 nM and is effective in killing inactive *M.tb* as well as exponential *M. tb* unlike the current first line TB drug, rifampicin which is ineffective against inactive *M.tb.*[1] Lassomycin is an AMP that exhibit unique biological activity because it activates the target enzyme rather that inhibiting it.[40] Lassomycin binds to the acidic *N*-terminal pocket of ClpP1P2 and increases the ATPase activity leading to decoupling of ATPase from ClpP1P2 proteolysis activity. ClpC1P1P2 complex is essential ATP-depended protease responsible for the viability of the mycobacteria.[5]

Docking and mutations studies have shown that lassomycin binds to Gln17 by hydrogen bonding, Arg21 and Pro79 of the *N*-terminus domain of ClpC1. Gln17 was found to be critical for the binding of lassomycin whereas Arg21 and Pro79 were less essential.[11,46] Arginine residues on lassomycin tail are reported to form hydrogen bonding with the Gln of the ClpC1 *N*-terminal domain of the caseinolytic protease. Previously reported solution state NMR structure of lassomycin (Figure 11) was a cyclic unthreaded peptide.

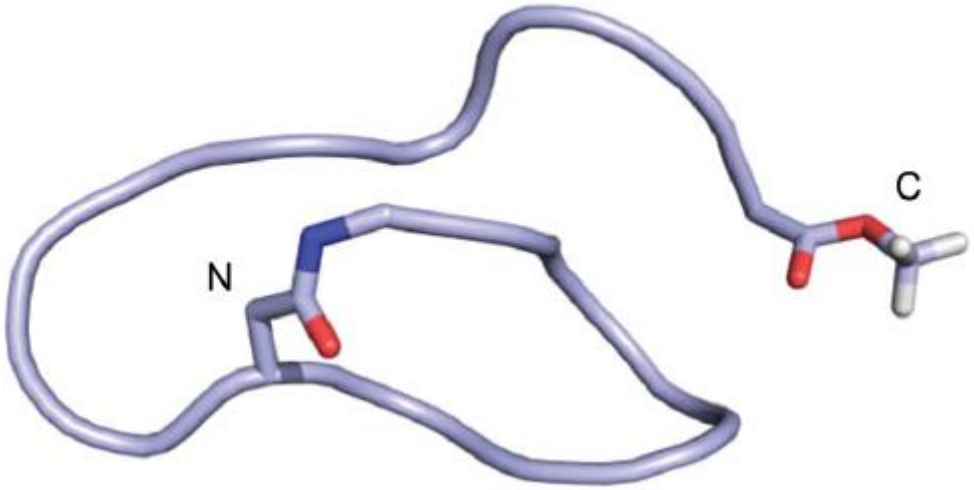


Figure 11: Unthreaded lassomycin structure previous reported.[13]

It was not a lasso peptide without a knot topology which is a characteristic of other homologous lasso peptides as shown in Figure 10.[13,42] However, recent biological evaluation of the synthetic lassomycin based on the reported unthreaded structure and its *C*-terminal amide analogy showed no activity against *M.tb* for both compounds.[13] According to a temperature dependent NMR study on synthetic lassomycin, it was suggested that the natural lassomycin exist in a threaded conformation that does not unfold upon heating to 40 $^{\circ}$C contrary to the originally proposed unthreaded structure.[43]

1.5.2 Cyclomarin A

Cyclomarin A is another cyclic AMP from marine *Streptomyces* CN3-982 (Figure 12).[5] It is active against *M.tb* with cidal concentration value of 0.3 µM and 2.5 µM against bacteria in culture broth medium and human-derived macrophages, respectively.[43] It kills both active and dormant, non-replicative mycobacteria.[25] Cyclomarin A was found to be effective against MDR *M.tb* unlike the resistance which was shown by *Bacillus subtilis, Enterococcus faecalis, Escherichia coli, Pseudomonas aeruginosa,* and *Staphylococcus aureus.*[1] Cyclomarin A binds to the *N*-terminal domain of ClpC1 leading to uncontrollable proteolysis

by the ClpP protease machinery. Cyclomarin A binding does not affect the ATPase activity of ClpC1 and no bactericidal activity has been observed in the panel of Gram-positive and Gram-negative bacteria despite them containing ClpC1.[25]

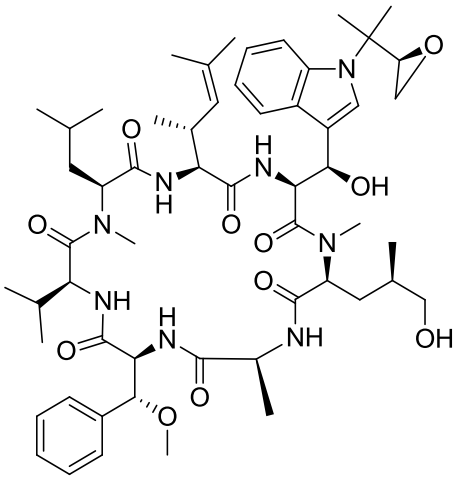


Figure 12: Structure of Cyclomarin A.[27,47]

Apart from showing activity against *M.tb* recent research showed that it has anti-malaria properties. Cyclomarin A selectively inhibits *PfAp3Ase* of *Plasmodium falciparum* in a nanomolar range, but the human homologue in FHIT.[47]

1.5.3 Comparison of binding sites and activities of aforementioned AMPs

Figure 13 shows the binding sites of ecumicin, cyclomarin A, and lassomycin on ClpC1.

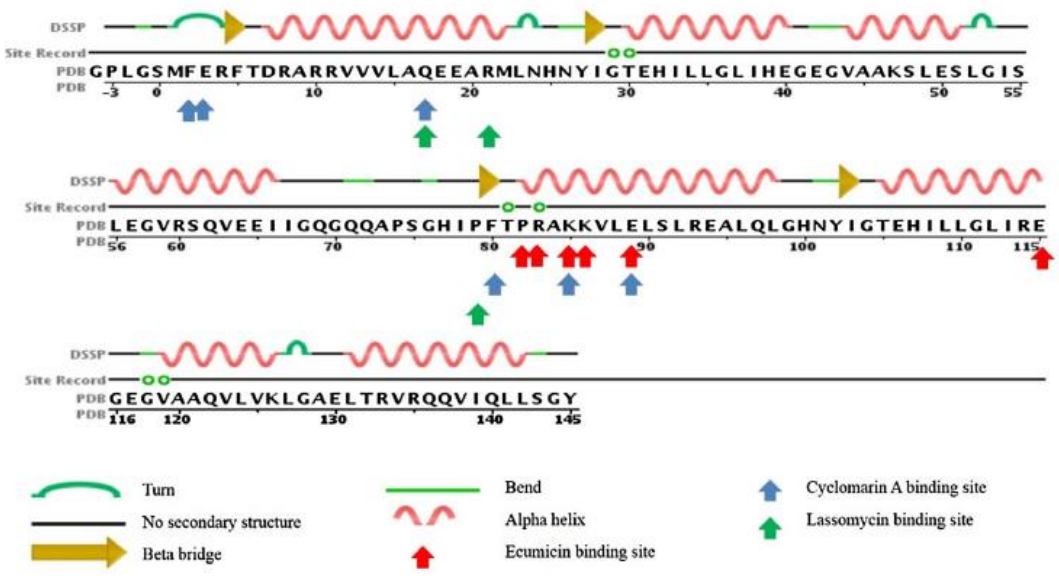


Figure 13: Binding sites of ecumicin, cyclomarin A, and lassomycin on ClpC1.[11]

Cyclomarin A, and lassomycin share the same binding site on Gln 17 whilst ecumicin, Cyclomarin A shares the same binding site on K85. Binding sites of one or two of the three AMPs are confined within a particular region of the ClpC1.

Table 1 shows the anti-tuberculosis activity of cyclomarin A, lassomycin and ecumicin. Ecumicin is more potent that lassomycin and Cyclomarin is the least potent among them when tested against the *M.tb* strains mentioned in Table 1.

Table 1: Anti-tuberculosis activity of cyclomarin A, lassomycin, and ecumicin.[1]

M. tuberculosis	**Cyclomarin A**	**Lassomycin**	**Ecumicin**
MIC	MIC_{50} **(µg/ml)**	MIC_{90} **(µM)**	MIC_{90} **(µM)**
H37Rv	0.08	0.41-0.83	0.16
MDR	0.08-0.125	1.56-3.1	0.31
XDR	N.D.	0.78-3.1	0.31-0.62
Clinical isolates	0.08-0.3	1.56-3.1	0.31-0.62

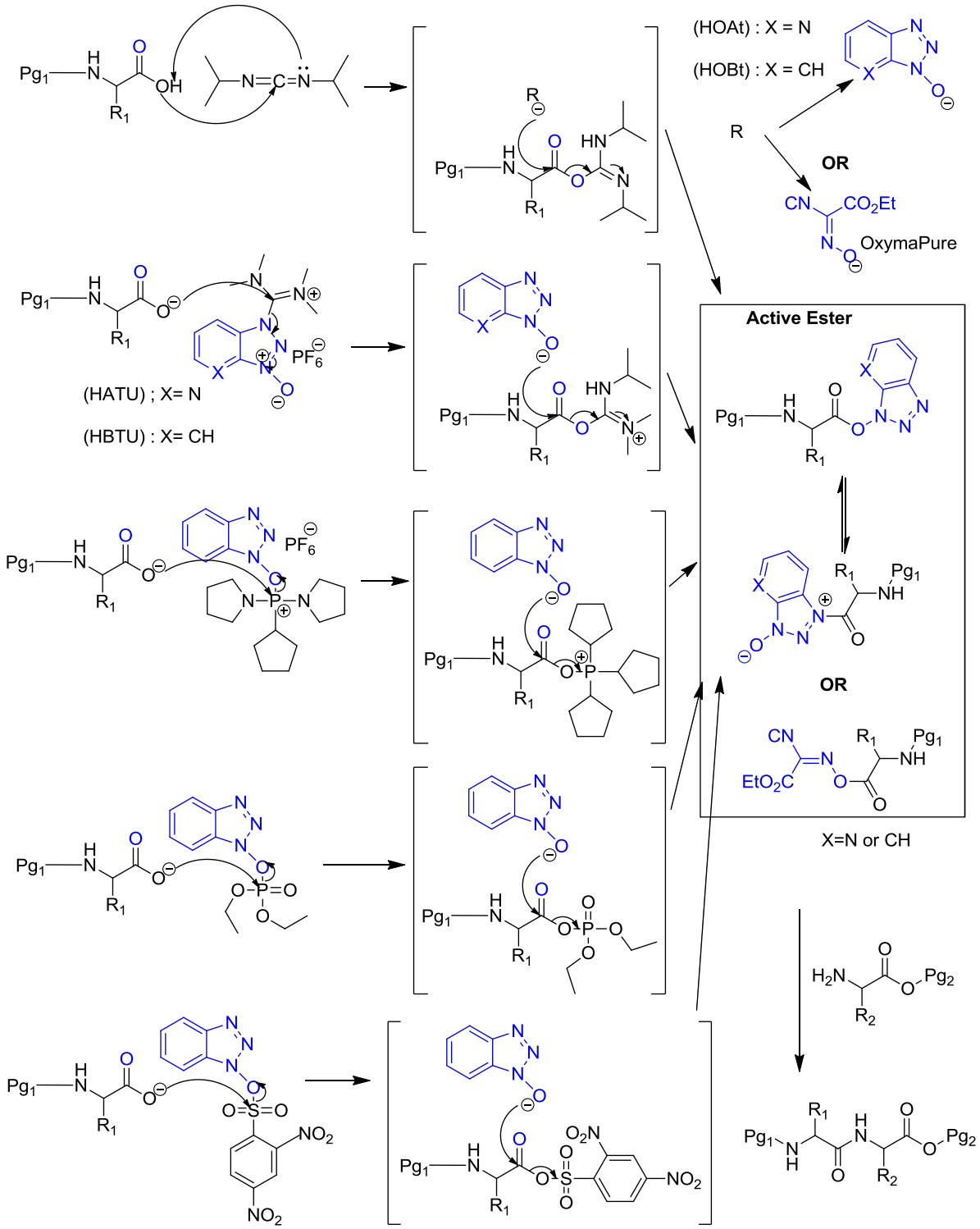
N.D. Not determined

1.6 Peptide synthesis

Peptide formation is a condensation reaction or amide bond formation between a carboxylic acid and an amine of two amino acids.[48] This reaction is favored at high temperature because of both thermodynamic and kinetic reasons. Mixing an acid and base will favor formation of a stable salt instead of an amide but the reaction conditions can be changed to favor the formation of an amide when the temperature is elevated to 160-200 ^{o}C, conditions which are not compatible with other functionalities and substrate.[48,49] Activating the carboxylic group of the amino acid into a carboxylic ester derivative by attaching it to a leaving group will allow the weak nucleophile amino group to react at an ambient temperature.

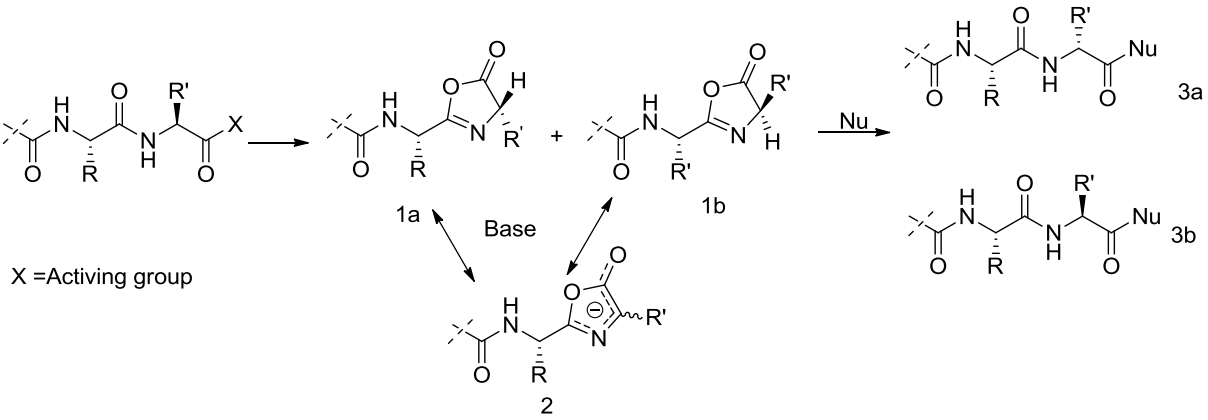
Many activating or coupling reagents have been developed that exhibits numerous favorable properties in different peptide synthesis conditions with varieties of peptide structures and derivatives. These properties include but not limited to little racemization/epimerization, shorter reaction time, compatibility with the solvent type and resins, minimum side products, temperature compatibility, safety, costs and efficiency for fragment coupling or cyclization of linear/macro peptides.[49-52] Some are best at coupling *N*-methylated amino acid or dialkyl amino acid while others are good at ester formation. Carbodiimides, phosphonium-based reagents, aminium/uronium- based reagents and oxyma-uranium-based reagents are among

these peptide coupling reagents often used.[51,53] Carbodiimides coupling reagents are often used with additives to reduce racemization/epimerization. Scheme 1 shows the mechanism of the amino acid carboxylic group activation by various coupling reagents used in peptide synthesis.



Scheme 1: Activation of amino acid carboxylic group via different types of coupling reagents.[49,54]

Epimerisation is the interconversion of epimers in peptides synthesis and is facilitated by the formation of the oxazolone during the nucleophilic attack by the amine group.[49,53] Epimerisation results in a change of chirality and production of enantiomers or diastereoisomers which are difficult to purify. Purification can be challenging as special chiral columns are required to separate the epimers.[48] Scheme 2 shows the epimerization formation in peptide synthesis.



Scheme 2: Formation of epimers in peptide synthesis.[53,55]

1.6.1 Peptide synthesis methods

There are various methodologies or strategies used to synthesize peptides namely; liquid phase, solid phase, microwave, and recombinant technology.[37,56,57] Each methodology has its own strengths and weaknesses. Depending on the nature of the peptide, synthesis can be a combination of the synthetic strategies mentioned above.

1.6.1.1 Liquid phase strategy

Liquid phase strategy (LPS) is when synthesis is done in solution phase.[58] It is suitable for short peptides with less than eight amino acids produced in large quantities. Scale up is relatively cost effective and ease.[59] The formation of side products can be easily detected and can be used for ligation technology. Intermediate products can be deprotected and purified to give the final peptide in high yield.[58] However, it has long reaction time.[58] It is not easily automated and the purification work is labor intensive.[59] An additional step is required to protect the C- terminal of the first amino acid.

1.6.1.2 Microwave assisted

The microwave energy facilitates unfolding of the folded and aggregated peptides into unthreaded peptides that are easy to couple, Figure 14.[60]

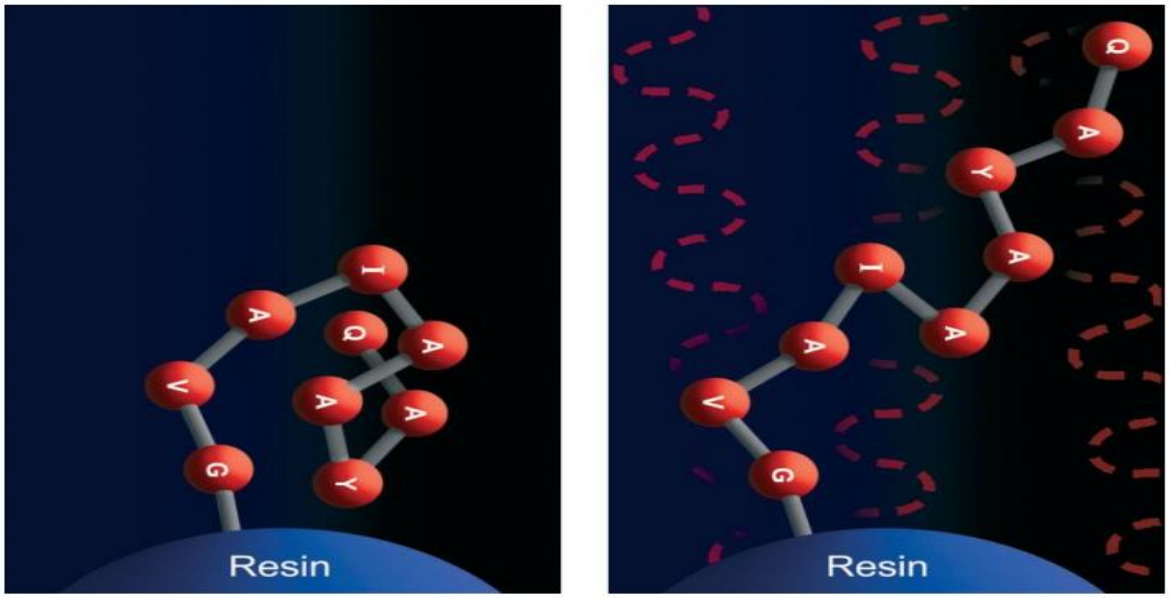


Figure 14: Effects of microwave energy on synthesis of difficult peptide sequences.[61]

Microwave assisted peptide synthesis is when microwave radiation is used to heat the reaction mixture during coupling and deprotection stages of peptide synthesis.[62] Microwave assisted peptide synthesis reduces the reaction time, saves energy, and has high yield and purity of the crude product.[63,64] Hence it is more effective for coupling difficult peptides as shown in Figure 14 above.[62,65,66] Microwave assisted strategy uses less solvents than conventional (manual or automatic) solid peptide synthesis. There is less need for double or triple coupling as in SPPS as reaction goes to completion in few minutes over a single coupling.[67] However, chances of dehydration and racemization with some amino acids are increased if not properly optimized especially for cysteine and histidine amino acids.[61]

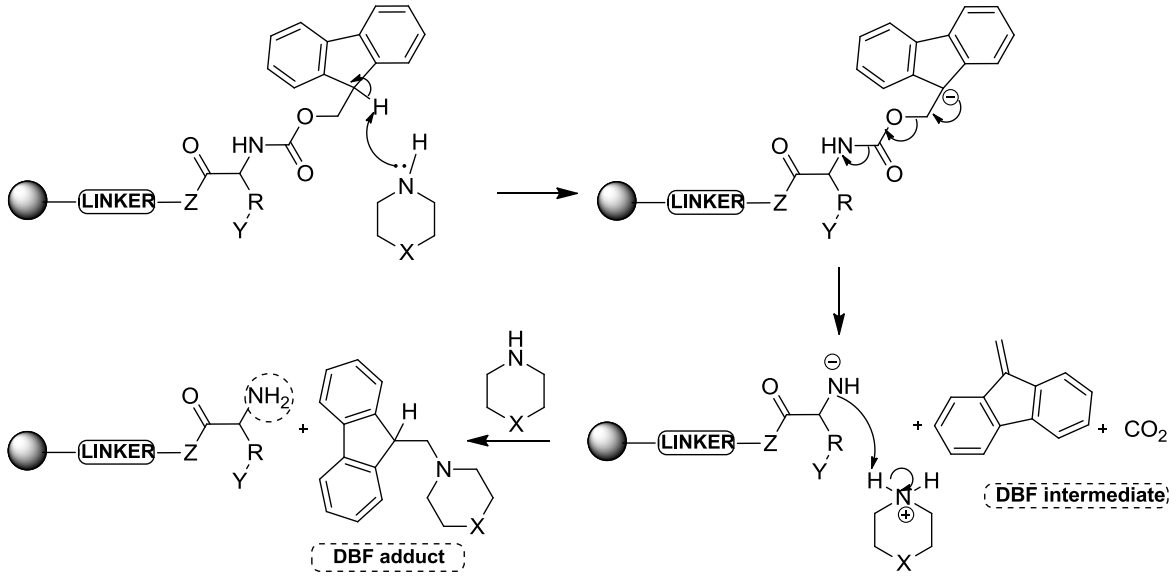
1.6.1.3 Solid Phase Peptide Synthesis (SPPS)

Two methods for SPPS are namely 9-fluorenylmethyloxycarbonyl (Fmoc) strategy and the *tert*-butyloxycarbonly (Boc) strategy.[58] For the Fmoc strategy, the *N*-terminus of the amino acid is protected by the Fmoc group which can be removed by a mild secondary base such as piperidine (20-50) % in dimethylformaamide (DMF) or 1,8-Diazabicyclo[5.4.0]undec-7-ene (DBU) .[68] The side chain protecting groups must be stable to the base and only be removed by an acid such as trifluoroacetic acid (TFA) at the final cleavage when the peptide is also cleaved from the resin.

A Boc protecting group is used to protect the *N*-terminus of the amino acid for the Boc strategy to be employed. Since t-Boc group is removed by TFA in dichloromethane (DCM)

or dimethylsulphoxide (DMSO), the side chain protecting groups must be TFA stable to prevent premature cleavage. Cleavage by TFA produces isobutylene, carbon dioxide and protonated amine which must be neutralized before the next coupling. Strong acids such as hydrofluoric (HF) or trifluoromethanesulfonic acid (TFMSA) in the presence of suitable scavengers, such as anisole are used to finally cleave the peptide from the resin and to remove all the protecting groups.

The milder conditions and ease to handle chemicals makes the Fmoc strategy more widely used. It starts with the *C*-terminal of the amino acid being attached to an insoluble support called a resin through a linker on the resin. Amino acids are coupled one at a time until the *N*-terminus amino acid is reached. After every reaction of the growing peptide chain, by-products are removed by filtration and washing. Base labile protecting group, 9-fluorenylmethyloxycarbonyl (Fmoc), (Scheme 3) protects the alpha amino group and the acid labile protecting group protects the side chain groups on amino acids.[68] Scheme 3 shows the mechanism for the removal of Fmoc protecting group by secondary amine for the formation of free amine in SPPS.



Scheme 3: The removal of Fmoc group by secondary amine for the formation of a free $–NH_2$ in SPPS. R = amino acid side chain; Y= side chain protecting group; Z=O, NH; X=CH_2, NH, and N(CH_3).[68]

These developments by B. Merrifield in 1963 and L. A. Carpino and G. Y. Han in 1970 made SPPS to be the fasted and cheapest way of synthesizing peptides.[69] It is best for long peptides in small quantities. Purification is ease because the solution is filtered by draining leaving the attached peptide on the resin without manipulative loses.[70] It is highly automated and has

short production cycles compared to LPS. However, it has its own drawbacks. Coupling and deprotection does not go to completion in SPPS. There is always accumulation of mixtures of by-products and aggregation of growing peptides even when washing is done thoroughly with the appropriate solvent, temperature, pH and time.[58] Protein synthesis is not feasible with SPPS since the average length of a protein is 250 amino acids. It is very expensive for large scale production and requires two extra steps of linkage and cleavage.[59]

Deprotection is dependent on factors such as resin swelling, peptide aggregation, time, peptide sequence, reaction phase and solvent type.[71] Recent studies by Albericio *etal* shows that the reaction is effective when polar aprotic solvents are used such as DMF, DMSO, N-methyl-2-pyrrolidone (NMP), tetramethylurea (TMU) and is very slow in medium to a polar aprotic such as tetrahyrofuran (THF), methyltetrahydrofuran (MeTHF) and toluene.[72] Although piperidine is the widely used base for removing the Fmoc group, it sometimes causes deletion sequences due to incomplete removal of the Fmoc group in several peptide sequences.[71] Alternative combination of piperidine/DBU has been reported to be more effective when deprotecting difficult peptide sequences with very little or no deletion and racemization.[71]

1.6.2 Resins Support

Solid support resins are classified mainly into three types: polystyrene (PS), polyethylene glycol-polystyrene (PEG-PS) and hydrophilic PEG-based resins.

PS resins are cross-linked polymers with 1% of divinylbenzene PS(DVB) and a loading capacity range of 0.4-1.5 mmol/g. 1% DVB is added to make them insoluble in hydrophobic solvents and to avoid precipitation in aprotic organic solvents.[73,74] PS are best in nonpolar solvents and good in some polar solvents like *N, N*-dimethyl formamide (DMF) and tetrahydrofuran although not good in water.[70] PS resins perform well in small to medium peptides and are cheap although limited for very hydrophobic peptides which aggregate. PS resins are chemically and mechanically stable and have wide spectrum of loading levels.[72]

PEG-PS is a low DVB cross-linked PS grafted with PEG by an ether link.[70,73] It is amphiphilic and allows solvation by both polar and non-polar solvents including water. PEG-PS(s) are good for long chain peptides although relatively expensive. For example Tentagel resins, has a broader range of swelling in polar solvents although it is hygroscopic and its backbone is more reactive compared to PS. This exposes the backbone to damage

consequently leakage of PEG or PEG derivatives resulting in reduced process yield and purity.[72]

Another group of resin supports are the hydrophilic PEG or Poly (ethylene glycol)-poly (*N*,*N*-dimethylarcralyamide)-copolymer (PEGA). PEG or (PEGA) are best for water and protein studies although they easily get damaged if shrunk or dried. ChemMatrix are better PEGA, with no PS, good handling properties and compatible for small to long peptides.[73]

The choice of resin support is important in SPPS strategy. Resin support determines the physical properties such as swelling. Swelling is an important property as it affects the diffusion of reagents and the accessibility of the reactive sites hence the kinetics of the reaction. Different resin supports are compatible with different solvents and this will affect the chemistry and conditions under which the resin is stable. The solid support must be stable to a range of temperatures and mechanical stirring.[75] Biocompatibility is a point to consider on whether the resin support can swell in aqueous buffers used during biochemical assays. Resin support bead diameter affects the kinetics due to surface area to volume ratio. Beads with smaller sizes have faster reaction kinetics. However, if the bead size is too small, filtration can be prolonged. Size distribution of beads is important as too inhomogeneous bead sizes can cause different quantities of the final product mixture. Bead size is usually measured in Tyler Mesh size which is inversely proportional to the bead diameter.[75]

1.6.3 Solvent type

Like any other chemical reactions, the choice of solvent can promote or suppress the intended reaction due to interaction of the solvent with reagents or substrates. Additionally, solvent type can affect the swelling of the resin, hence the loading capacity. Solvents with high resin swelling abilities are preferred to those with low resin swelling.[40] Table 2 shows the swelling properties of Fmoc based SPPS resins in various solvents.

Table 2: Overview of the three subgroups of resins for Fmoc –based SPPS and their swelling properties.

Resin subgroups	Commercial name	Initial Loading (mmol/g)	Approximate swelling (mL/g) DCM	DMF (NMP)	Ether	Water	TFA	THF	MeOH
PS (1% DVB)	Amino methylated PS	0.4-1.5	7	4	4	N.A	2	9	1.6
PEG-PS	Amino TentaGel (TG)[a]	0.15-0.3	6	5	2	3.6	N.A	5.0	3.6
PEG based	Amino PEGA[b]	0.2-0.4	13	11	N.A	16	NA	13	13

	ChemMatrix (CM)	0.4-0.6	11	8	N.A	11	14	N.A	9

[a] The swelling volumes are for standard grade TG, [b] The swelling properties listed are for 0.2mmol/g resins[73]

Recent studies show that THF has better swelling, and solubility properties than DMF. Altogether, N-methyl-2-pyrrolidine (NMP) is the best candidate to replace DMF as a SPPS solvent based in comparison of their properties such as resin swelling, viscosity, solubility of SPPS reagents, coupling reaction profile and Fmoc cleavage profile.[72]

1.6.4 Linkers

Linkers are bifunctional molecules that facilitate the attachment of the growing peptide as well as the final cleavage step.[73] Integral linkers are those whose support is part of the linker (e.g. 2-chlorotrityl resin). Non-integral linkers are independent and bifunctional molecules that are attached to the solid support through an ether link (e.g. Wang resin) or amide bond. Varieties of linkers release peptide acid, amide, esters, thioesters and secondary amides when cleaved from the resin. Thus the linker is chosen based on the desired *C*-terminal functional group Table 3.

Table 3: Shows types of resin linkers, commercial names, their *C*-terminal functionality and stability.[73]

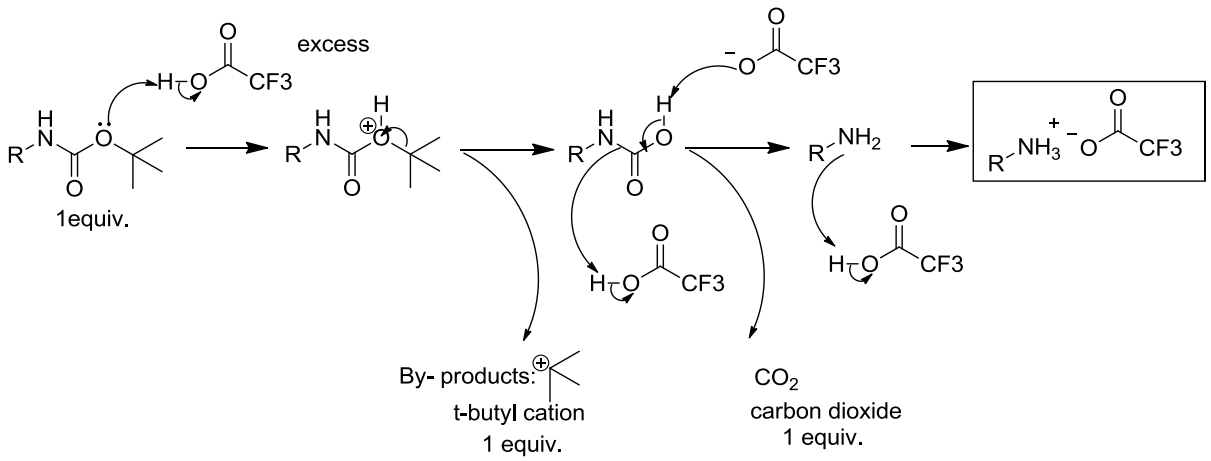
Linker type	Name	*C*-terminal functionality	Stability
Amino methyl	Rink amide linker	Peptide amide	Base
	Sieber linker	Peptide amide	Base
	Pal linker	Peptide amide	Base
Hydroxyl methyl	Wang/PHB	Peptide acid	Acid
	HMPA	Peptide acid	Acid
	HMBA	Protected peptide acid, amide, alcohol and hydrazine	Acid
2-chlorotrityl Variants		Peptide acid and amide	Base
	Rink acid linker	Peptide acid	Base
	SASRIN linker	Peptide acid	Base
Others	Aryl hydrazide linker	Peptide amines or esters	Base

BAL	*Ortho*-Paldehyde linker (*o*-BAL)	Peptide acids, aldehyde, thioester	Base
Safety catch	4-sulfamylbutyl/Kenner safety-catch	Peptide thioesters	Base

Non-integral linkers are recommended because they provide control and flexibility during the synthetic process. Linkers which are stable throughout the synthetic process including the final cleavage stage are preferred to those that are even acid labile which can cause unwanted side reactions. Amino alkyl and amino benzyl are more acid stable linkers.[73]

1.6.5 Cleavage mixture

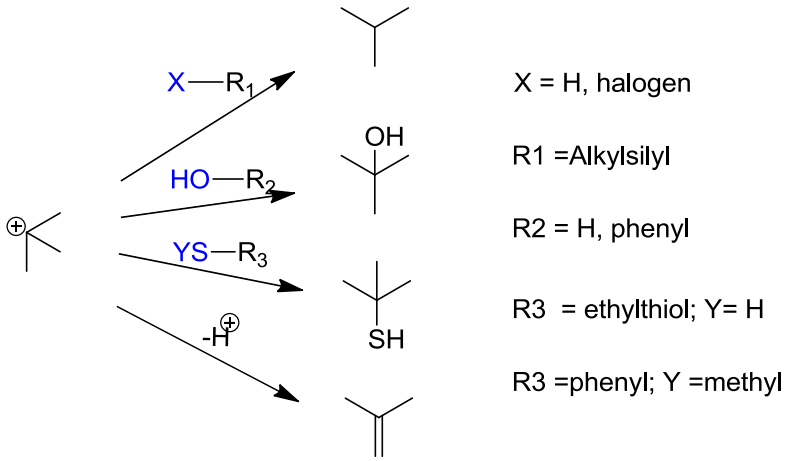
In the Fmoc SPPS strategy, hydroxyl side chain groups are commonly protected by *tert*-butyl and thiols while the carboxylic acids are protected by triphenylmethyl (trityl or trt): indoles, imidazoles and amines by (Boc), and guanadinium by 2,2,4,6,7-Pentamethyldihydrobenzofuran-5-sulfonyl (Pbf) protecting groups. All these protecting groups and the resin are cleaved with TFA based cleavage cocktails. Highly reactive cationic species are generated from the protecting groups and the handles or linkers on the resin (Scheme 4) below.[76] Unless these cationic species are quenched or trapped they will react with the nucleophilic groups on the side chain residues of the amino acid thereby modifying the peptide. In order to avoid and/or suppress these reactions, small amount of nucleophiles called scavengers are added to the cleavage mixture.[76] Scheme 4 shows the *t*-butyl cations formed during deprotection of BOC by TFA.



Scheme 4: Boc deprotection mechanism[57]

These scavengers preferentially react with cations formed instead of the deprotected nucleophilic groups on side chains of the peptide thereby preventing undesired peptide modification. The scavengers involve water, trialkylsilanes and thiols for example ethane dithiol (EDT). Apart from its bad smell, EDT is an excellent scavenger for *t*-butyl cations, trityl protecting group in the cysteine residues and prevent acid catalyzed oxidation of tryptophan residue. Trialkylsilanes such as triisopropylsilane (TIS) and triethylsilane (TES) are odorless effective substitutes of EDT for Trp (Boc) and Arg (2,2,5,7,8-pentamethylchroman-6-sulfonyl), (Pmc) containing peptides (Scheme 4).[77,78]

Thioanisole speeds up Arg(Pmc/Pbf/(4-Methoxy-2,3,6-trimethylbenzenesulfonyl), (Mtr)) cleavage in TFA although it causes partial removal of tButhio, tBu or Acm in Cys residues.[79] Tetrafluoroboric acid (HBF_4) (1M) in TFA is an effective cleavage and deprotection cocktail. Rink Amide and Wang resins are cleaved within 30-60 minutes at 4°C and MBHA resin requires more than 90 minutes at 25°C. It completely cleaves the Boc protecting group from lysine, tBu from Thr, Tyr Ser, Asp and Glu residues and 4,4'-Dimethoxybenzhydryl (Mbh) from Gln and Asn.[80] Risk of Trp alkylation is greatly minimized when HBF_4 is used instead of TFA only because it cleaves the Mtr group of arginine in less than an hour. Deprotection of multiple Arg (Mtr) associated peptide can be easily done within a short time of 15 minutes by using the trimethylbromide cocktail hence preventing Trp alkylation.[81] Scheme 5 shows the nucleophiles that scavenge carbocation during cleavage.



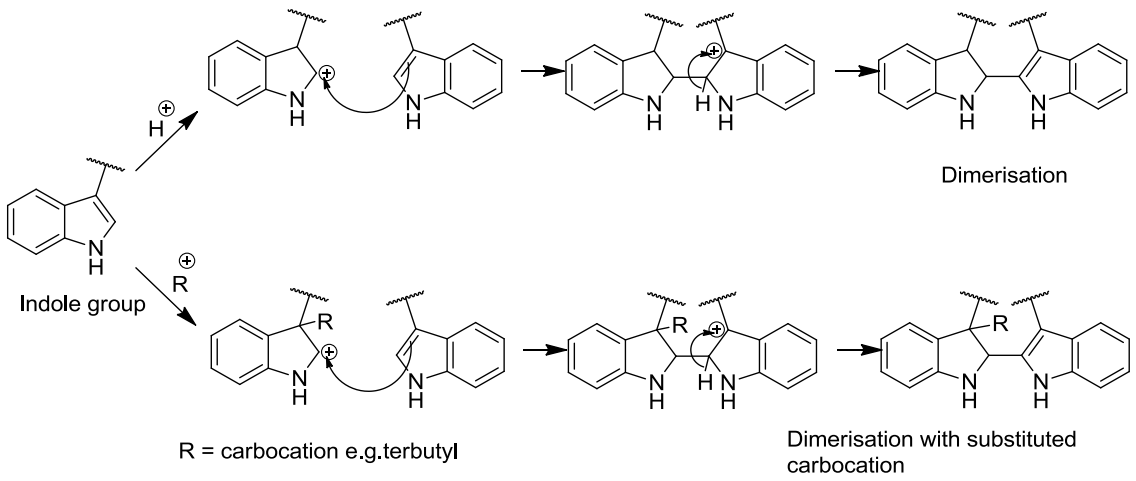
Scheme 5: Carbocation formed during cleavage are quenched by nucleophiles.[77,78]

Resin bound peptides must be thoroughly washed especially when DMF is used as the solvent because it is nonvolatile and any basic residual DMF will weaken TFA's acid properties. Mild acid like acetic acid which cannot cleave the peptide from the resin can be

used to wash the PEG and polyacrylamide resin support as it holds DMF.[82] The cleavage reaction is effective when polar aprotic solvents are used such as DMF, DMSO, NMP, TMU and is very slow in medium to a polar aprotic solvents like, for example THF, MeTHF and toluene.[72]

1.6.5.1 Side reaction during deprotection

Tryptophan is one of such amino acids that are greatly affected by side reactions during deprotection because of its indole side chain group. In acidic media, the free indole moiety can protonate and dimerizes to give undesired by-product. It can react with the carbocation formed from its protecting group or other side chain protecting groups resulting in a number of side reactions. Hence for a tryptophan based peptide, cleavage time must be optimized to suppress these reactions in addition to the presence of scavengers in the cocktail (Scheme 6).[83,84]



Scheme 6: Indole dimerization and side chain reaction after Boc deprotection.[83,84]

1.7 Drug derivatization and modification

Peptide novel lead compounds have quite a number of drawbacks apart from their activity profile against targeted receptors. Peptides are enzymatically unstable and have poor membrane permeability. Enzymatic degradation will reduce the fraction absorbed and the half-life of the peptide. Their different chemical and physical properties can present both chemical and physical challenges such as isolation, synthesis, solubility and purification.[85] Modifying these lead compounds will solve such problems and enhance the pharmacological and pharmacokinetic profile of the lead peptide in order to increase its stability, potency, crystallinity, taste specificity and to improve delivery to its site of action.[85,86]

1.7.1 Enhancing peptide stability by chemical modification

Chemical modification is when potential enzymatic cleavage sites on the peptide are altered to improve stability of the peptide. Chemical modification is in three categories namely modified peptides, pseudo peptides and peptide mimetics.[86] Table 4 below summarizes the afore mentioned categories.

Table 4: Chemical modifications of peptides.[86]

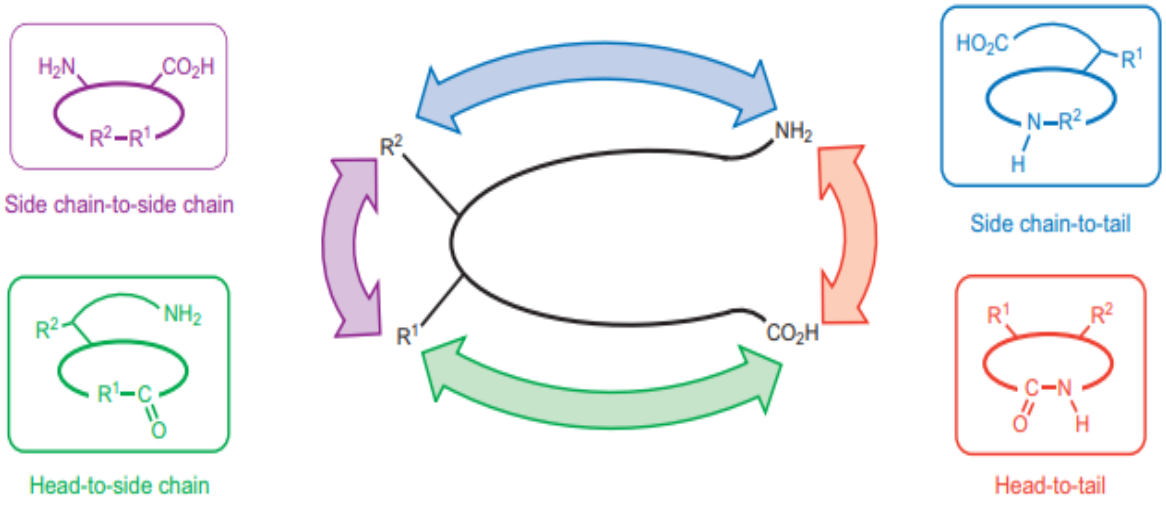
Name	Definition	Example
Modified peptide	Peptide derivatives containing relatively small modifications that do not alter the peptide bond. These derivatives can be considered as peptides in chemical nature	End modifications, cyclization, chirality changes, noncoded amino acids, N-amide nitrogen alkylation
Pseudo peptide	Peptide derivatives containing peptide bond modifications consisting of the replacement of some chemical groups. These derivatives are only partially peptide in chemical nature.	Amide bond surrogates Peptoids Azapeptides
Peptide mimetics	Organic molecules that no longer contain any peptide bonds but mimic the pharmacological activity of peptides	Rationally-designed peptide mimetics Randomly-identified mimetics

1.7.1.1 N-amide alkylation

N-amide alkylation reduces intramolecular hydrogen bonding potential and diminishes structural regularity thereby enhancing or improving the aqueous solubility of the peptide.[85,87] N-amide alkylation reduces the peptide structural flexibility by restricting the torsional angel between the carbon-carbon bond and the carbon nitrogen bond; this configures the peptide in a certain conformer that prevents proteolysis by enzymes.[88,89] It can as well improve receptor binding by hydrophobic interactions by alkyl group that can probe the deep pockets of the receptors.

1.7.1.2 Cyclization

Global restriction in peptide conformation is done through cyclisation.[88] Peptide cyclization decreases conformational freedom of flexible linear peptides, and often increases receptor binding affinities by reducing unfavorable entropic effects.[90] When peptides are cyclized, they become more constrained. Because of the constrained structure, cyclic peptides become more selective in their affinity to specific receptor cavities. Furthermore these constrained structures results in high stability against enzymatic degradation hence prolonging half-life time.[91-93] Cyclization of peptides exists in different combinations which are head to tail (C-terminus to N-terminus), head to side-chain, side-chain to side-chain and side-chain to tail with side-chain to side-chain being the most common (Scheme 7).[90,92,93]



Scheme 7: Four different ways of peptide cyclization.[92]

Cyclization efficiency in micro cyclization is minimized due to competing side reactions such as dimerization or cyclodimerization of linear peptide precursors. Dilute conditions in micro molar solutions can suppress these side reactions although it has drawbacks of costs associated and handling problems.[93] Theses side reactions can be minimized by cyclizing a peptide while it is still bound on the resin provided the resin loading is low. Under these conditions, intramolecular cyclic bonds are favored over inter-molecular bonding.[94] Figure 15 shows different types of side chain to side chain cyclization.

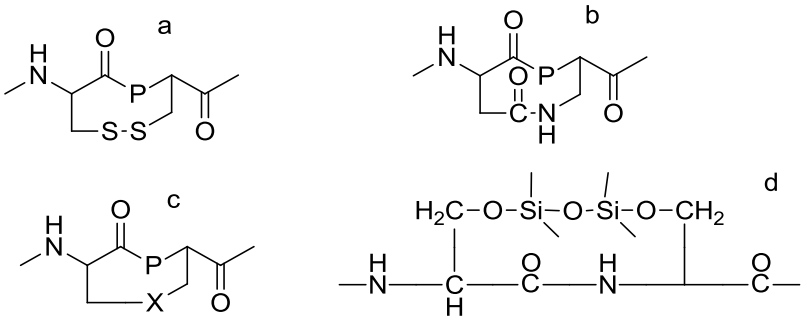


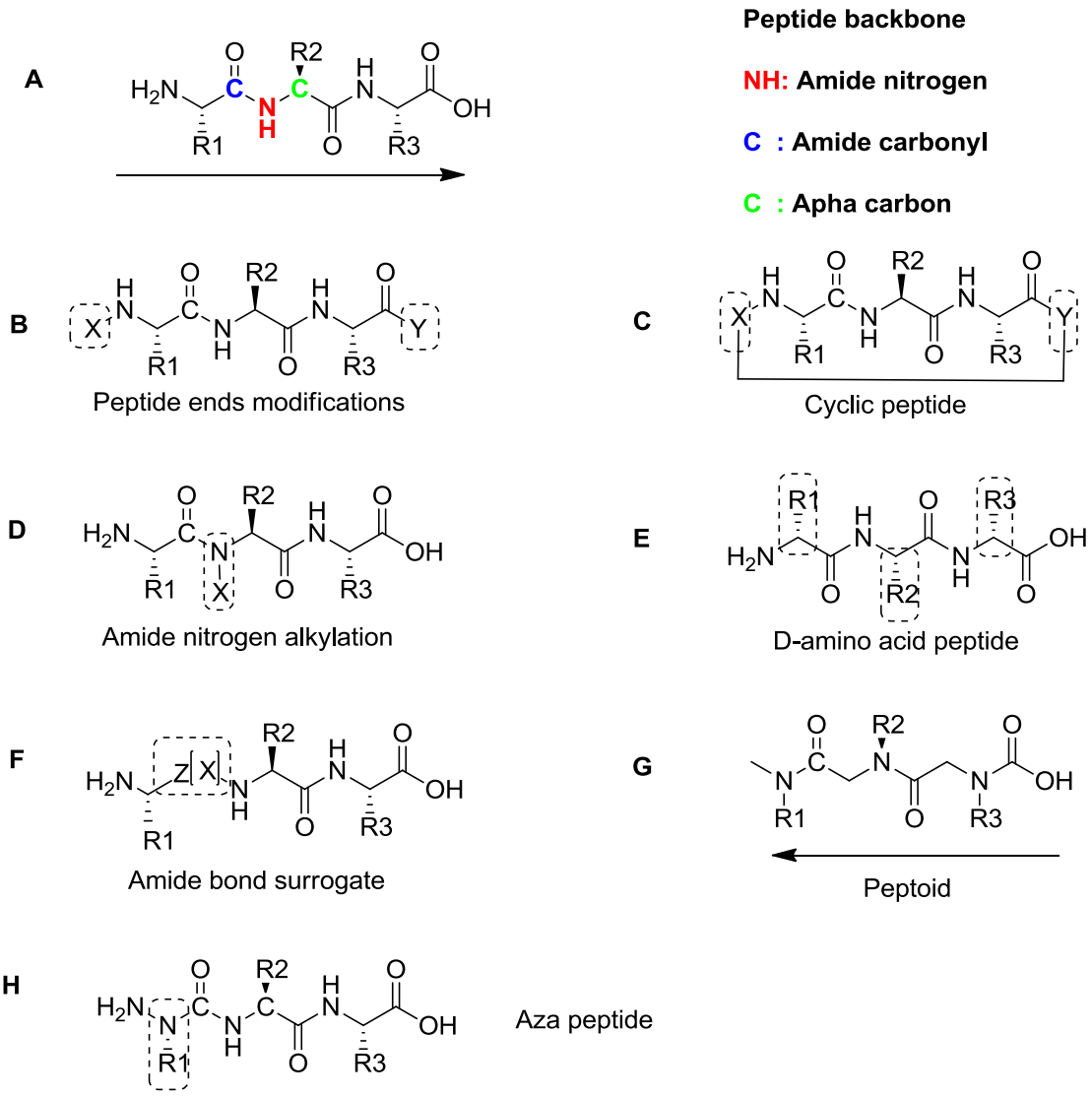
Figure 15: Covalent side-chain to side-chain cyclization a) Disulphide; b) Lactam; c) Ether/thioether/lactone; d) Disiloxane; P-Peptide.[88]

1.7.1.3 Peptide ends modification

Modifying either the C-terminus or the *N*-terminus of the peptide can increase peptide stability from proteolytic degradation. This is because many exopeptidases in plasma, liver and kidney affect therapeutic peptides.[95] Common terminal modifications are *N*-acetylation and *C*-amidation. Pegylation is another form of peptide end modification that increases peptide bio-availability, blood half-life and reduces proteolytic degradation, cell toxicity and non-specific uptake in tissue.[31] Pegylation is the covalent addition of polyethylene glycol (PEG) to a peptide.[96]

1.7.1.4 Peptoids

Peptoids are oligomers of N-substituted glycines, a class of compounds that mimic the structure of peptides.[97] The tertiary amide of peptoid is resistant to enzymatic degradation which give a competitive advantage of peptoids as a better peptidomimetics.[98] Peptoids are more flexible than peptides because of the absence of amide backbone proton which is responsible for inter- and intra-chain hydrogen bonding that causes formation of α-helices, and β- sheets. Peptoids are not readily denatured by solvents and temperature changes as the peptides.[98,99] Scheme 8 shows different peptide structural modification that can be used to prevent enzymatic degradation.



Scheme 8: Peptide modification changes that increase enzymatic stability. X and Y are any chemical group or atom. R_1, R_2 and R_3 are amino acids side chain groups.[86]

1.8 Limitations of peptides drugs, Ecumicin

Despite their favorable properties, peptides have several drawbacks that limit their therapeutic applications. Their unfavorable physiochemical properties, such as low bioavailability, variable solubility and limited stability make their systemic delivery difficult.[87,100] Peptides production costs are extremely high compared to small molecules of the same molecular weight by more than 10-fold.[101] This is evidently seen in the commercial large scale production of Enfuvirtide commercially known as Fuzeon, a 36- amino acid peptide chemically synthesized in a total of 106 steps, the majority (99) being in the SPPS. It is a membrane fusion inhibitor for the treatment of HIV and it cost US$25000 per year for treatment.[101] These peptides tend to undergo denaturation, aggregation, and adsorption which

limit their active concentration and proper function *in vivo.*[102] Some peptides have poor specific bio-distribution due to high conformational flexibility, resulting in a lack of receptor selectivity and activation of different target receptor leading to side effects.[102]

Although ecumicin has good activity, it is still limited by a long synthetic route, low *in vivo* activity and low solubility.[21,103] Thus this study aims to address these limitations.

In this study we will focus on derivatizing ecumicin to produce compounds with potentially greater potency.

1.9 Aims and objectives of the project

1.9.1 Aim

- This project is aimed at designing and synthesizing bioavailable ecumicin derivatives with anti-tuberculosis activity using the solid phase peptide synthesis strategy.

1.9.2 Objectives

The objectives of this project were to:

- Understand the structure activity relationship (SAR) of ecumicin by modifying the cyclic ring to investigate the effect of the ring size on the activity or binding by incorporating two cysteine residues.
- Develop a shorter synthetic route by replacing the lactone bond with the disulphide bridge.
- Improve the solubility of ecumicin by introducing polar amino acids.
- Synthesize and incorporate a peptoid analogue of a natural amino acid into the ecumicin sequence to prevent enzymatic degradation of the peptide.

1.9.3 Hypotheses and Questions

1.9.2.1 Question

Our main research question is, can naturally occurring caseinolytic protease inhibitors be synthesized and derivatized to address the issue of Tuberculosis?

- Will the replacement of the lactone bond with a disulphide bond improve solubility, structural conformation and activity against TB bacteria?
- Will incorporation of arginine improve solubility and the binding of ecumicin to the acidic regions of the protease?

- Will substituting arginine (pKa 12.48) with the less basic lysine (pKa 10.79) affect solubility and binding?
- Will increasing the residual chain of ecumicin affect its biological activity?
- Will a peptoid version of ecumicin improve solubility and conformational stability?

1.9.2.2 Hypotheses

a. *N*-methylated peptides and peptoids will have better antimicrobial properties than peptides because they have increased bioavailability as a result of their proteolytic enzyme stability.
b. By incorporating arginine, derivatives will have increased solubility and activity because of its basicity and strong hydrogen bonding to the *N*-terminal acidic region of the Clp1C1.

CHAPTER 2: Ecumicin derivatives

2.1 Introduction

This Chapter describes the synthesis of ecumicin derivatives as potential *Mycobacterium Tuberculosis* caseinolytic protease inhibitors.

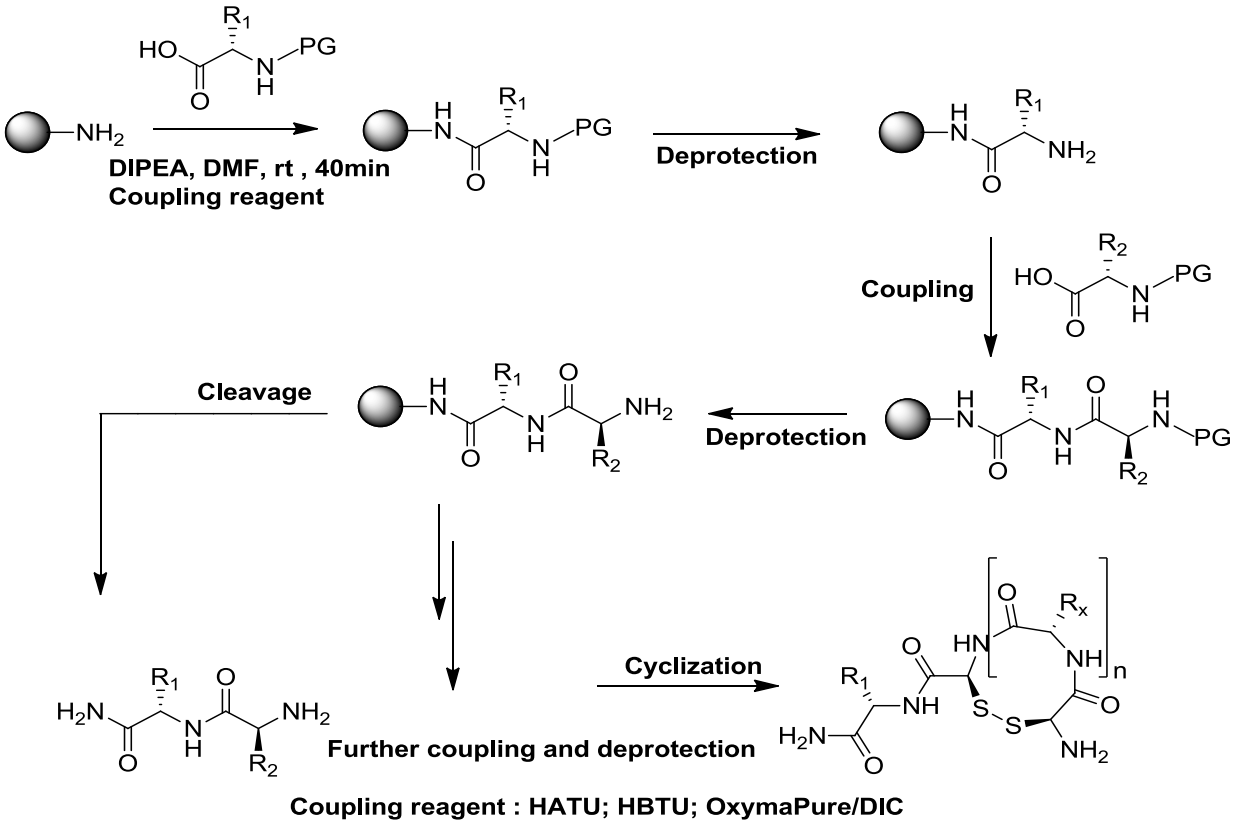
The use of natural amino acids for the synthesis of ecumicin peptide derivatives is essential for a quite number of reasons. Highly functionalized unnatural amino acids are difficult to synthesize and expensive as reported for the synthesis of Fmoc-*N*-methyl-4-methoxyl-L-tryptophan. This unnatural amino acid is synthesized in inclusively 8 steps in more than 100 hours.[103]

The reported overall yield for the synthesis of ecumicin over 30 steps was only 2.4% with a MIC_{90} value of 312 nM.[103] Thus we decided to use natural amino acids and feasible modifications to substitute the highly functionalized unnatural amino acids that will still enable ecumicin to bind to the protease.

Peptide drugs that are difficult to synthesize can only serve a limited number of patients because of their high prices due to exorbitant production costs. This is evidently seen in the most expensive Anti retro viral (ARV) drug, Enfuvirtide commercial known as fuzeon a 36 amino acid that cost approximately US$25000 per year for treatment.[104,105] Furthermore highly hydrophobic peptides like ecumicin poses solubility challenges during bio assays and even when administered to patients.[8,106] Hence the peptide can be successfully synthesized but will not be soluble in bio-compatible solvents and this make the whole effort fruitless. As a result, derivatizing the peptide to be more ionic or hydrophilic will facilitate the necessary biological assay and subsequent clinical trials administration.[107] Enfuvirtide is administered subcutaneously because it is not orally soluble.

The cyclic lactone bond on ecumicin involves quite a number of steps and is time consuming and hence it is costly. Modifying the cyclic bond by using an ease and cheap disulphide bond will eliminate a number of steps and save costs and time in addition to the importance of the disulphide bond mentioned in Chapter 1. Disulphide bridges are natural structural elements in proteins hence they give an essential structural network that affects the protein's tertiary structure.[108]

Manual and automated Solid-Phase Peptide Synthesis (SPPS) according to the Fmoc strategy (Scheme 9) was used for the synthesis of the peptides and the conditions are detailed in Table 6.



Scheme 9: Showing the SPPS with the final cleaved and cyclized structures.[48,92,109,110]

Liquid Chromatography Mass Spectrometry (LCMS) and Nuclear Magnetic Resonance Spectrometry (NMR) were the two techniques that were used for characterization. LCMS is a technique that allows separation of sample components by liquid chromatography before detection of their molecular mass by the sensitive and highly specific mass spectrometer (MS).

The samples to be analyzed were injected and carried into a reverse phase C18 column using solvent system selected based on the polarity of the peptide. Various run time and solvent gradients were investigated to find a method that did not co-elute components. The eluted components were then ionized by the MS to give the molecular ion peaks of all the components in the sample.

2.2 Purification

Purification was done on a C18 reverse phase column using preparative High Pressure Liquid Chromatography (prep-HPLC). The run time, solvent system and gradient was deduced from those determined during the LCMS analysis.

2.3 Biological studies

The minimum inhibitory concentrations (MIC) were determined using the broth assay microplate dilution method. Bacterial selectivity was done using bacterial MIC test. Bacterial strains; E.*coli* ATCC25922, P. *aeruginosa* ATCC 27853, S.*aureus* ATCC29913, and B.*subtilis* ATCC 2002 were used.

2.4 Results and discussion

2.4.1 Synthesis of PS01

The first derivative PS01 shown in the Figure 16 is a 15 amino acid peptide with two cysteine amino acids added on the 4th and 15th position of the sequence.

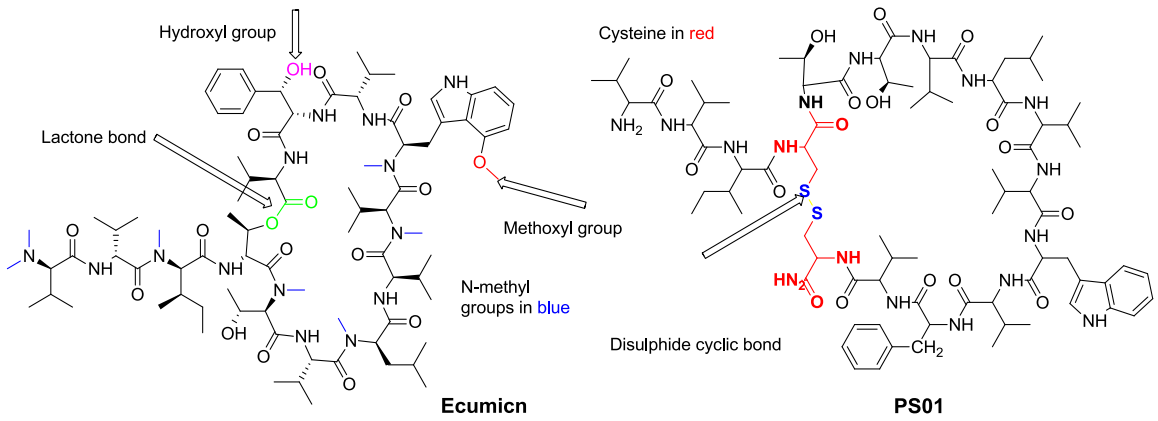


Figure 16: Ecumicin[19] and Ecumicin derivative, PS01.

Cysteine disulphide cyclic bond was used to form the ring instead of a lactone bond which is present in the original ecumicin structure.[90,109] Hence, the rink amide resin which would afford an amide ending was used to grow the peptide chain from the *C*- terminal of the derivative because there was no need of a carboxylic end to complete the lactone bond. This also would prevent the *C*-terminus enzymatic degradation by exopeptidases.[95] The *C*-terminal amidation increases peptide stability against proteolytic degradation.[85]

2.4.1.1 Synthesis of PS01 by manual and automated SPPS using HBTU as the coupling reagent

HBTU coupling reagent was used initially as it is cheap and works efficiently with most peptide sequences. However, it was observed that coupling only occurred until the 5th amino

acid (tryptophan) and coupling of subsequent amino acid was unsuccessful. Amino acid coupling times were varied between 20 minutes and 40 minutes, either single or double coupling respectively on both the automated peptide synthesizer and for manual synthesis. However, despite varying synthesis conditions, the LCMS showed a molecular ion peak corresponding to 5 amino acids with mass to charge ratio (*m/z*) of 652.9004$[M+H]^+$ (ESI^+) and calculated *m/z* being 651.8193 (Figure 17). This suggested that HBTU was not the best coupling reagent for this peptide because of steric hindrance. This could be explained because of the hydrophobic nature of the peptide which makes it difficult to couple.

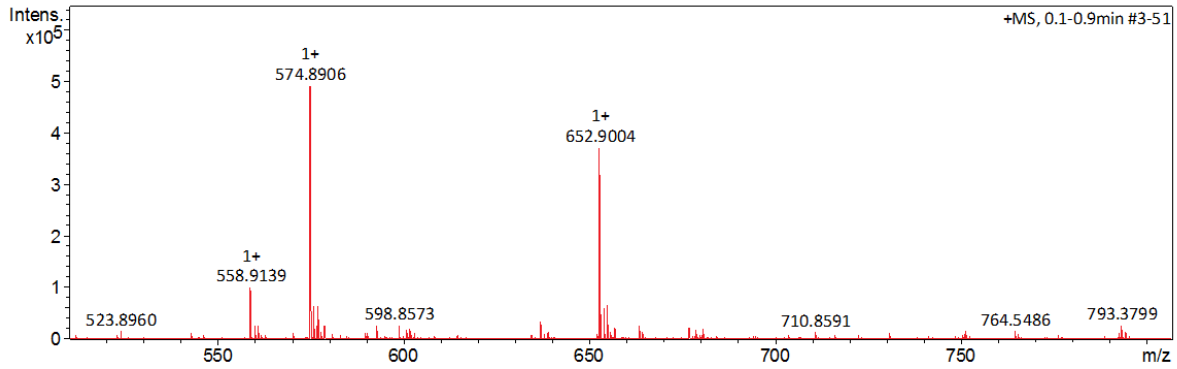


Figure 17: Molecular ion peak of the 5 amino acids which were successfully coupled during the synthesis of PS01.

2.4.1.2 Synthesis of PS01 by manual SPPS using HATU as the coupling reagent

HATU coupling reagent is a variant of the HOAt coupling reagents (Scheme 1). HOAt coupling reagents couple fast, more efficiently and with less epimerization when compared to HOBt coupling reagents.[49,50] The extra nitrogen on HOAt forms a hydrogen bond that stabilizes the activated intermediate.[111] HATU has also been proven to be efficient in coupling sterically hindered sequences.[48] The synthesis was carried out under bubbling inert nitrogen gas. Each coupling was conducted over a period of 30 minutes but double couplings were done for each amino acid to improve the yield of the peptide. Double coupling is usually employed for difficult coupling peptides sequences. During the synthesis, the peptide mass was analyzed after each coupling (Table 5).

Table 5: PS01 LC-MS masses found after each coupling.

Amino acid no.	Sequence	Calculated Mass	Mass Found	Retention time
4	**V**FVC	$C_{22}H_{35}N_5O_4S$ 465.2410	466.2460$[M+H]^+$	
5	**W**VFVC	$C_{33}H_{45}N_7O_5S$ 651.3207	652.3248$[M+H]^+$	3.84
6	**V**WVFVC	$C_{38}H_{54}N_8O_6S$ 750.38870	751.3001$[M+H]^+$	5.44
7	**V**VWVFVC	$C_{43}H_{63}N_9O_7S$ 849.4571	850.3532$[M+H]^+$	5.82
8	**L**VVWVFVC	$C_{49}H_{74}N_{10}O_8S$ 962.5412	963.4277$[M+H]^+$	6.94
9	**V**LVVWVFVC	$C_{54}H_{83}N_{11}O_9S$ 1061.6096	1062.4843$[M+H]^+$	8.63
10	**T**VLVVWVFVC	$C_{58}H_{90}N_{12}O_{11}S$ 1162.6573	1163.5150$[M+H]^+$	10.87
11	**T**TVLVVWVFVC	$C_{62}H_{97}N_{13}O_{13}S$ 1263.7050	1264.5504$[M+H]^+$	11.16
12	**C**TTVLVVWVFVC	$C_{65}H_{102}N_{14}O_{14}S_2$ 1366.7141	1368.5306$[M+2H]^+$	12.51
13	**I**CTTVLVVWVFVC	$C_{71}H_{113}N_{15}O_{15}S_2$ 1479.7982	1480.6120$[M+H]^+$	13.84
14	**V**ICTTVLVVWVFVC	$C_{76}H_{122}N_{16}O_{16}S_2$ 1578.8666	1579.6676$[M+H]^+$	10.6-21.0
15	**V**VICTTVLVVWVFVC Cyclic	$C_{81}H_{129}N_{17}O_{17}S_2$ 1675.9194	-	-

A side reaction peak was observed at 4.72 minutes when tryptophan was added [**W**VFVC] as shown in the Figure 18 below. This indicated that coupling tryptophan was incomplete. This could be because of the bulky nature of tryptophan that hindered coupling despite the long coupling time of 40 minutes and double coupling which was done. Improvements can be

done by either triple coupling or increasing time of coupling as well as using a less hindered coupling reagent such as OxymaPure since HATU is bulky.

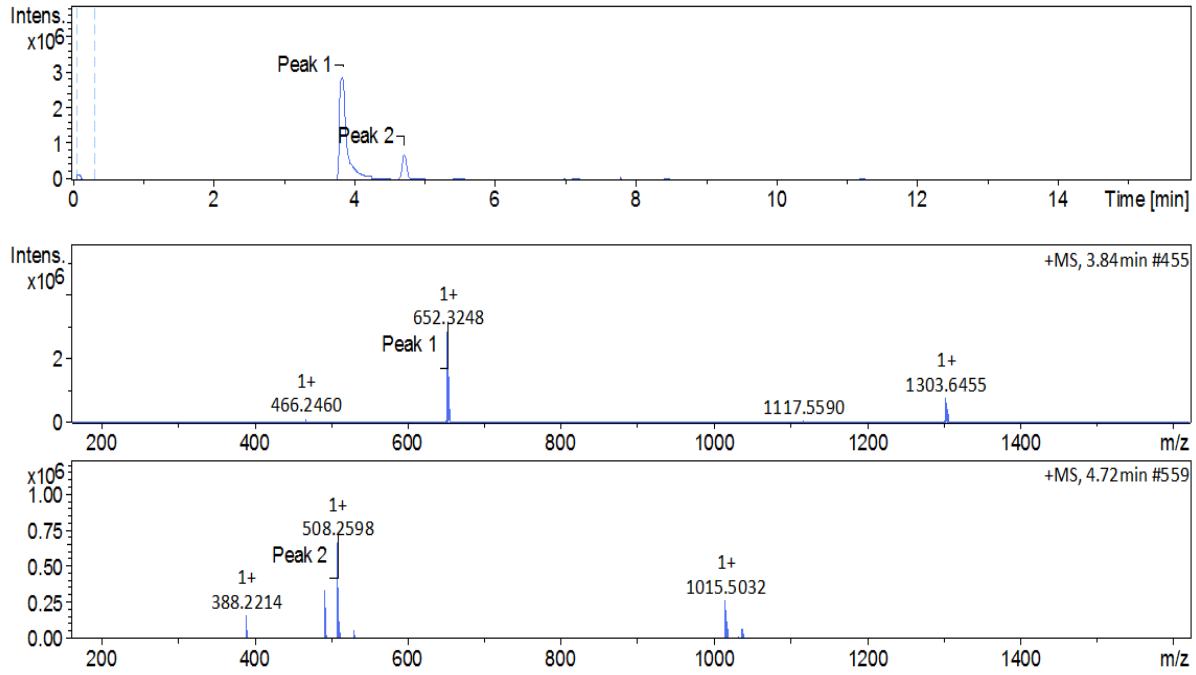


Figure 18: Molecular ion peak of the 5 amino acids which were successfully coupled during the synthesis of PS01.

Other methodologies could be used such as microwave assisted coupling. Coupling the 6th [**V**WVFVC] amino acid further showed more side reactions fragments that could not be assigned.

For the 14th amino acid, masses of 1579.6676 $[M+H]^{1+}$ and 790.3399 $[M+2H]^{2+}$ were found with the full mass having low intensity as shown on the Figure 19.

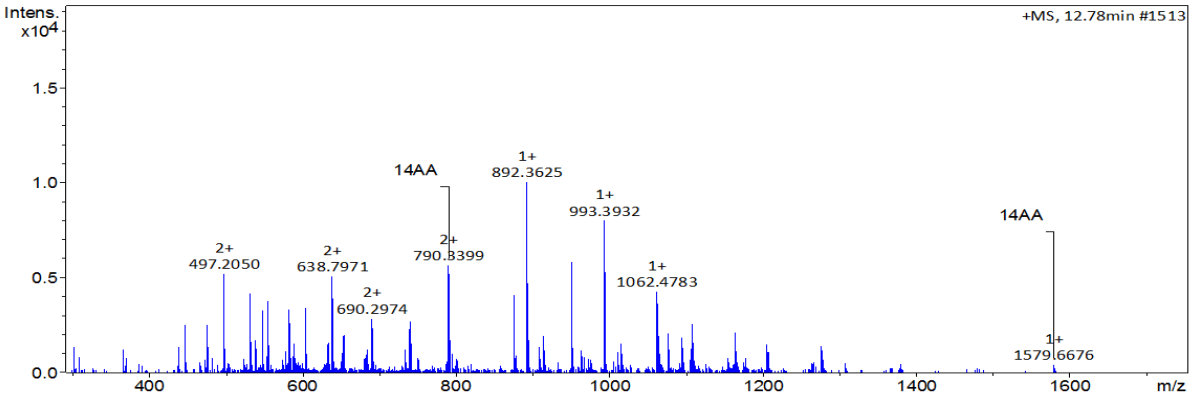


Figure 19: Molecular peak of the 14 amino acids which were successfully coupled during the synthesis of PS01.

This could suggest that poor ionization or the presence of many impurities in the total sample matrix suppressed the ionization.

Even though double coupling was done with an excess of 4 equivalents, the reaction could not go to completion as seen from the 5th amino acid to the 14th amino acid. This was however expected given the general drawbacks of SPPS mention earlier in Chapter 1. This could suggest a folding conformer of the peptide sequence that sterically hindered coupling and the steric hindrance increased as the chain grew. This is a common drawback of peptides drugs that aggregate or fold during synthesis especially hydrophobic sequences causing slow or incomplete deprotection and incomplete coupling.[112] This aggregation is mostly observed from the 5th or 6th amino acid to the 21th amino acid.[113]

2.4.1.3 Synthesis of PS01 by manual SPPS using OxymaPure as the coupling reagent

OxymaPure is an oxime which has been found to be a very efficient and effective additive in the carbodiamide coupling reagents for peptide coupling.[114] OxymaPure is readily available, stable, less explosive than common coupling reagents and is a very good epimerization suppression additive.[54,114] Compared to HATU, OxymaPure is a small molecule which offers less steric hindrance when coupling. Hence this gives OxymaPure a competitive advantage over HATU when sterically hindered amino acids are coupled. An attempt was made to synthesize PS01 using OxymaPure/DIC coupling reagents starting from the 5th amino acid to the final amino acid. All reaction conditions were kept constant except for the coupling reagents which were changed. A summary of synthesis conditions are shown in Table 6.

Table 6: Summary of peptide synthesis conditions

Coupling reagent	Resin	Coupling time(min)	Deprotection/ time (min)	Cyclization	Cleavage mixture
[HATU(0.19M), or OxymaPure/DIC (0.19M)] &1.5ml DIPEA (1.0M)	Rink amide HMBA (150.3mg)	30 per coupling (double)	3ml (20% piperidine in DMF, (5min×2	10equiv of $I_{2(s)}$ to AA loading capacity in 5ml (1:4, H_2O:DMF) for 3hrs	5ml (94:2.5:2.5:1, TFA:EDT:H_2O: TIS) for 3hrs

There were significant differences that were observed when OxymaPure/DIC was used as coupling reagent. Full peptide was successfully synthesized although there were a lot of fragments as shown in Figure 20.

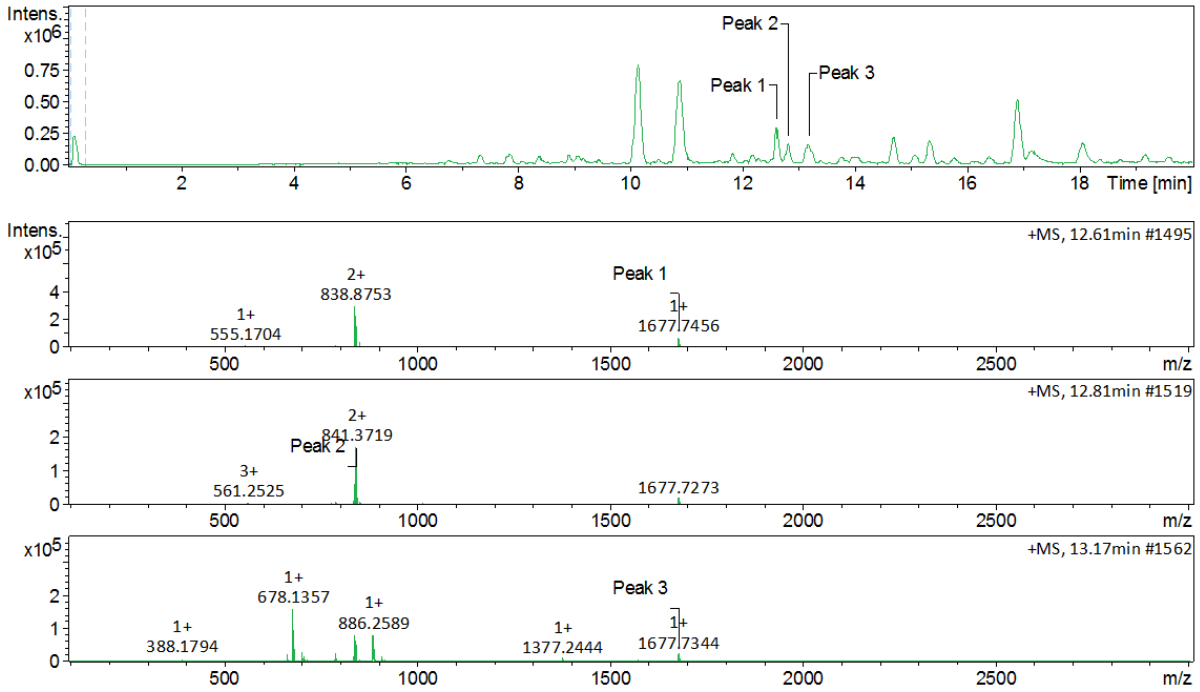
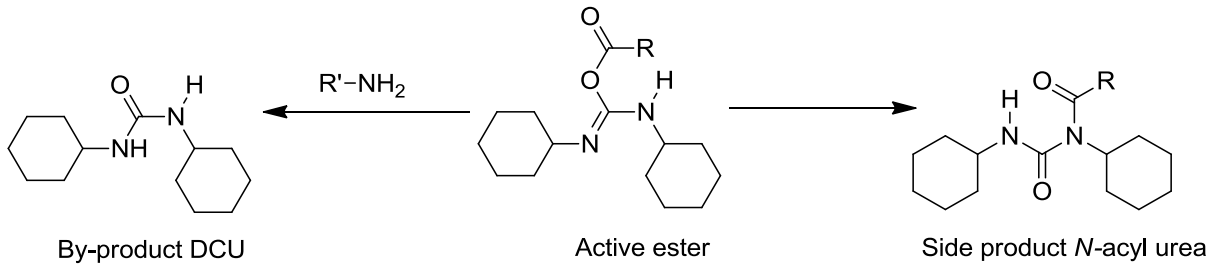


Figure 20: Molecular peaks of the 15 amino acids which were successfully coupled during the synthesis of PS01 using OxymaPure.

Spectrum from the 5th amino acid until the 13th amino acid showed similarities with the one observed when HATU was used. The intensities for the 14th and the 15th amino acid 1677.7456 $[M+H]^{1+}$ were higher when OxymaPure was used instead of HATU. This could suggest that OxymaPure could be a better alternative for HATU particularly for this peptide. Despite this advantage over HATU, OxymaPure has its drawbacks when used with DIC. OxymaPure forms side products' *N*-Acyl urea and dicyclohexylurea (DCU) which are insoluble in most solvents as shown in Scheme 10.[49] The peptide showed 3 conformers based on the method used for the final peptide which elute at 12.61, 12.81 and 13.17 minutes respectively. The peptide was not considered for purification and for testing because of too many fragments.



Scheme 10: Side reactions when DIC is used.[49]

2.4.2 Replacement of Tryptophan with Tyrosine

Many side reactions that were observed from the 5th amino acid all the way to the last amino acid of the peptide might have been caused by the presence of tryptophan. Therefore, substituting tryptophan with another amino acid that is less likely to be affected could possibly improve the yield of the peptide. However, it is important to carefully choose an amino acid that resembles tryptophan in terms of its pharmacological properties so that it will not possibly inactivate the peptide. One of such amino acid is tyrosine; it has been found that replacement of tryptophan with tyrosine does not affect the biological activity of the drug.[115] Hence another derivative PS06 was synthesized with tyrosine instead of tryptophan.

2.4.2.1 Synthesis of PS06 by manual SPPS using HATU as the coupling reagent using

Figure 21 shows the amino acid sequence of the PS06 peptide. Compared to PS01 with tryptophan, there was a great change from the 5th amino acid as minimal side reactions were observed.

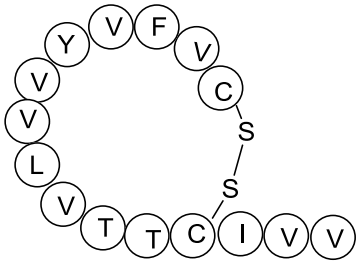


Figure 21: PS06 amino acid sequence.

We observed an intense peak 3 (Figure 22) which correspond to the desired molecular mass of 5 amino acid, and a minute Peak 1 corresponding to the mass of 4 amino acid sequence.. This confirms the effectiveness and ease with which tyrosine couples to valine with less side reactions and minimal modification during global cleavage of the peptide.

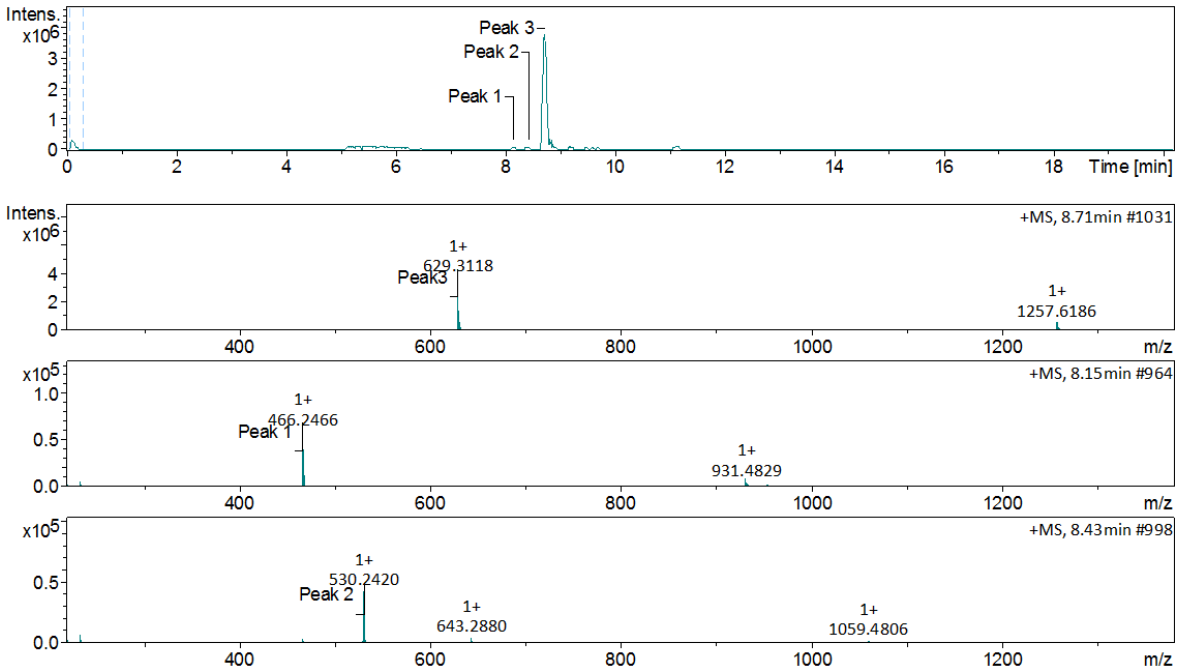


Figure 22: Molecular peaks of the 5 amino acids which were successfully coupled during the synthesis of PS06

6th amino acid coupling

Coupling valine to tyrosine showed that coupling was incomplete as there was the 5th amino acid peak 2 shown in Figure 23. Peak 1 is a deletion sequence (CVFVV).

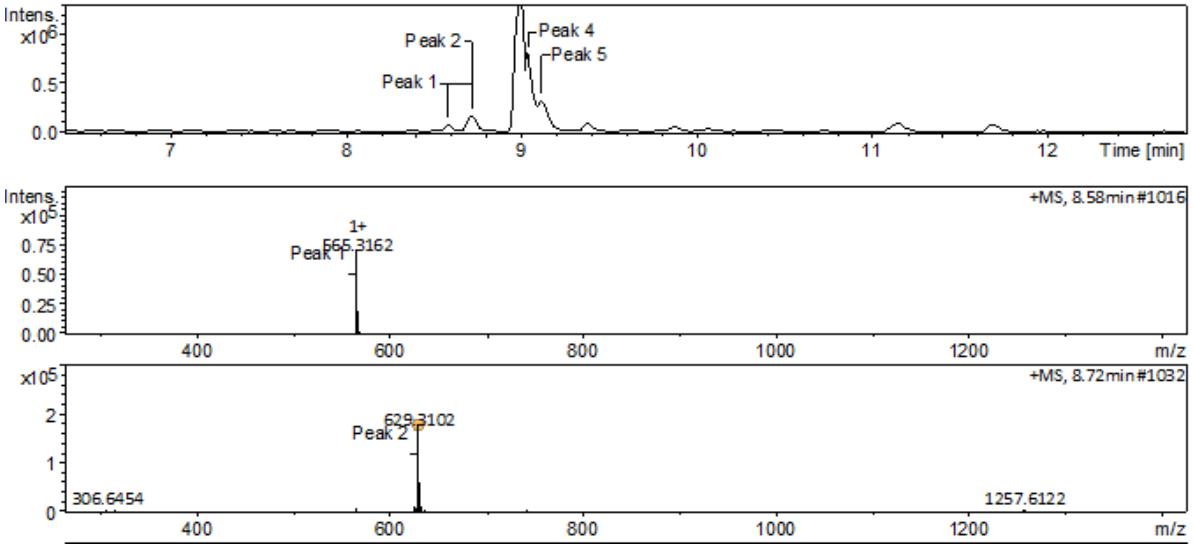


Figure 23: Molecular peaks 1-2 of the 6 amino acids which were successfully coupled during the synthesis of PS06.

Increasing coupling time to 1 hour and using OxymaPure coupling reagent can improve the coupling of tyrosine and valine, hence avoid deletion sequences. Peaks 3-5 are conformers for the 6th amino acid (Figure 24).

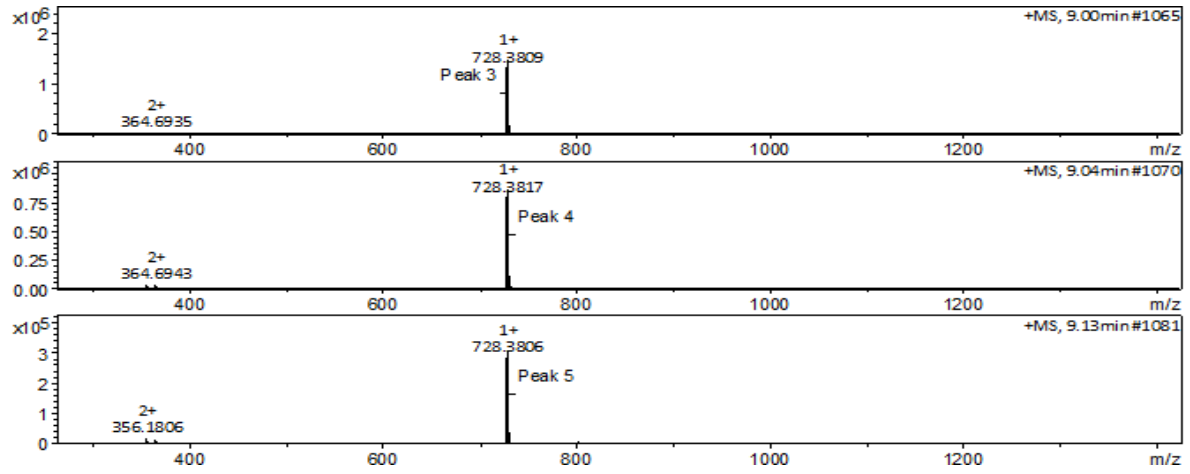


Figure 24: Molecular peaks 3-5 of the 6 amino acids which were successfully coupled during the synthesis of PS0

7th amino acid coupling

Addition of the 7th amino acid valine was incomplete and produced conformers as shown in Figure 25.

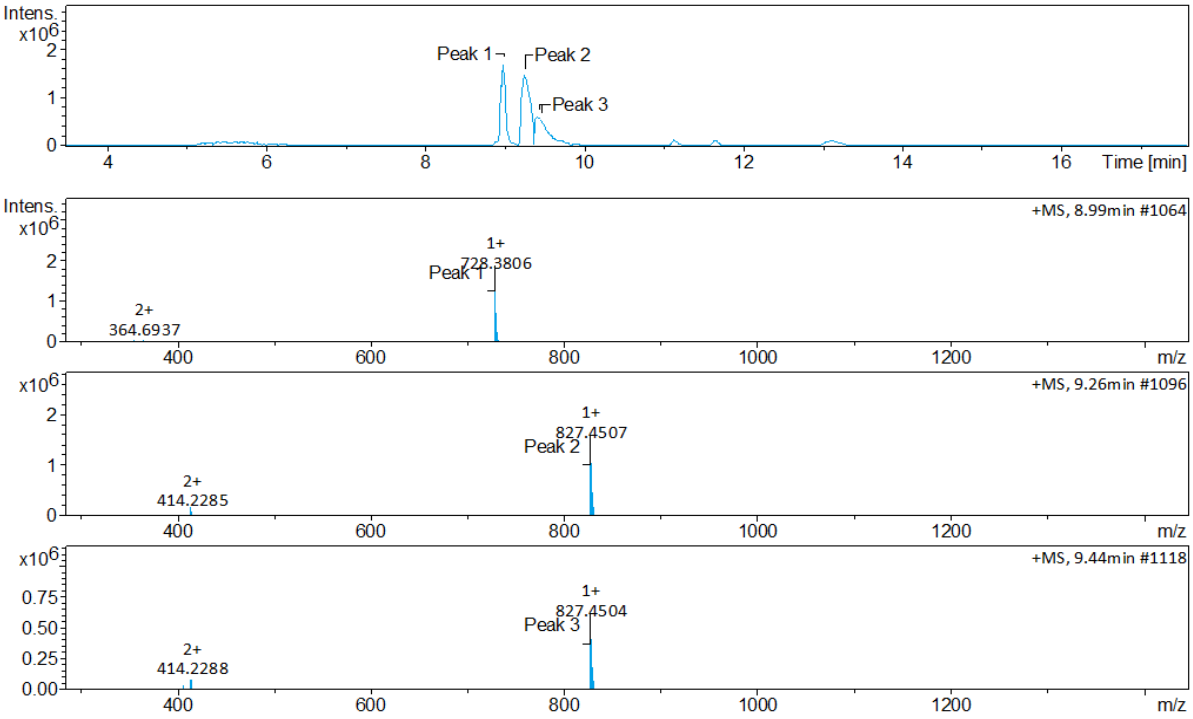


Figure 25: Molecular peaks of the 7 amino acids which were successfully coupled during the synthesis of PS06.

Peak 1 is the 6th amino acid peak (CVFVYV) which shows that coupling of valine to valine was incomplete. Peak 2 and 3 are the 7th amino acids conformers produced at retention time 9.26 and 9.44 minutes respectively. The peptide folding that is produced after the 6th amino

acid coupling might have partially locked the *N*-terminal such that coupling of the oncoming amino acid was sterically hindered.

8th amino acid coupling

Coupling the 8 amino acid was successful as shown in Figure 26 peak 4. Results for the 8th amino acid coupling revealed that deletion and incomplete coupling occurred. Peak 1 confirms the presence of 6th amino acid sequence (CVFVYV) and peak 2 showed the presence of the 7 the amino acid sequence (CVFVYVV). Peak 3 is a deletion sequence where the 7th amino acid, valine did not couple (CVFVYVL). This indicates how difficult this peptide is to couple and supports the predicted trend for difficult SPPS.[61]

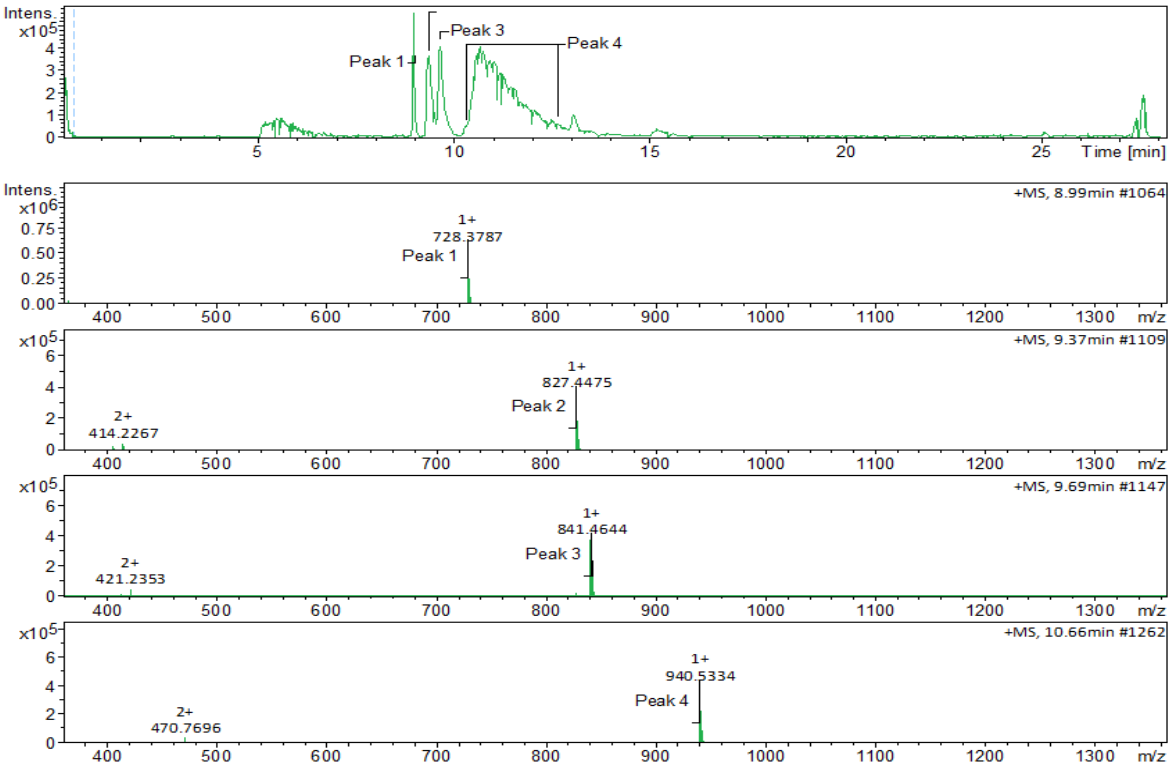


Figure 26: Molecular peaks of the 8 amino acids which were successfully coupled during the synthesis of PS06.

9th amino acid coupling

The addition of the 9th amino acid was successful although there were deletion sequences as shown in Figure 27. All peaks observed after coupling the 8th amino acid were also observed after coupling the 9th amino acid. This indicated incomplete coupling of the 9 the amino acid as peak 5 represents the 8th amino acid. Another deletion sequence (CVFVYVVV), peak 4 was also observed as a result of omission of leucine showing that coupling of the 8th amino acid was incomplete. Formation of β- sheets due to consecutive valine amino acid might have hindered coupling of leucine.[116,117]

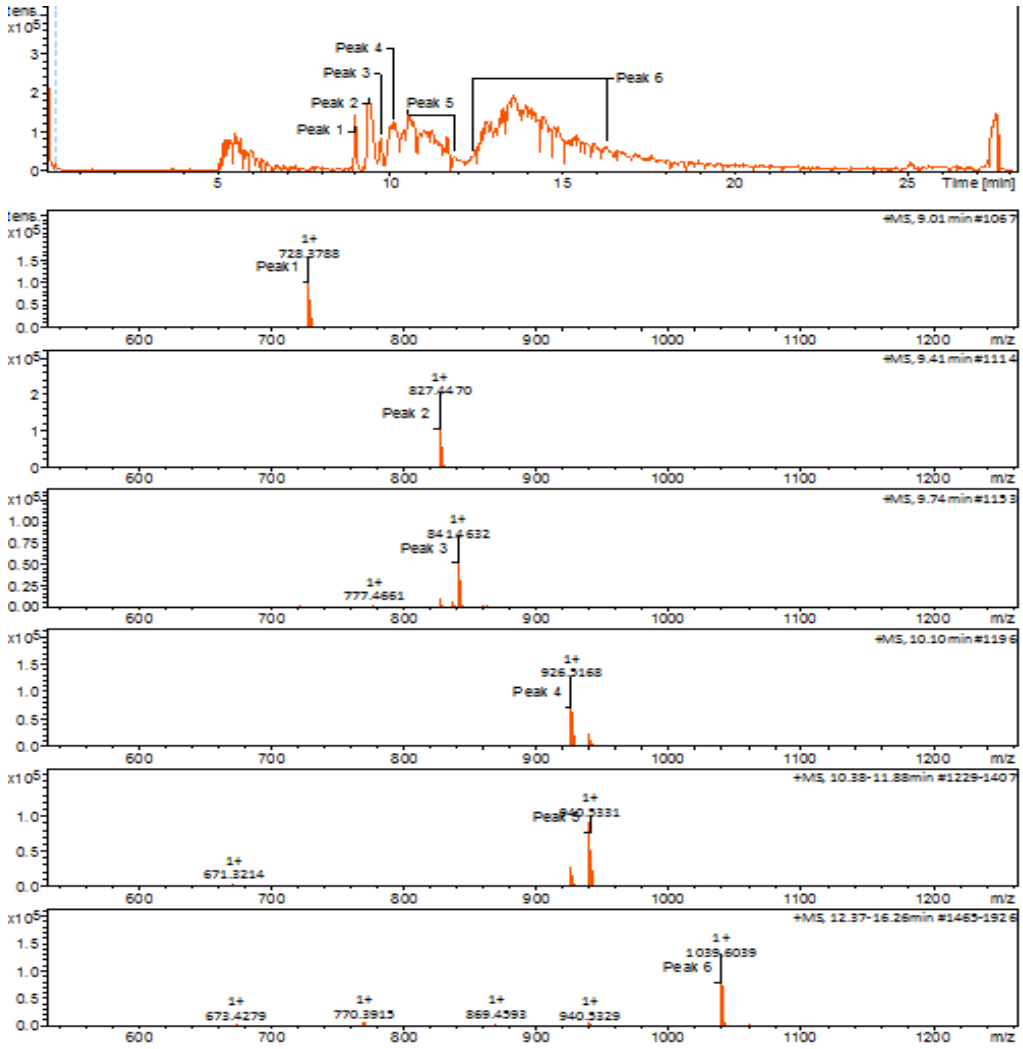


Figure 27: Molecular peaks of the 9 amino acids which were successfully coupled during the synthesis of PS06.

Tailing was observed particularly for the 8th amino acid peak from 10 to 14 minutes. As the chain grew, so was the deletion peptide. As the hydrophobic character increases so was the retention time as can be seen from the 6th amino acid to the 9th amino acid in Table 7. The eight peptide chain peak tailed for about 2 min which can be a result of its strong interaction with stationary phase.

Table 7: PS06 LC-MS masses found for particular coupling.

Amino acid no.	Sequence	Calculated Mass	Mass found	R_t
6	**V**YVFVC	$C_{36}H_{52}N_7O_7S$ 727.3727	728.3809 $[M+H]^+$ 728.3817 $[M+H]^+$ 728.3806 $[M+H]^+$	9.00 9.04 9.13
7	**V**VYVFVC	$C_{41}H_{62}N_8O_8S$ 826.4411	827.4507$[M+H]^+$ 827.4504$[M+H]^+$	9.26 9.44
8	**L**VVYVFVC	$C_{47}H_{73}N_9O_9S$ 939.5252	940.5334$[M+H]^+$	10.70
9	**V**LVVYVFVC	$C_{52}H_{82}N_{10}O_{10}S$ 1038.5936	1039.6039$[M+H]^+$	13.60
15	**V**VICTTVLVVYVF VC (cyclic)	$C_{79}H_{128}N_{16}O_{18}S_2$ 1652.9034	1653.7400$[M+H]^+$ 1653.7390$[M+H]^+$	

PS06 was successfully synthesized although it had many fragments shown from the chromatogram (Figure 28). Two cyclic PS06 conformers were observed at 9.32 minutes and 9.55 minutes.

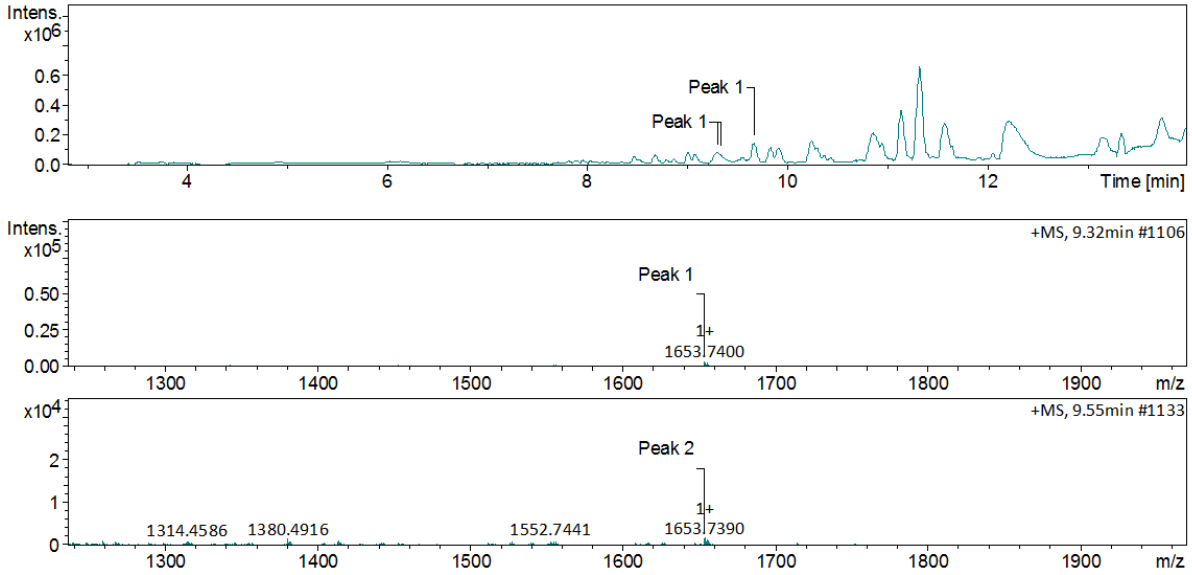


Figure 28: Molecular peaks of the 15 amino acids which were successfully coupled during the synthesis of PS06.

The separation was challenging. Firstly it could not be dissolved in bio assay friendly solvents but only in 100% DMSO. This was going to pose some further problems for a potential clinic trial. This was anticipated due to its hydrophobic nature because of being comprised of many non-polar amino acids. Different combinations of solvents were tried and still would not dissolve the peptide. These include water, acetonitrile, methanol, Isopropanol. In some cases when attempting to dilute DMSO with other solvents, the peptide could immediately crush out of solution. This posed a serious challenge especially in purifying the peptide as the solvents which are compatible with prep-HPLC columns caused the sample to immediately crush out when introduced into the mobile phase.

Consequently this would block the capillaries and column and potentially cause subsequent damage of the instrument. The peptide had another drawback of aggregating when it was left in DMSO solution over a long period of time even when stored at 18 degrees. Efforts to dissolve it again in DMSO were fruitless as the jelly peptide could not dissolve even when heated to 50 degrees. This is a common problem with peptide drugs.[85] This further demanded us to find other modification that could be done to improve the solubility properties of the analogues without compromising the activity.

2.4.3 Lassomycin residue

Lassomycin is active against *M.tb as* described in Chapter 1. One of the interesting features of lassomycin is its basic residual chain (RRNI) which comprised of arginine groups that follow each other. This makes it more basic and ease to dissolve in biologically friendly solvents for a biological test. It was also reported that the arginine groups are essential for activity of lassomycin by forming hydrogen interactions with the *N*-terminus of ClpC1 particularly the Gln17 residue of the receptor.[46] Hence adding this residue to the ecumicin sequence could possibly improve both the activity of ecumicin and its solubility.

However, this attempt did not work out as the derivative PS07 could not be successfully synthesized (Figure 29). We rationalized that the arginine groups that were following each other might not have coupled successfully. To solve the problem, we decided to remove one arginine group from the four peptide residue.

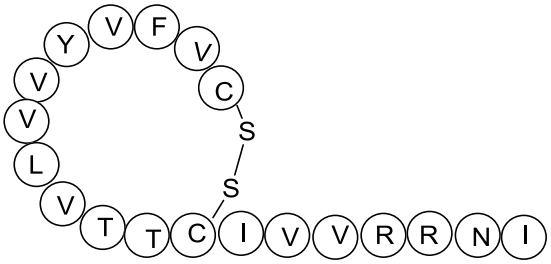


Figure 29: PS07 amino acid sequence.

2.4.3.1 Synthesis of PS09 by manual SPPS using HATU as the coupling reagent

Figure 30 shows PS09 derivative with 1 arginine group instead of 2. However, the synthesis of this derivative was unsuccessful.

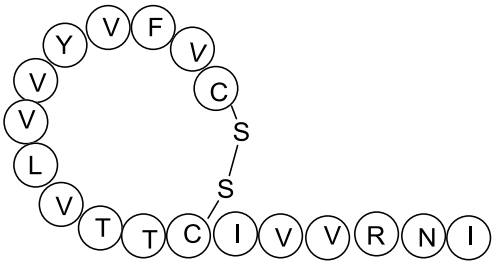


Figure 30: PS09 amino acid sequence.

2.4.3.2 Synthesis of PS09 by manual SPPS using HATU as the coupling reagent

Figure 31 shows the peptide sequence for PS10.

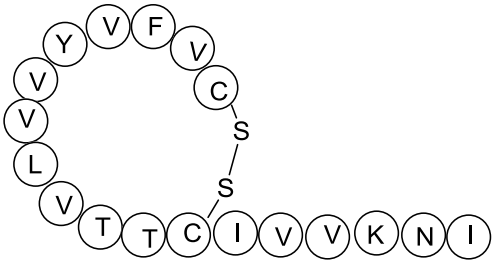


Figure 31: PS10 amino acid sequence.

Arginine pKa is 12.48 and is more basic than lysine which has a pKa of 10.79. However, lysine is ease to couple and ease to remove side chain protecting group compared to arginine. Hence substituting arginine with lysine would slightly lower the basicity of the peptide but improving synthesis. PS10 is one of these derivatives where arginine was substituted with lysine. However, this peptide could not be successfully synthesized.

2.5 Conclusion

Ecumicin derivative PS01 was successfully synthesized when OxymaPure was used although it had many fragments which made purification difficult. HATU was not effective especially for the last two amino acids. Replacing tryptophan with tyrosine improved yield and reduced side reactions. However, synthesis of lassomcyin arginine containing residues was unsuccessful. Thus we replaced isoleucine, leucine and valine with cationic lysine in the next Chapters.

CHAPTER 3: Ecumicin cationic derivatives

This Chapter describes ecumicin derivatives where hydrophobic amino acids, isoleucine, leucine and valine are substituted with cationic amino acids. As described in Chapter 1 (section 1.5), cationic amino acids improve peptide permeability, solubility and possibly binding affinity, we decided to substitute some of the aforementioned hydrophobic amino acids with cationic lysine in the sequence of the peptide to afford various derivatives.

3.1 Synthesis of PS08 by manual SPPS using HATU as the coupling reagent

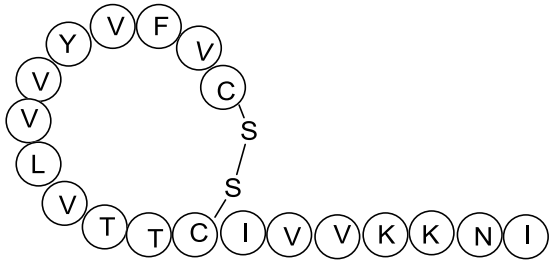


Figure 32: PS08 amino acid sequence.

As reported in Chapter 2 PS07, PS09 and PS10 were not successfully synthesized even though the peptides consisted of cationic amino acids, but PS08 (Figure 32) was successfully synthesized as shown in (Figure 33). The calculated or expected UHPLC-HRMS (ESI^+) *m/z* mass for PS08 $C_{101}H_{169}N_{23}O_{23}S_2$ is 2136.2203, and the found mass was 1069.6078$[M+2H]^{2+}$.

A gradient elution method employing water and acetonitrile in 18 minutes was used in the UHPLC, buffer A, 0.1% formic acid in H_2O; buffer B, 0.1 formic acid in CH_3CN and the column temperature was set to 20 °C. Acetonitrile was allowed to increase from 5% to 95% in 18 minutes.

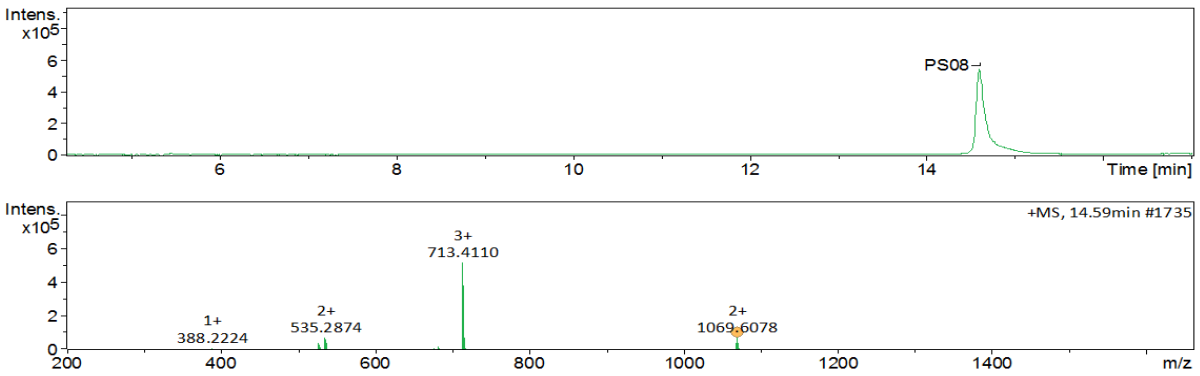


Figure 33: Molecular peak of the 19 amino acids which were successfully coupled during the synthesis of PS08

This derivative was successfully synthesized manually using double coupling method of 40 minutes per coupling cycle and HATU as the coupling reagent. The derivative dissolved only in 100% DMSO and no combinations of solvent could dissolve it. When dissolved in DMSO, upon addition of few drops of either of acetonitrile, methanol, isopropanol or water, the peptide precipitated immediately.

Despite the success in synthesis, its crude yield was very low, 2.4%. There were many challenges in synthesizing PS08 as unwanted side reactions were observed. One of the reasons that catalyzed low yield was the difficulty in dissolving and purifying the peptide. It was only dissolved in 100% DMSO as other solvent combination could not dissolve it. This could suggest that the addition of lysine groups insignificantly improved the peptide solubility. Being soluble in DMSO only posed problems during purification as the peptide had high chances of crushing out when separating using water-acetonitrile as solvents. Consequently, separation was associated with capillary blockages and pressure built ups. This also could have resulted in sample loss. Hence more lysine groups were added to improve peptide solubility as observed with cationic peptides such as the "KLAKLAK".[118,119] We anticipated that the lysine groups will bind to the acid region of the C-terminus of the protease.

KLAKLAK

The AMP sequence 'KLAKLAK' has been widely used in the synthesis of various active novel drugs against cancer cells.[118-120] It is an antibacterial agent which is effective and is less toxic.[121] The D- derivative of $(KLAKLAK)_2$ showed selective cytotoxicity towards gram positive and negative bacteria and not mammalian cell types. The peptide's poly cationic nature results in its selectivity which facilitates cell translocation across the negatively charged bacterial membrane and limited permeability across the zwitterionic lipid bilayer of mammalian cell types.[122] The derivatives overall effects and facilitates lipid bilayer disruption resulting in membrane potential dissipation and bacterial death.[121] Lysine-leucine-rich α-helix amphipathic peptide amphiphile (PA) micelles have been reported to have disrupted the membranes of human breast cancer cells causing cell death.[123]

3.2 Synthesis of PS15-PS18 by manual SPPS using HATU as the coupling reagent

Having observed from either PS06 or PS08's 8th amino acid (Figure 26 Chapter 2 above) that fragmentation and unwanted peaks intensified, we decided to substitute certain amino acids of interest with other amino acids that could possibly provide better desired properties. We

concluded that coupling of leucine (L) to valine was not highly favorable and produces side reactions based in Figure 26 in Chapter 2. This challenge might be due to peptide aggregation or folding during synthesis especially for hydrophobic sequences which causes slow or incomplete deprotection and incomplete coupling as observed for valine-leucine coupling in PS06 and PS08.[112] This aggregation is mostly observed from the 5th or 6th amino acid to the 21st amino acid.[113]

Aggregation is among the chief contributors that causes some peptide and protein sequences to be difficulties to synthesis.[112] Peptide and protein aggregation is mainly caused by the formation of parallel β-sheets through intermolecular hydrogen bonding between polypeptides strands as shown in Figure 34 below.[116,117] A series of glutamine, isoleucine, leucine, phenylalanine, threonine, tyrosine or valine can cause β-sheets, which cause incomplete solvation during peptide synthesis resulting in deletions.[124] Studies have shown that the probabilities of valine and leucine to form β-sheets is greater than alanine which is in turn greater than glycine (V, L > A > G).[19]

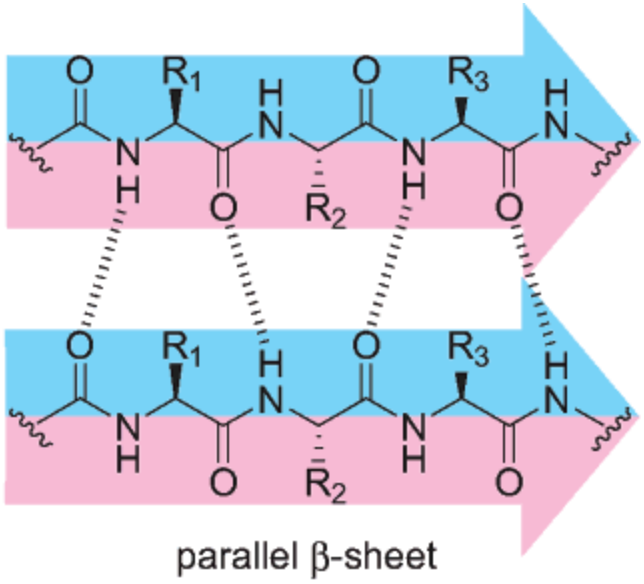


Figure 34: Parallel β-sheet in peptides and proteins.[116,117]

Another contributor to peptide aggregation is the edge to edge dimerization of β-sheets strands of the peptide.[19,125] Studies of artificial β-sheets that dimerizes with valine and threonine side chains showed substantial preference for T-T and V-V pairing over T-V pairing as shown in Figure 35. Dimerization is preferred among the hydrophobic amino acids valine, leucine, alanine and isoleucine hence it is sequence selective.[19]

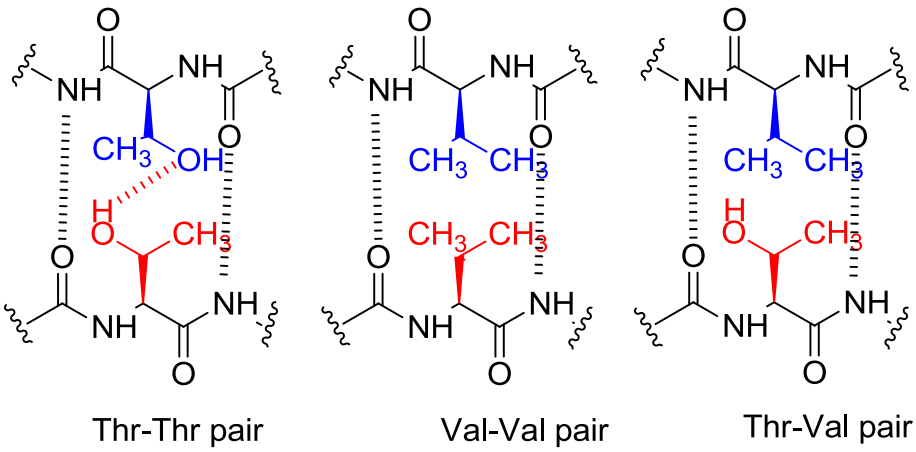


Figure 35: Interactions among Valine and Threonine pairing β-sheets.[19]

The studies of dimerization were done for antiparallel artificial β-sheets. This could suggest why coupling leucine to valine was associated with a lot of side reactions. The 6th and 7th valine amino acids coupled together before leucine could have possibly formed these β-sheets and consequently resulted in incomplete solvation and deletion. To minimize or break the β-sheets, it is recommended to substitute asparagine for glutamine or serine for threonine, adding a proline or glycine every third amino acid or shifting the sequence.[124]

A polar amino acid, lysine was used to replace leucine. Lysine was used mainly to improve the cationic properties of the peptides and consequently its solubility in solvents and improving the peptides' cell membrane permeability (PS15 and PS16, Figure 36).[28,34,35]

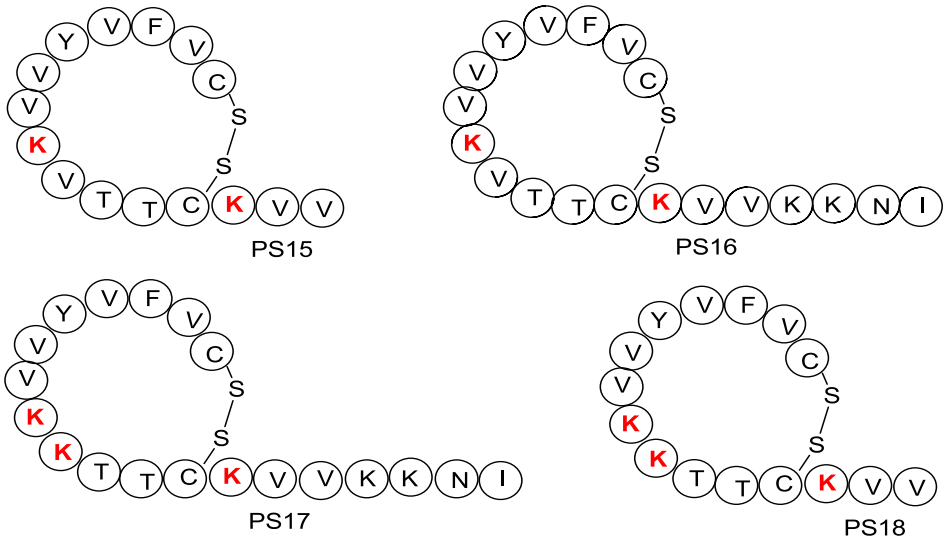


Figure 36: Lysine cationic derivatives

On the other two derivatives, two lysine groups were added following each other replacing leucine, valine and also isoleucine as shown (PS017 and PS018, Figure 36). Other than improving solubility, we anticipated that lysine will increase the activity, ease of synthesis and yield.

These peptides were manually synthesized on rink amide resin using HATU/DIPEA double coupling method of 30 minutes per coupling cycle. Synthesis conditions are summarized in Table 8.

Table 8: Summary of peptide synthesis conditions

Coupling reagent	Resin	Coupling time(min)	Deprotection/ time (min)	Cyclization	Cleavage mixture
HATU(0.19M) & 6ml DIPEA (1.0M)	Rink amide HMBA (750.0mg)	30 per coupling (double)	12ml (20% piperidine in DMF, (5min×2	10equiv of $I_{2(s)}$ to AA loading capacity in 15ml (1:4, H_2O:DMF) for 3hrs	10ml (94:2.5:2.5:1, TFA:EDT:H_2O: TIS) for 2hrs

Cold diethyl ether was used to wash the peptide and precipitate it out of the cleavage solution and soluble by-products. There was a great improvement in terms of solubility of these peptides. A small amount of peptide that was cleaved after the final coupling and was dissolved in 1:1(water: acetonitrile). However, purifying the whole peptide with this solvent ratio proved difficult as the peptide crushed out of solution. Large volumes were required to dissolve the peptide which was impractical when separating the peptide using prep-HPLC. The optimum ratio was found to be the 2:3 (ACN: DMSO) as a solvent.

3.3 PS15 and PS16 results and discussion

PS15 was successfully synthesized and the results showed cyclized and uncyclized peptides. The cyclic calculated or expected HRMS (ESI^+) *m/z* mass for PS15 $C_{79}H_{130}N_{18}O_{18}S_2$ is 1682.9252, and found mass was 841.8746 $[M]^{2+}$ at t_{R1} 8.78 minutes and uncyclic calculated or expected HRMS (ESI^+) *m/z* mass for PS15 $C_{79}H_{132}N_{18}O_{18}S_2$ is 1684.9408, and found mass was 843.4248 $[M]^{2+}$ t_{R2} 8.99 minutes. HRMS-LC data is shown on Figure 37.

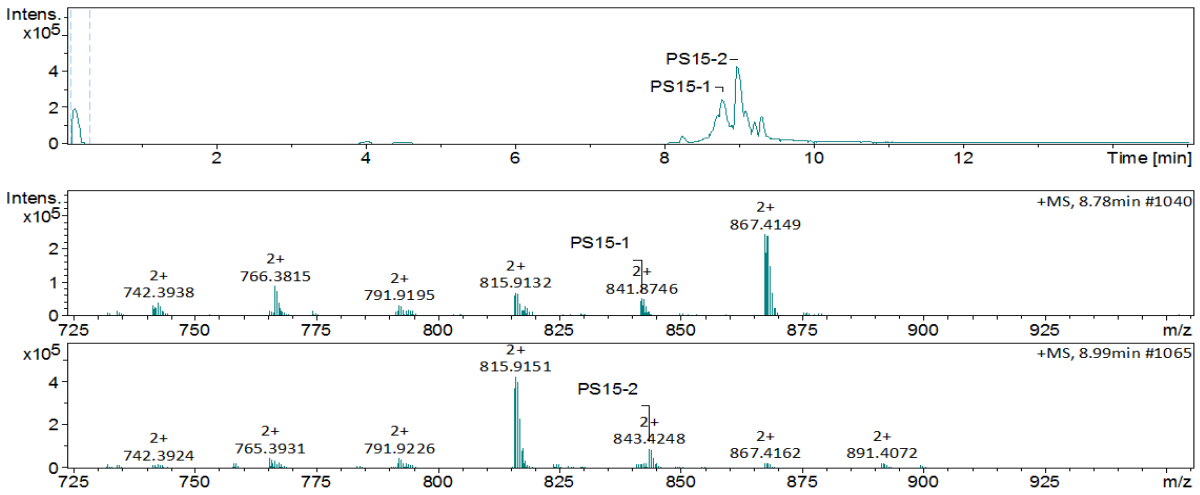


Figure 37: PS15 LC-MS Spectrum.

Gradient elution method employing, water and acetonitrile in 10 minutes was used in the UHPLC, buffer A, 0.1% formic acid in H_2O; buffer B, 0.1 formic acid in CH_3CN and the column temperature was set to 20 °C. Acetonitrile was allowed to increase from 5% to 70% in 10 minutes.

The peptides were not separated both from each other and from the impurities even after a series of attempts. The retention time for the cyclized and uncyclized peptide was from 8.01 minutes to 8.59 minutes respectively and the crude yield was 12.48%.

Purified PS16 showed the peak at 7.57 minutes (Figure 38). The calculated or expected HRMS (ESI^+) *m/z* mass for PS16, $C_{101}H_{171}N_{25}O_{23}S_2$ is 2166.2421, and found mass was 1084.0834 $[M+2H]^{2+}$ at t_{R1} 7.57 minutes.

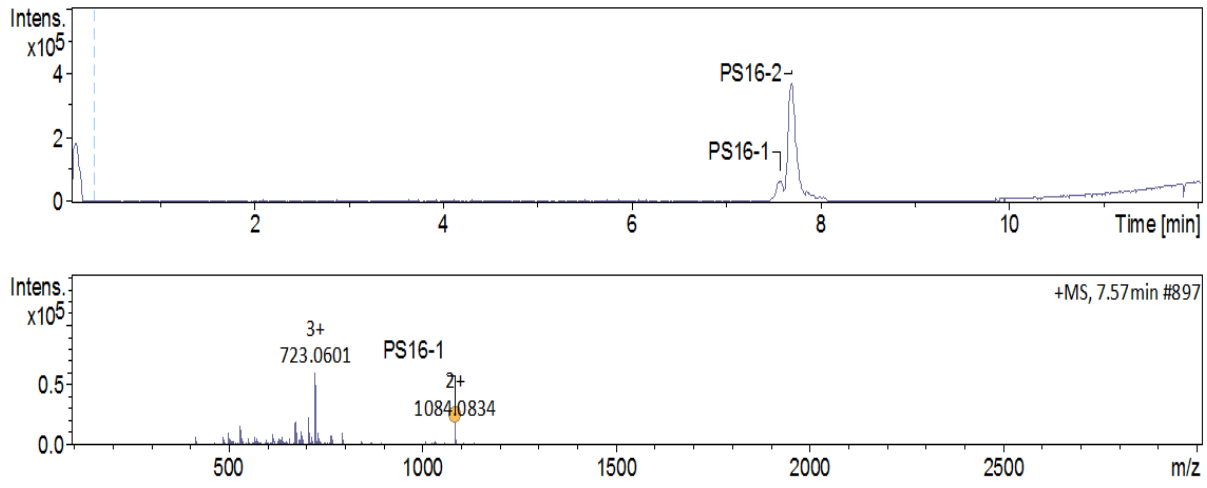


Figure 38: PS16 LC-MS Spectrum.

A gradient elution method employing water and acetonitrile in 10 minutes was used in the UHPLC, buffer A, 0.1% formic acid in H_2O; buffer B, 0.1 formic acid in CH_3CN and the column temperature was set to 20 °C. Acetonitrile was allowed to increase from 5% to 95% in 10 minutes. The crude percentage yield of 25.7% was obtained.

3.4 PS17 and PS18 results and discussion

PSI7 and PS18 were both successfully synthesized. The calculated or expected HRMS (ESI^+) *m/z* mass for PS17, $C_{102}H_{174}N_{26}O_{23}S_2$ is 2195.2687, and found mass was 1099.1447 $[M+2H]^{2+}$ at t_R5.50 minutes. Figure 39 shows the UHPLC-HRMS data observed. A gradient elution method employing water and acetonitrile in 9 minutes was used in the UHPLC, buffer A, 0.1% formic acid in H_2O; buffer B, 0.1 formic acid in CH_3CN and the column temperature was set to 20 °C. Acetonitrile was allowed to increase from 15% to 95% in 9 minutes. The crude percentage yield of 5.7% was obtained.

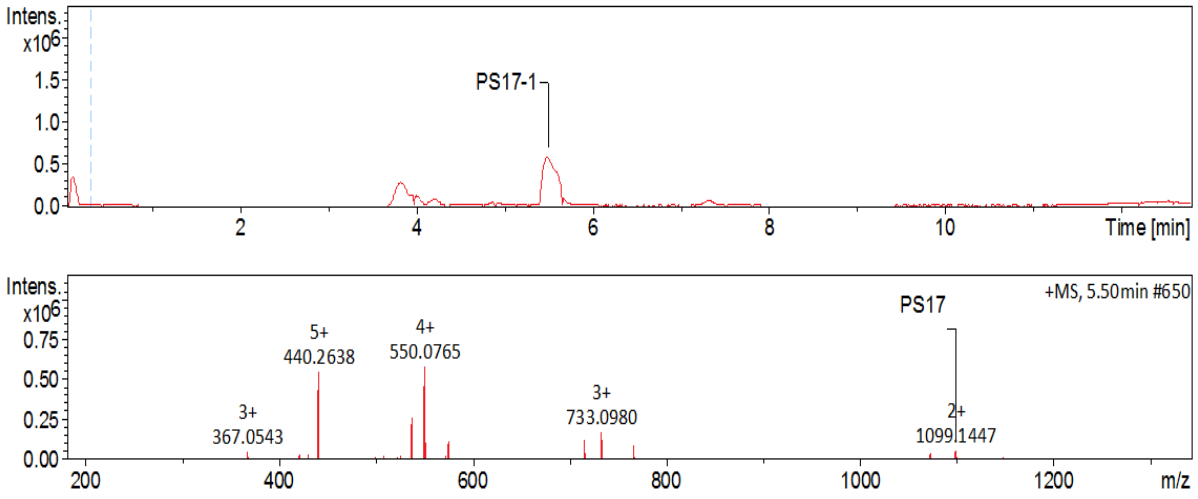


Figure 39: PS17 LC-MS Spectrum.

The calculated or expected HRMS (ESI^+) *m/z* mass for PS18, $C_{80}H_{133}N_{19}O_{18}S_2$ is 1711.9517, and found mass was 857.8445 $[M+2H]^{2+}$ at t_R7.61 minutes Figure 40 shows the UHPLC-HRMS data observed.

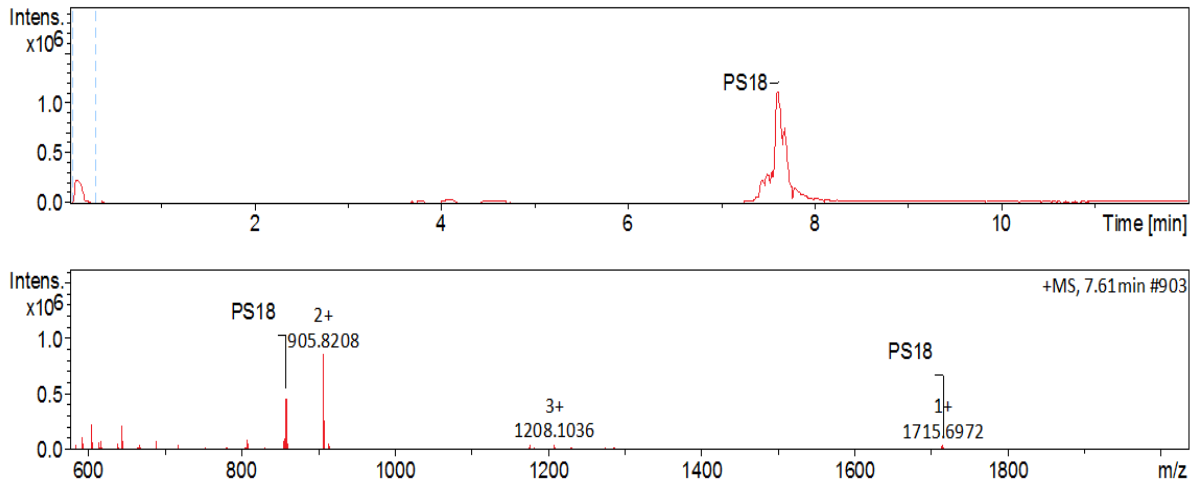


Figure 40: PS18 LC-MS Spectrum.

A gradient elution method employing water and acetonitrile in 10 minutes was used in the UHPLC, buffer A, 0.1% formic acid in H_2O; buffer B, 0.1 formic acid in CH_3CN and the column temperature was set to 20 °C. Acetonitrile was allowed to increase from 5% to 95% in 10 minutes. The crude percentage yield of 6.05% was obtained.

The Table 9 below shows the data summary for the synthesized peptides.

Table 9: LCMS masses found for data cationic peptides.

Peptide	Sequence	Calculated Mass	Mass found	R_t/min	Crude yield/ %
08	INKKVVICTTVLVVYVFVC	$C_{101}H_{169}N_{23}O_{23}S_2$ 2136.2203	1069.6083$[M+2H]^{2+}$	14.60	2.46
15	VVKCTTVKVVYVFVC	$C_{79}H_{130}N_{18}O_{18}S_2$ 1682.9252 (cyclic) $C_{79}H_{132}N_{18}O_{18}S_2$ 1684.9408(uncyclic)	841.6746 $[M+2H]^{2+}$ 843.4248 $[M+2H]^{2+}$	8.78 8.99	12.48
16	INKKVVKCTTVKVVYVFVC	$C_{101}H_{171}N_{25}O_{23}S_2$ 2166.2421	1084.0834 $[M+2H]^{2+}$	7.57	25.07
17	INKKVVKCT	$C_{102}H_{174}N_{26}O_{23}S_2$	1099.1447$[M+2H]^{2+}$	5.50	5.75

	TVKKVYVFVC	2195.2687			
18	VVKCTTVKKVYVFVC	$C_{80}H_{133}N_{19}O_{18}S_2$ 1711.9517	1715.6972 $[M+4H]^+$	7.61	6.05

3.5 Conclusion

Cationic lysine improved the synthesis of the derivatives. However, more work needs to be done to improve purification and synthetic procedures as the yields were low. With this in mind, we decided to incorporate *N*-methylated amino acids and peptoids to the derivatives.

CHAPTER 4: *N*-Methylated peptides and Peptoid

4.1 Synthesis of *N*-methylated peptides

The incorporation of *N*- methylated amino acids and peptoids into peptide sequences modifies the peptide backbone, reduces the peptide's hydrophobicity and increases stability to enzymatic degradation.[88,126] Consequently improving the solubility and the half-life of the peptide.[86,95,96]

In this Chapter we discuss the synthesis of *N*- methylated peptide derivatives; PS19, PS20, PS21 and peptoid derivative PS22 shown in Figure 41.To achieve this synthesis, we adopted the same methods used for the synthesis of other peptides reported in Chapter 3 except that the coupling cycle for *N*-methylated amino acids was 1 hour instead of 30 minutes.

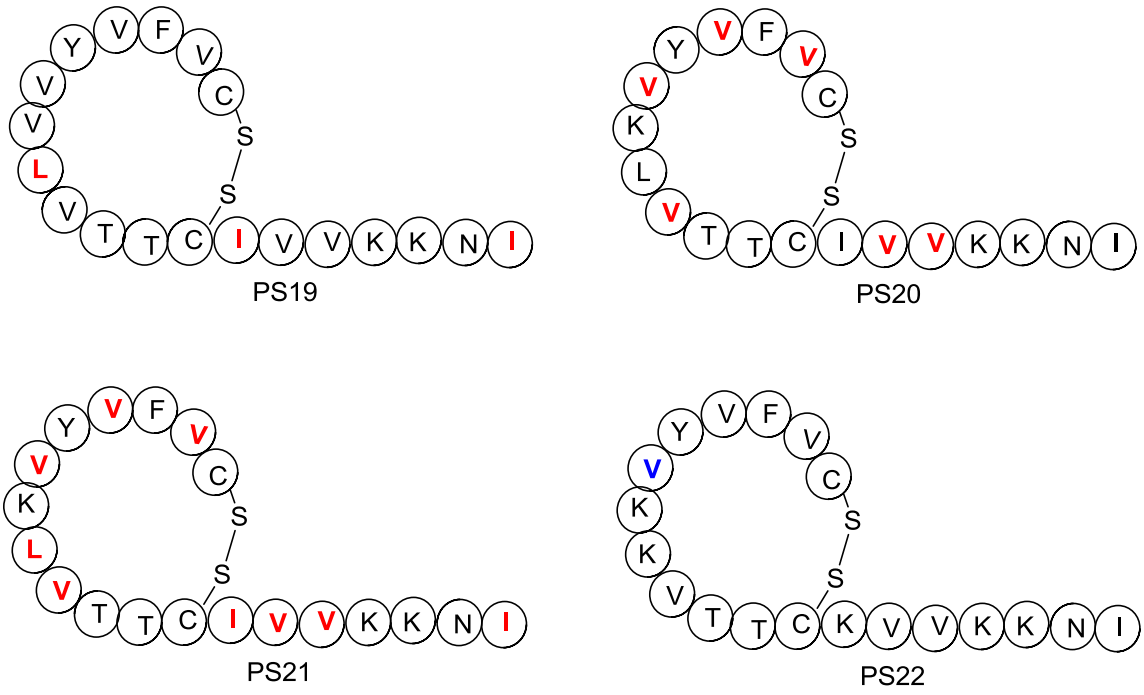


Figure 41: *N*-methylated amino acid and peptoids substituted peptide derivatives: *N*-methylated amino acid residues are in red and peptoid residue is in blue color.

PS19, PS20 and PS21 could be successfully synthesized up to the 13th, 14th, and 8th amino acid respectively. It was observed that the 13th, 14th and 8th amino acids were *N*-methylated isoleucine (*N*MI), *N*-methylated valine (*N*MV) and *N*-methylated leucine (*N*ML) for PS19, PS20 and PS21 respectively. Thus, the change in structure caused by the addition of sterically hindered *N*- methylated amino acids restricted further coupling to the chain. Generally,

coupling of sterically hindered *N*- methylated amino acids is difficult and in most cases results in epimerization and peptides that are very difficult to separate when standard coupling reagents and methods are used.[127,128] In this Chapter we outline the synthesis of various *N*-methylated peptides and Table 10 shows a summary of the LCMS results obtained from the *N*-methylated peptides mentioned above in Figure 41.

Table 10: HRMS results for PS19, PS20 and PS21 the synthesized *N*-methylated peptides.

Peptide	Sequence	Formula and calculated mass	Found mass	Retention Time (min)
PS19	INKKVVICTTVLV VYVFVC	$C_{104}H_{175}N_{23}O_{23}S_2$ 2178.2673	-	-
PS19-13 amino acids	ICTTVLVVYVFVC	$C_{71}H_{114}N_{14}O_{16}S_2$ 1482.7979	1485.7352 $[M+3H]^+$	6.05
PS20	INKKVVICTTVLK VYVFVC	$C_{108}H_{184}N_{24}O_{23}S_2$ 2249.3408	-	-
PS20-14 amino acids	VICTTVLKVYVFV C	$C_{80}H_{132}N_{16}O_{17}S_2$ 1652.9398	1653.8767 $[M+H]^+$ 1653.8757 $[M+H]^+$ 827.4414 $[M+2H]^{2+}$	4.30 4.60 7.06
	Uncyclized peptide	$C_{80}H_{134}N_{16}O_{17}S_2$ 1654.9398	1655.8909 $[M+H]^+$ 828.4485 $[M+2H]^{2+}$	7.22 7.59
PS21	INKKVVICTTVLK VYVFVC	$C_{111}H_{190}N_{24}O_{23}S_2$ 2291.3877	-	-
PS21-8 amino acids	LKVYVFVC	$C_{52}H_{84}N_{10}O_9S_2$ 1024.6143	1025.6215 $[M+H]^+$	-

Red: *N*-methylated amino acid

4.1.1 PS19 results and discussion

(*N*MI) and (*N*ML) were used to substitute isoleucine and leucine respectively in PS19 with the intention to understand their effects on the peptide's activity, solubility and enzymatic stability. (*N*ML) was coupled on the 8th amino acid position whilst (*N*MI) was coupled on the 13th and 19th amino acid position as shown in Figure 41.

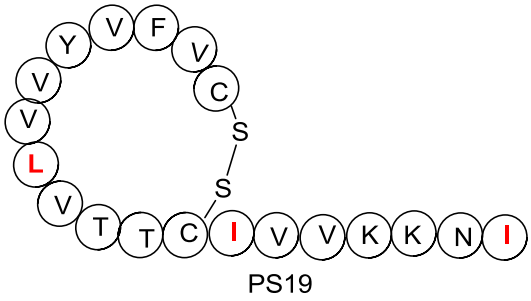


Figure 42: PS19 structure.

Coupling proceeded without any deletion sequence(s) from the second amino acid to the 6th amino. After coupling the 7th amino acid (valine), we observed peak 1 and peak 2 as shown in Figure 43. Peak 1 corresponds to the first 6 amino acid (CVFVYV) while peak 2 showed successful coupling of the 7th amino acid. This implied that valine coupling was incomplete.

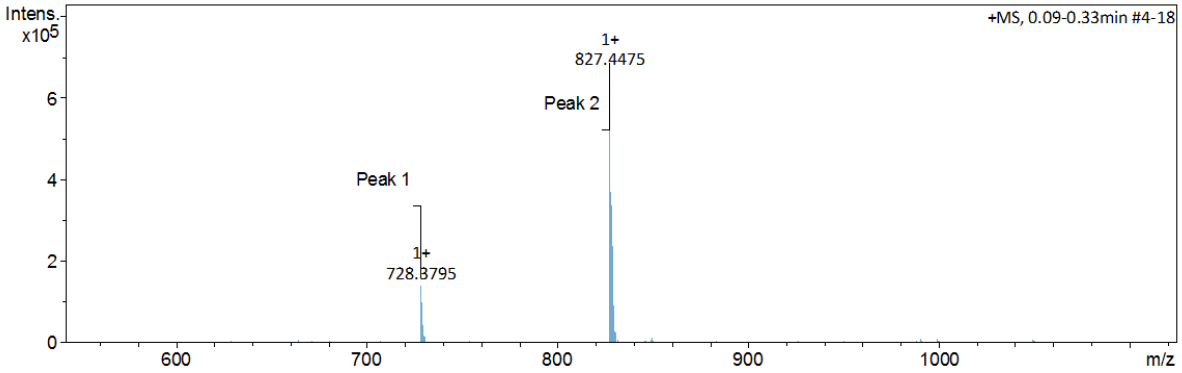


Figure 43: PS19-7 amino acid sequence MS results.

Incomplete coupling could suggest that the addition of the 7th amino acid, valine was difficult. Hydrophobic amino acids following each other have a tendency to aggregate and prevent coupling of the oncoming amino acid. Hence increasing coupling time and triple couple could improve coupling.

8th amino acid coupling

Coupling (*N*ML) was successful as shown in Figure 44 peak 2 although a deletion sequence peak 1 was formed. The deletion sequence (CVFVYV**L**) was formed as a result of coupling (*N*ML) to (CVFVYV), a sequence that was observed when the 7th amino acid (valine) was incompletely coupled.

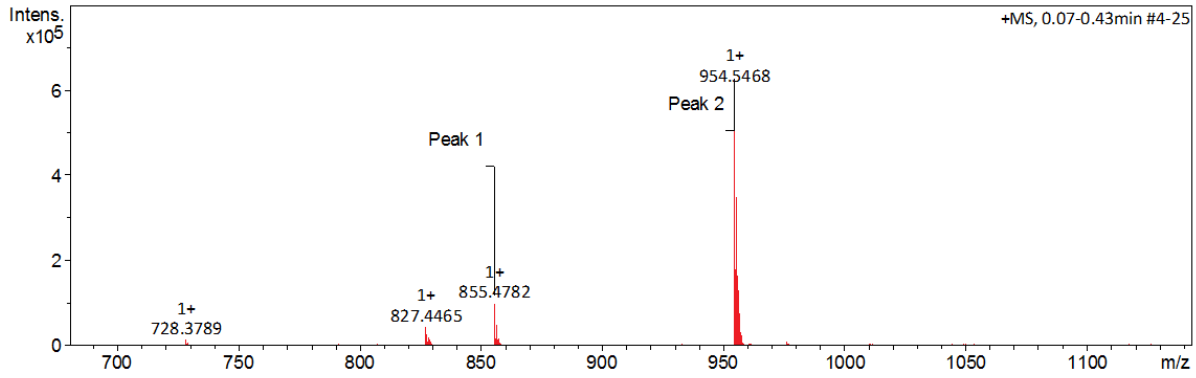


Figure 44: PS19-8 amino acid sequence MS results.

9th amino acid coupling

Coupling the 9th amino acid, (valine) was successful as shown in peak 2 Figure 45. A new deletion sequences (CVFVYVVV) shown as peak 1 (Figure 45) was formed implying an omission of (*N*ML). The presence of peak 1 showed that there was incomplete coupling of (*N*ML) despite the fact that coupling was done twice at 1 hour per each cycle.

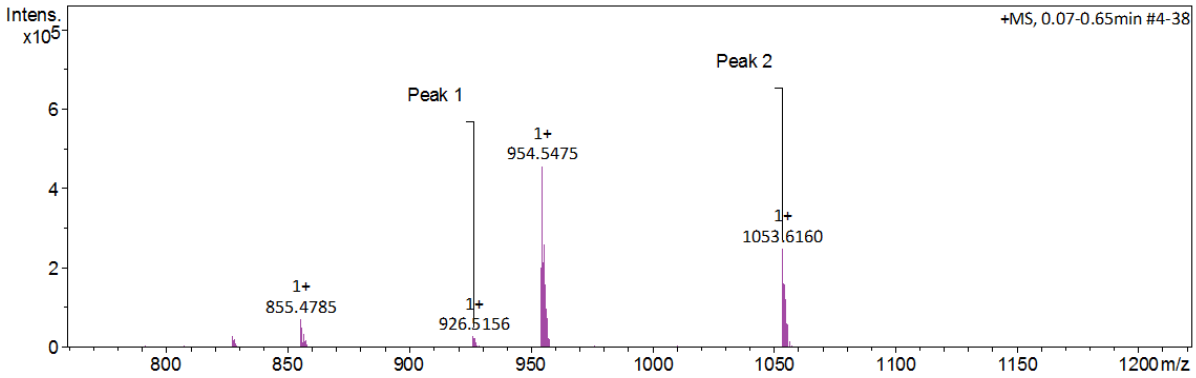


Figure 45: PS19-9 amino acid sequence MS results.

(*N*ML) was sterically hindered because of the presence of the methyl group on the nitrogen atom which prevents coupling especially when a bulky coupling reagent like HATU is used. Coupling to hydrophobic sequence that has high propensity to form β-sheets could have further prevented coupling of (*N*ML) especially when there are valine amino acids following each other. Hence to improve coupling of (*N*ML) to valine, less bulky coupling reagents such as Diisopropylcarbodiimide (DIC) and OxymaPure and COMU could be used. Furthermore using microwave assisted coupling could also help in synthesizing such difficult sequences.

10th amino acid coupling

The 10th amino acid was coupled successfully and was associated with several deletion chains. Figure 46 shows peaks 1-3 corresponding to deletion sequences and peak 4 corresponds to the 10th amino acid chain.

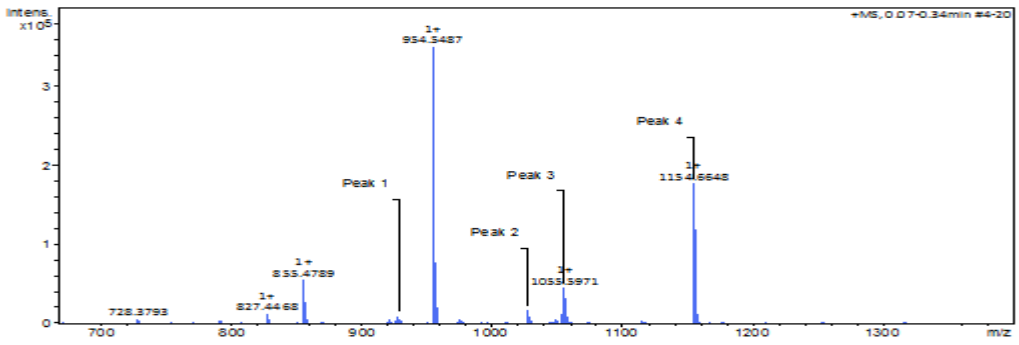


Figure 46: PS19-10 amino acid sequence MS results.

Peak 1 with identified sequence, CVFVYVVT revealed that threonine was coupled to the 7th amino acid sequence. This could suggest the extent at which aggregation inhibits solvation that facilitate coupling such that even after coupling 3 amino acids, the sequence was incompletely consumed. Peak 2 with sequence (CVFVYVVVT) was a growing deletion sequence that was observed after coupling the 9th amino acid where (*N*ML) did not couple. Peak 3 with sequence (CVFVYVVLT) showed incomplete coupling of valine amino acid, the 9th amino acid. From this observation we suggested that valine a hydrophobic amino acid could have been sterically hindered to couple to another hydrophobic (*N*ML).

11th amino acid coupling

As the chain grew, new deletion sequences were formed mainly due to incomplete coupling. This was also observed when the 11th amino acid (threonine) was coupled resulting in sequences (CVFVYVVLTT) and (CVFVYVVVTT) which corresponds to peak 1 and peak 2 respectively shown in Figure 47. Peak 3 represent the desired 11th sequence.

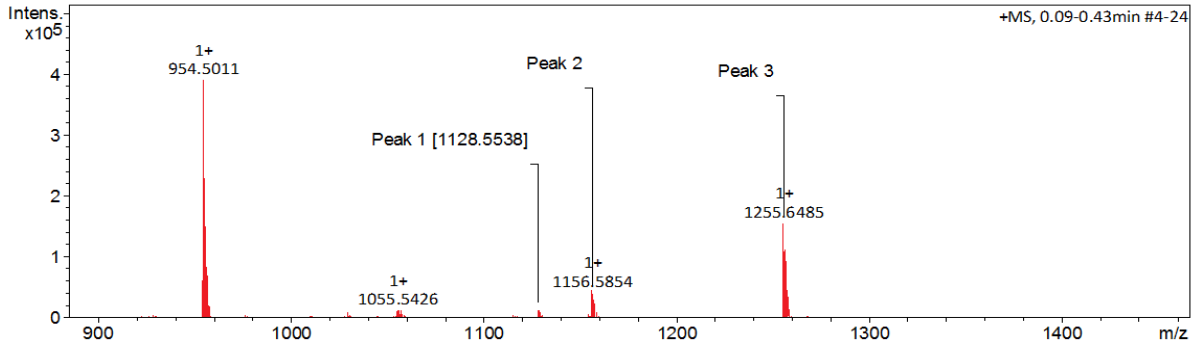


Figure 47: PS19-11 amino acid sequence MS results.

12th amino acid coupling

Coupling the 12th amino acid (cysteine) resulted in another new deletion sequence (CVFVYYVVLC)**,** peak 1 (Figure 48). Peak 2 shows successful coupling of cysteine. This observation confirms that for this particular sequence, it is difficult to couple cysteine to *N*ML because the sequence (CVFVYYVVL) was still present after addition of three more amino acids.

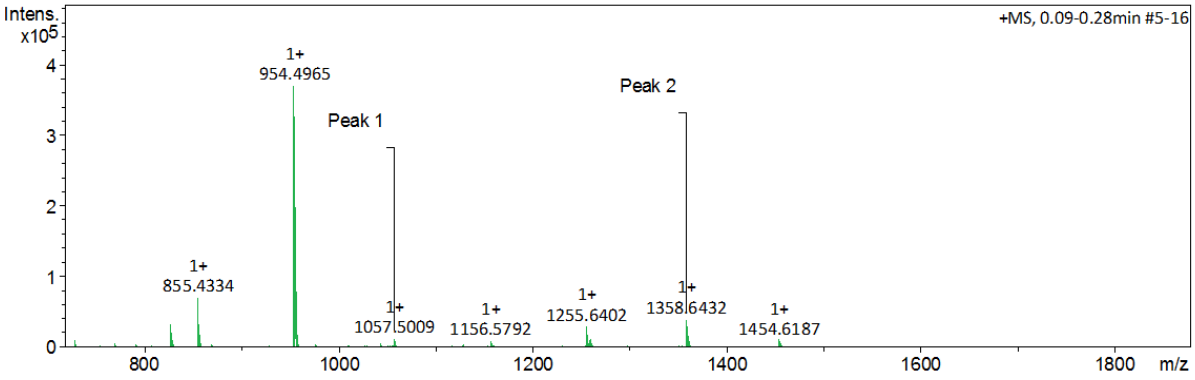


Figure 48: PS19-12 amino acid sequence MS results.

13th amino acid coupling

Coupling the 13th amino acid was a success. However, 3 deletion sequences were formed represented by peaks 1-3 (Figure 49). These sequences are (CVFVYYVVLI)**,** (CVFVYYVVLCI), and CVFVYYVVLTTI respectively.

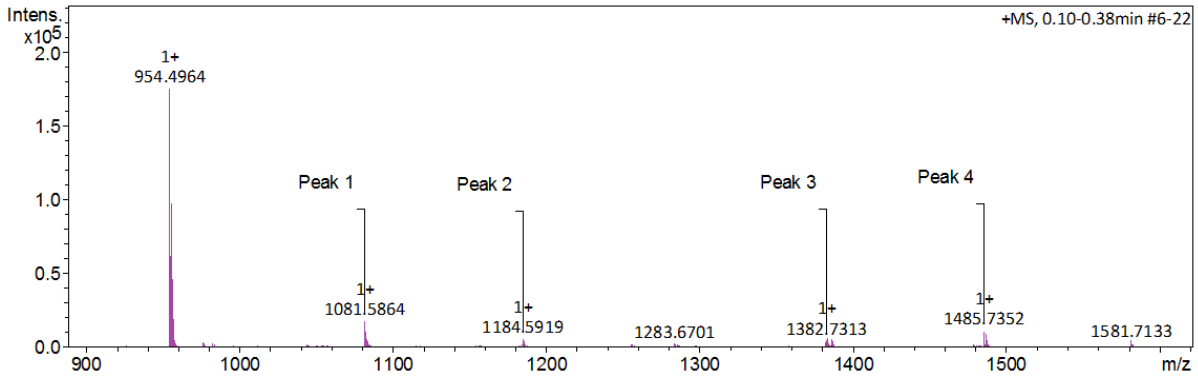


Figure 49: PS19-13 amino acid sequence MS results.

Peak 1, (CVFVYYVVLI) showed that the 8th amino acid sequence (CVFVYYVVL) was still present to couple with the 13th amino acid. Peak 2 and peak 3 with sequences (CVFVYYVVLCI) and CVFVYYVVLTTI) respectively were growing chains of deletion sequences observed from the 12th amino acid coupling Figure 48. Peak 4 is the desired 13th amino acid sequence (CVFVYYVVLTTCI). Further coupling of subsequent amino acid showed that the peptide was successfully synthesized up to the 13th amino acid as shown in Figure 50 peak 5.

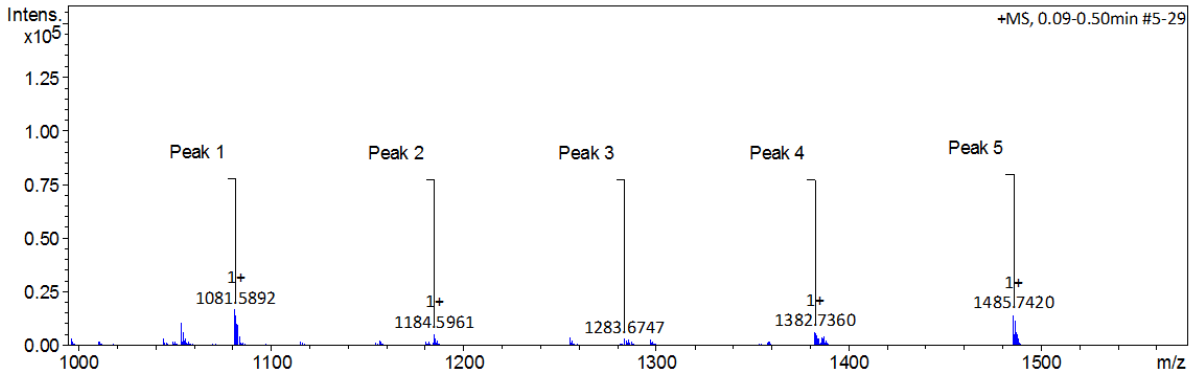


Figure 50: PS19-14 amino acid sequence MS results.

In summary, there were 5 overall deletion sequences that were observed after the 14th amino acid coupling which are CVFVYYVVLTTI), (CVFVYYVVLCI), (CVFVYYVVLI), (CVFVYYVVVTTI) and (CVFVYYVL). The first three deletion sequences were mainly caused by incomplete coupling of valine to (*N*ML), the 4th deletion sequence was as a result of incomplete coupling of (*N*ML) to the 8th amino acid, valine and the last was initiated by incomplete coupling of the 7th amino acid, valine. The peptide chain elongation ended when (*N*MI) was coupled. Other peaks observed in Figure 49 and 50 were fragmentation peaks. From the results observed, it is evident that coupling sterically hindered *N*-methylated amino

acid is difficult and produces deletion sequences. Also as explained in Chapter 3 hydrophobic amino acids such as valine and other amino acids like threonine when these amino acids are coupled following each other, they can aggregate due to formation of β-sheets which prevent solvation thereby causing incomplete coupling as observed after the 7th and 12th amino acid.[19] The deletion sequences (CVFVYVVVTTI) and CVFVYVVLTTI might be as a result of aggregation.

To improve the synthesis, a less sterically coupling reagent can be used such as OxymaPure or the reaction can be done in a microwave reactor at high temperatures. We can also substitute the 6th amino acid, valine with another amino acid that does not promote β-sheets formation.[19,124]

4.1.2 PS20 results and discussion

In this synthesis all valine amino acids on position 2, 4, 6, 9, 14 and 15 were substituted with (*N*MV) as shown in Figure 51.

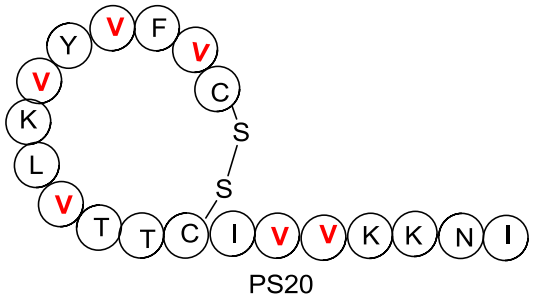


Figure 51: PS20 amino acid sequence

Peak 3 (Figure 52) shows the successfully synthesized 8th amino acid sequence for PS20 (CVFVYVKL).

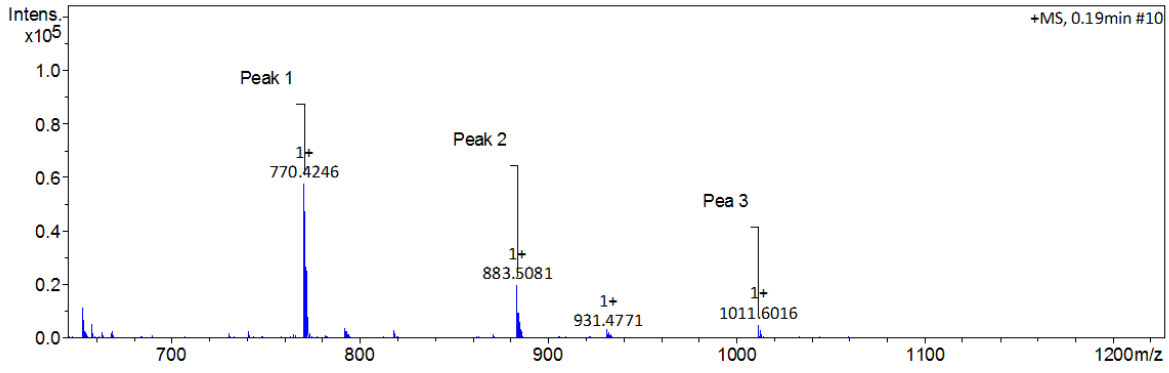


Figure 52: PS20-8 amino acid sequence MS results.

Coupling the 8th amino acid (leucine) showed that the 6th amino acid, (*N*MV) was incompletely coupled. Deletion sequences (CVFVYV) corresponding to peak 1 was observed implying incomplete coupling of lysine. Peak 2, (CVFVYVL) showed that leucine coupled to peak 1 resulting in another deletion sequence.

9th amino acid coupling

Coupling of *N*MV was successful (peak 3, Figure 53) and the deletion sequence produced during the coupling of the 8th amino acid grew to give the sequence CVFVYVLV, noted by Peak 2. Peak 3 shows the successful addition of (*N*MV). Deletion sequences (CVFVYV) corresponding to peak 1 was attributed to the incomplete coupling of lysine.

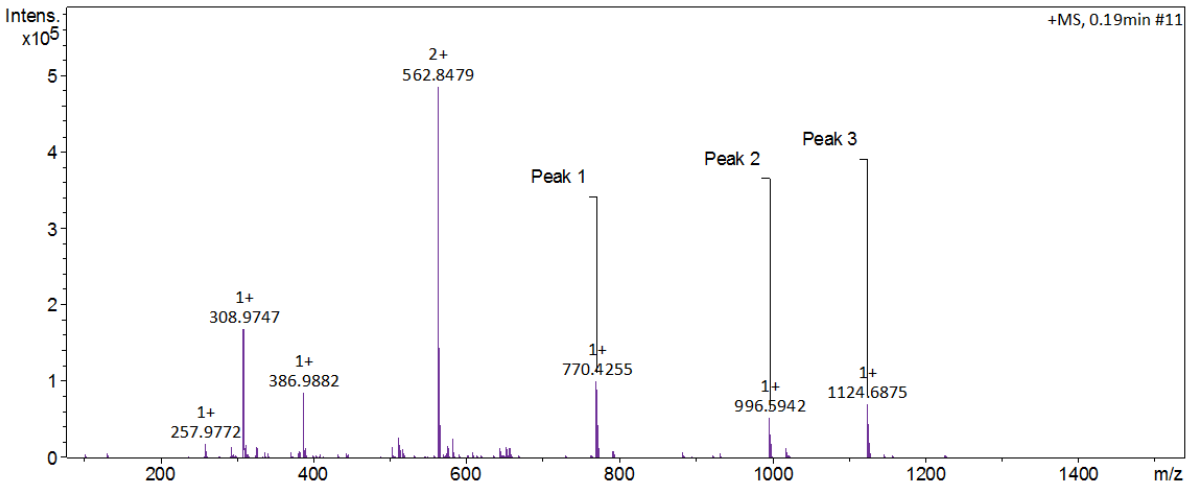


Figure 53: PS20-9 amino acid sequence MS results.

10th amino acid coupling

Figure 54 below shows the successfully synthesized 10th amino acid sequence for PS20 (CVFVYVKLVT) as peak 4.

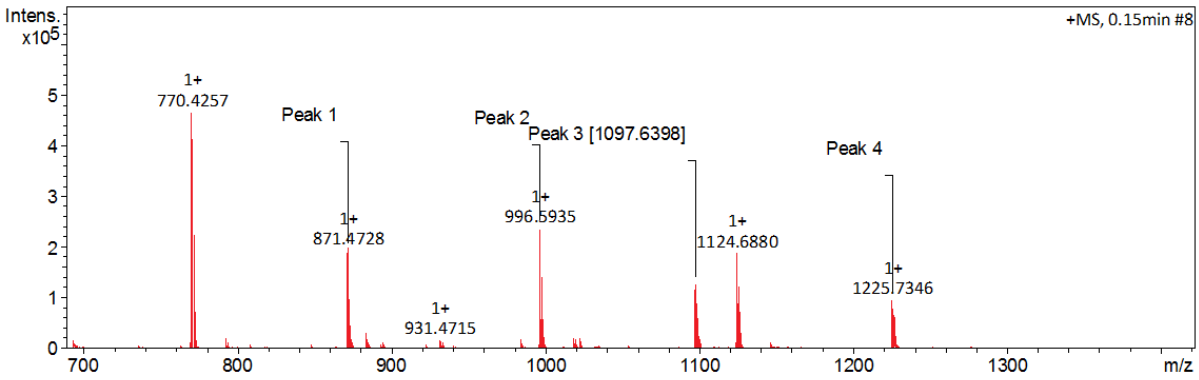


Figure 54: PS20-10 amino acid sequence MS results.

Coupling the 10th amino acid, threonine produced a new deletion (CVFVYVT), peak 1 showing that the sequence (CVFVYV) was still present. This showed that coupling to the 6th (*N*MV) was incomplete and was sterically hindered, proving again the challenges in coupling to an *N*-methylated amino acid. Peak 3 (CVFVYVLVT) is the growing deletion sequence for peak 2 (CVFVYVLV) which was initially observed after the 9th amino acid coupling in Figure 53 above.

11th amino acid coupling

Figure 55 show results for coupling the 11th amino acid, threonine. Peak 3 corresponds to the successful addition of threonine for the PS20 sequence (CVFVYVKLVTT).

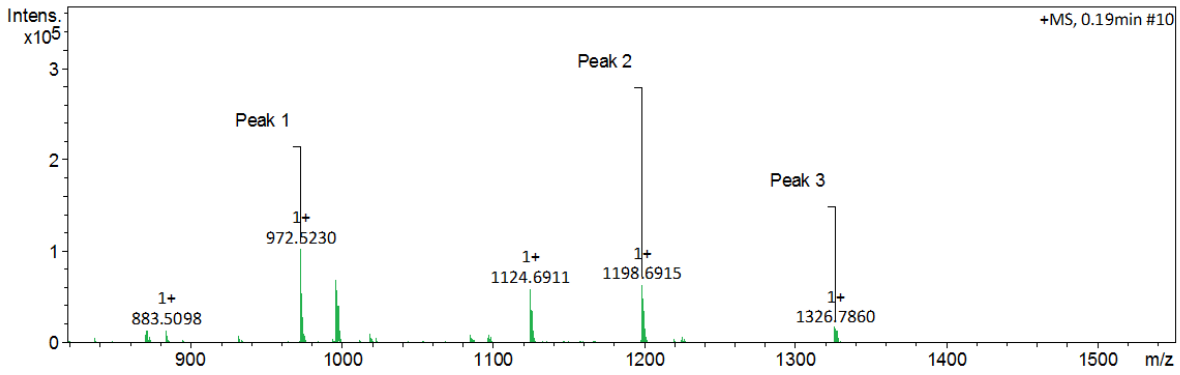


Figure 55: PS20-11 amino acid sequence MS results.

The deletion sequences (CVFVYVT) and (CVFVYVLVT) observed after the 10th amino acid coupling resulted in peak 1 (CVFVYVTT) and peak 2 (CVFVYVLVTT) after adding the 11th threonine.

12th amino acid coupling

Figure 56 below shows results for the coupling the 12th amino acid, cysteine. Peak 7 corresponds to the successful addition of cysteine for the PS20 sequence (CVFVYVKLVTTC).

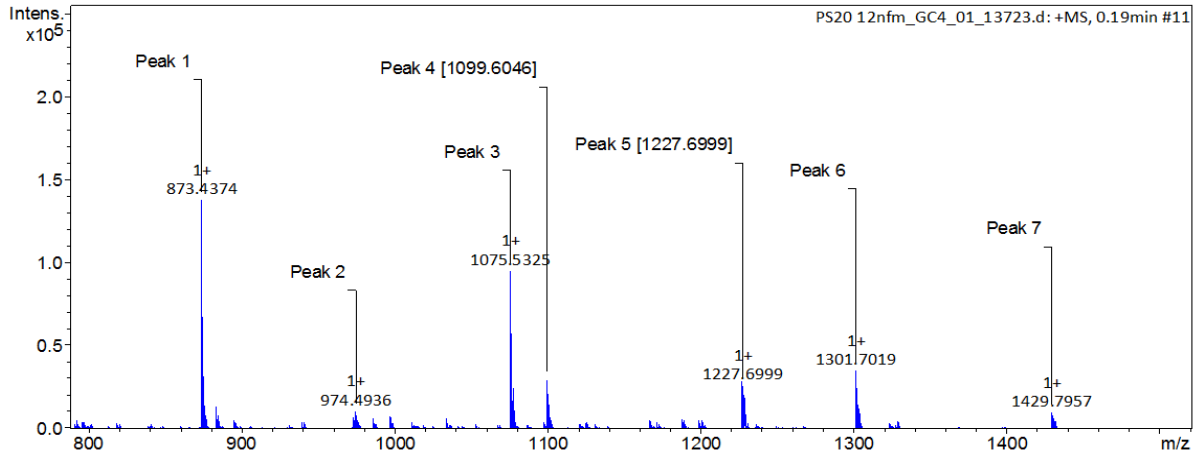


Figure 56: PS20-12 amino acid sequence MS results.

Peaks 1-6 are sequences formed after the addition of cysteine (CVFVYVC), (CVFVYVT), (CVFVYVTT), (CVFVYVLV), (CVFVYVLVTT), and (CVFVYVKLV) respectively. This observation can suggest that coupling of the 7th lysine amino acid resulted in a deletion sequence (CVFVYV) that partially remained uncoupled until the 13th amino acid. This can further imply that this sequence is highly sterically hindered and coupling the 7th amino acid might have played a significant role in determining the percentage yield of PS20-12 amino acid sequence. Peak 4 and 6 suggest that coupling to the 9th (*N*MV) was difficult.

13th amino acid coupling

Figure 57 above show results for coupling the 13th amino acid, isoleucine. Peak 1 corresponds to the successful addition of isoleucine for PS20 sequence (CVFVYVKLVTTCI). A bunch of deletion sequences resulted after the coupling of isoleucine from peak 3 to peak 8.

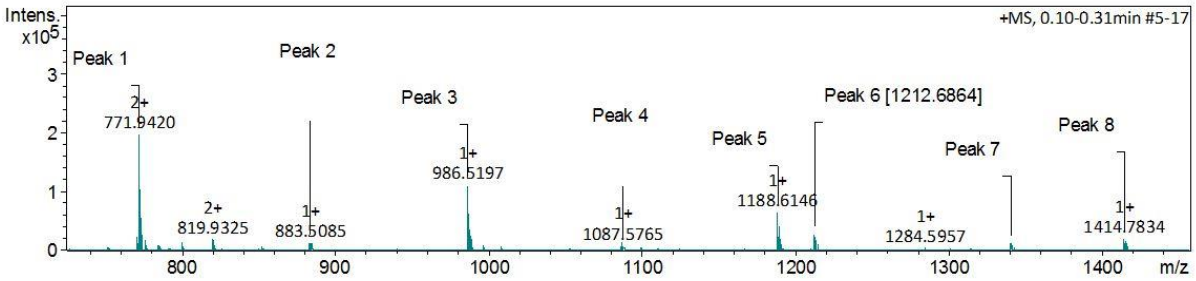


Figure 57: PS20-13 amino acid sequence MS results.

Peak 3 to peak 8 correspond to (CVFVYVTI), (CVFVYVTCI), (CVFVYVTTCI), (CVFVYVLVCI), (CVFVYVKLVCI) and (CVFVYVLVTTCI) respectively. Except for

peak 7, peaks 3-8 are as a result of incomplete coupling of lysine, the 7th amino acid. Sequences for peak 4 and peak 5 reveal that coupling of the 11th threonine was incomplete. This might suggest that the folding of the peptide prevented the coupling. In comparing peak 3 and peak 4, it was observed that there was incomplete coupling of cysteine because isoleucine coupled directly to threonine. This suggests that coupling cysteine to threonine might be difficult and should be improved.

14th amino acid coupling

Coupling (*N*MV), the 14th amino acid was successful as demonstrated by the presence of peak 1 in Figure 58 with the sequence (CVFVYVKLVTTCIV). Peaks 2-8 are observed deletion sequences as a result of coupling the 14th amino acid, (*N*MV) to deletion mentioned sequences. These are (CVFVYVIV), (CVFVYVTIV), (CVFVYVTCIV), (CVFVYVTTCIV), (CVFVYVLVCIV), (CVFVYVKLVCIV) and (CVFVYVLVTTCIV) respectively. Beyond the 14th amino acid, no further coupling was observed. Furthermore the LCMS results showed that coupling of (*N*MV) (6th amino acid) to tyrosine (5th amino acid) was incomplete although this 5 amino acid sequence did not further couple.

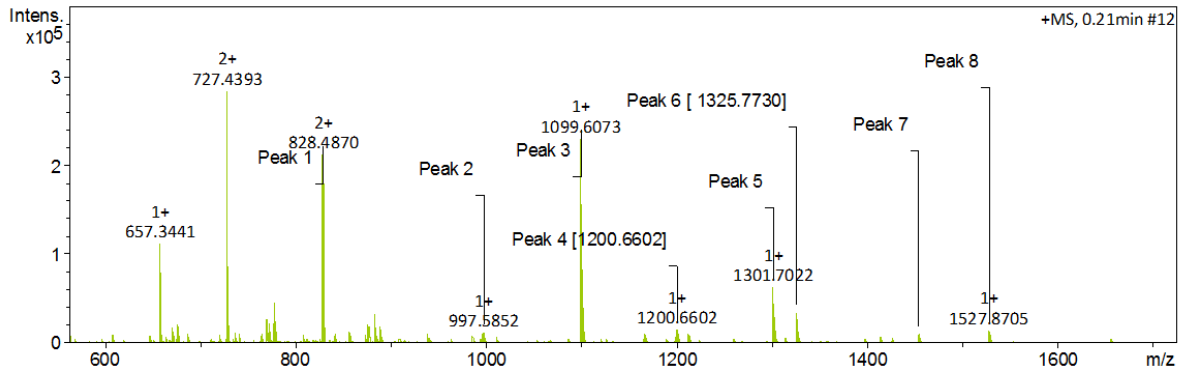


Figure 58: PS20-14 amino acid sequence MS results.

In summary we observed a total of seven deletion sequences which were primarily formed as a result of incomplete coupling of lysine to the 6th amino acid, (*N*MV). Lysine being a large molecule might have been sterically hindered by (*N*MV). To improve the coupling of lysine, coupling time could be increased, or the coupling reagent could be replaced with a better one such as OxymaPure and COMU. Finally microwave reactor at elevated temperature could be employed. Coupling of threonine to the 9th amino acid, (*N*MV) was incomplete showing that coupling to a sterically hindered *N*- methylated amino acid is not favorable. We also observed

that coupling of threonine following each other on this particular peptide could not go to completion as deletion sequences CVFVYVTCIV) and (CVFVYVTIV) were observed.

In conclusion coupling of *N*- methylated amino acids was only efficient when the peptide sequence was short ≤ 5 amino acids and when the *N*- methylated amino acids were alternated. As the number of *N*- methylated amino acid was increasing so was the deletion sequence and consequently the yield decreased. Further addition to the 14th *N*- methylated amino acid resulted in no further coupling being observed. In addition to the above mentioned reason, peptide folding as the chain elongated could have created a peptide matrix structure that sterically hindered the coupling of the oncoming amino acid. PS20-14 amino acid sequence showed conformers of both cyclized and uncyclized peptides in Figure 78 and 79 under the appendix section. A product mixture of cyclic and linear chain might suggest incomplete cyclization. Hence increasing iodine concentration or cyclizing time might improve the cyclic peptide yield. Also this mixture might be as a result of disulphide bond cleavage by soft nucleophiles when the ring system is thermodynamically unstable.[129] Improvement to this synthetic route can be done by varying the coupling reagents, using a microwave or by fragment coupling.

OxymaPure and COMU has been effectively used for the synthesis of IB-01212, a cyclodepsipeptide isolated from thermarine fungi *Clonostachys* sp. ESNA-A009.[128] Coupling of consecutive *N*-methylated amino acid was effective although the peptide was small with 6 amino acids. Hence less hindered coupling reagents could be a better option. Fragment coupling can be an alternative solution to this problem, although it may cause substantial levels of epimerization.[128] LC-MS results for the P20-13 amino acid sequence showed that there were conformers at 4.13, 4.25, 4.56, and 6.74 minutes in Figure 77 under the appendix section. These conformers subsequently reflected when the 14th amino acid was coupled as observed in Figure 78 under the appendix with retention times of 4.3, 4.60, 6.04, 6.88, 7.06, 7.22, and 7.59 minutes. Coupling the 14th (*N*MV) caused more conformers to be formed especially from the range 6-8 minutes' retention times.

4.1.3 PS21 results and discussion

All valine, isoleucine, leucine amino acids were substituted by (*N*MV), (*N*MI) and (*N*ML) respectively in the synthesis of PS21 with sequence illustrated in Figure 59. This was done to understand the overall effect on activity and solubility.

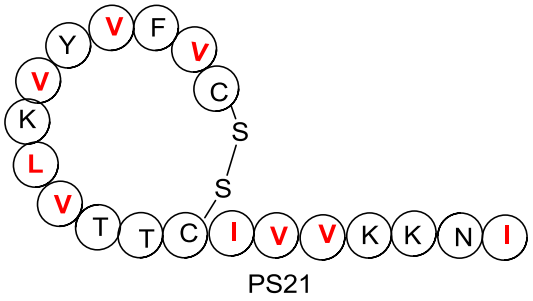


Figure 59: PS21 amino acid sequence.

5th amino acid coupling

Peak 2 correspond to 5th amino acid sequence (CVFVY) and peak 1 shows incomplete coupling of the 5th amino acid with sequence (CVFV). Surprisingly, we did not observe this when synthesizing the same portion of sequence for PS20. We suggested that the loading capacity might have been underestimated resulting in coupling with insufficient amino acid equivalence.

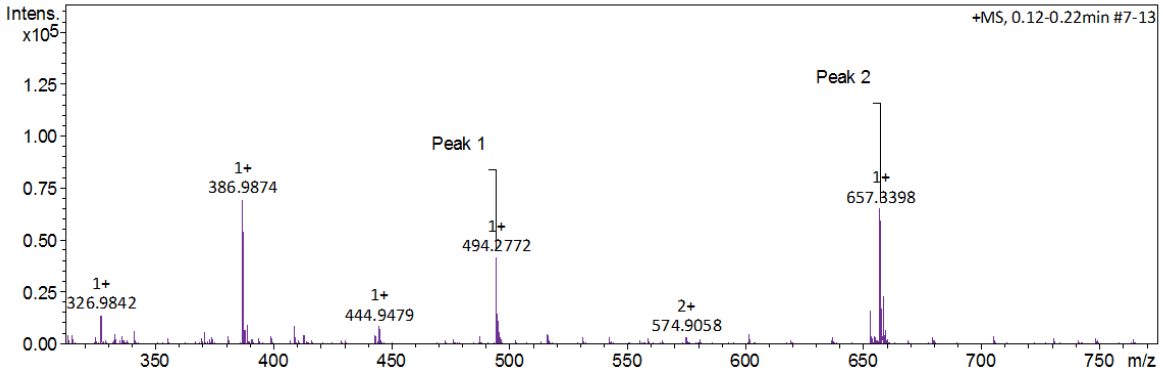


Figure 60: PS21-5 amino acid sequence MS results.

9th amino acid coupling

Results for coupling the 9th amino acid, (*N*MV) are illustrated on Figure 61. Coupling the first 8 amino acids was successful.

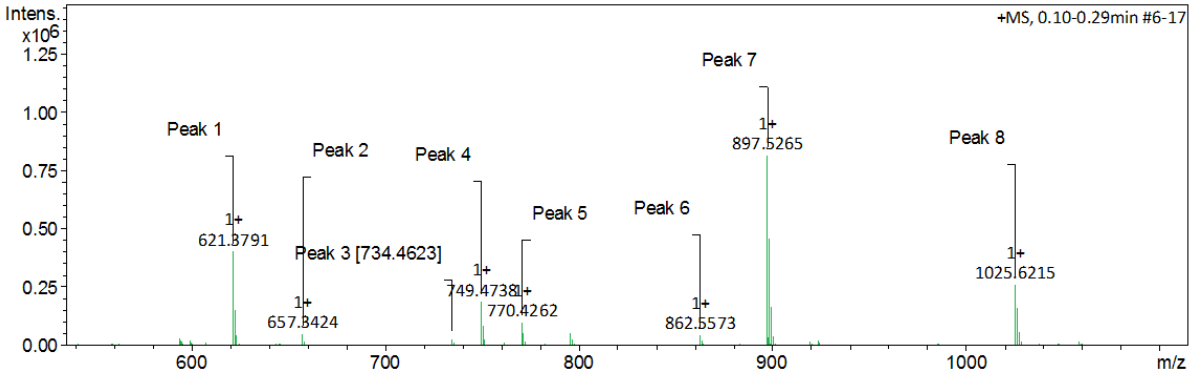


Figure 61: PS21-9 amino acid sequence MS results.

Peak 8 represents the mass of the 8th amino acid sequence (CVFVYVKL) as shown in Figure 61 although the 9th peak was not observed. Peaks 1-7 represent deletion sequences that were observed after the 9th amino acid coupling. Peak 1 corresponds to sequence (CVFVL). This sequence revealed that coupling tyrosine was incomplete and the deletion sequence then coupled with (*N*ML) (9th amino acid). Peak 3 corresponds to (CVFVVL), peak 4 corresponds to (CVFVKL) and peak 6 corresponds to (CVFVVKL) and peak 7 corresponds to 7th amino acid sequence (CVFVYVK). Peaks 3-6 resulted from coupling to the 4th amino acid deletion sequence.

10th amino acid coupling

Coupling the 10th amino acid, threonine results are illustrated in Figure 62. Results showed that the 9th amino acid did not couple at all resulting in sequence (CVFVYVKLT) observed as peak 6.

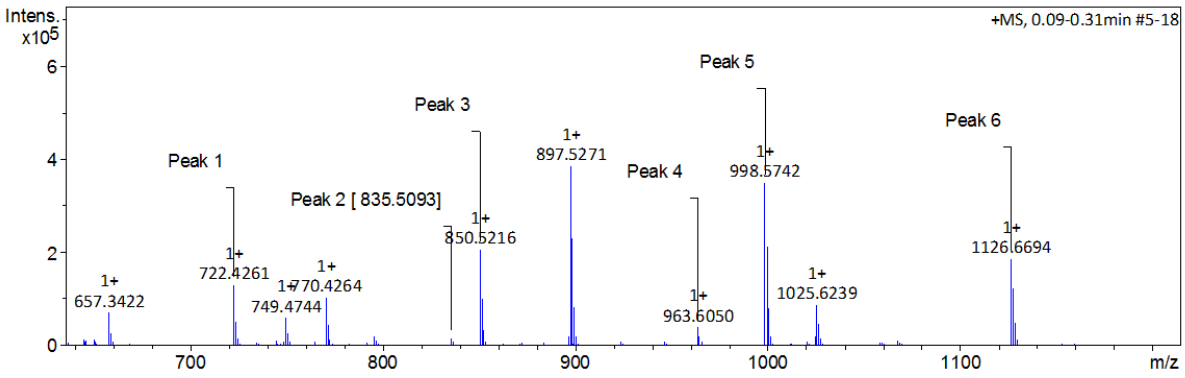


Figure 62: PS21-10 amino acid sequence MS results**.**

It is not surprising that did not couple because it is sterically hindered. Coupling to another sterically hindered (*N*ML) using a bulky coupling reagent, HATU could have caused steric hindrance. Further, the methyl group on the nitrogen atom of (*N*MV) enhanced the steric effect. Peak 1 corresponds to (CVFVLT), peak 2 corresponds to (CVFVVLT), peak 3 corresponds to (CVFVKLT), peak 4 corresponds to (CVFVVKLT) and peak 5 corresponds to (CVFVYVKT). All these deletion sequences observed were growing from the deletion sequences formed after the 9th coupling. Peak 1 (CVFVLT), peak 2(CVFVVLT) and peak 4(CVFVVKLT) sequences, revealed that coupling consecutive *N*-methylated amino acids was possible. However, we do not know to what extent these reactions were favored as we

did not probe the synthesis of these deletion sequences and furthermore due to time constrains.

We also suggested that deprotection of the 8th amino acid might have been accidently omitted by the peptide synthesizer. This resulted in no coupling occurring as the *N*-terminal was still protected with Fmoc. However, this analysis was done when the whole peptide sequence was complete hence it could not be coupled again.

11th amino acid coupling

Results for coupling the 11th amino acid, threonine are illustrated in Figure 63.

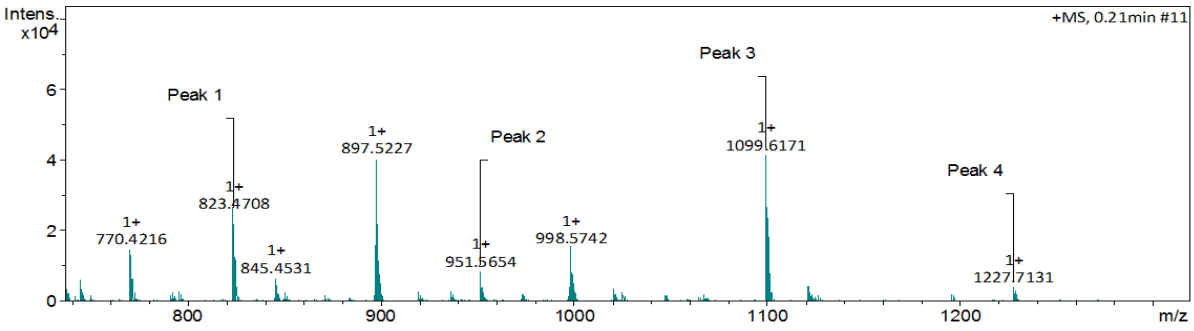


Figure 63: PS21-11 amino acid sequence MS results.

Deletion chains observed earlier in Figure 62 grew when the 11th amino acid, threonine was coupled. Peak 1 corresponds to (CVFVTT), peak 2 corresponds to (CVFVKLTT), peak 3 corresponds to (CVFVYVKTT) and peak 4 corresponds to (CVFVYVKLTT). This might suggest that among the deletion sequences that we observed after the 10th amino acid coupling, only these were kinetically and thermodynamically favored. This observation can further help in deciding sequences that could give better coupling and yields when modifying ecumicin derivatives.

12th amino acid coupling

Coupling cysteine produced several deletions sequences. This suggests that cysteine favorably couples to all these sequences. Figure 64 shows peaks of sequences that were observed after adding cysteine.

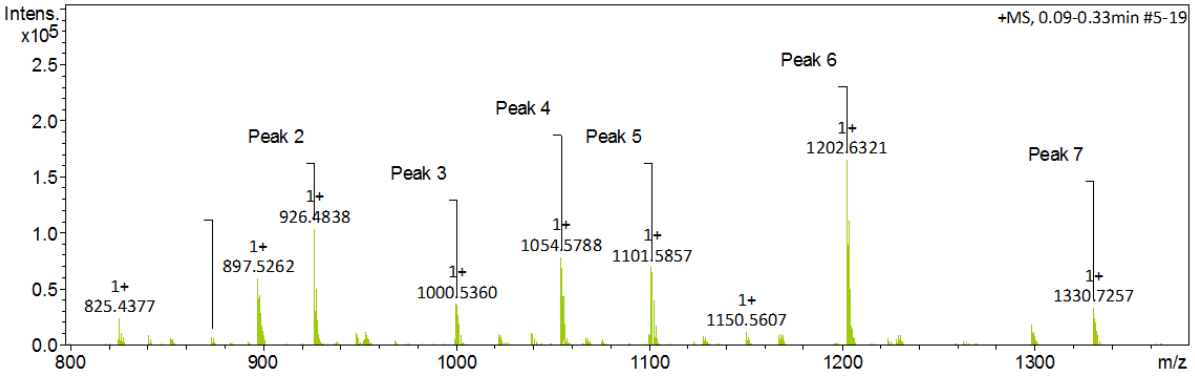


Figure 64: PS21-12 amino acid sequence MS results.

Peak 1 corresponds to (CVFVYVC) showing that the first 6 amino acid sequence was still present and confirming that coupling lysine to (*N*MV) was incomplete. This could have been facilitated by the bulky lysine side chain group which contributed to steric hindrance and preventing further coupling. This phenomenon was initially observed when synthesizing PS20 in Figure 52 which showed incomplete coupling of lysine. Hence to improve this coupling, a different coupling reagents which is less sterically hindered can be used. Peak 2 corresponds to (CVFVVTTC) and peak 3 corresponds to (CVFVYVKC). Peak 3 showed that there was still unreacted 7 amino acid sequence available (CVFVYVK). Hence as part of improving the synthesis of this peptide in future, coupling the 8th amino acid (*N*ML) can be done using another less sterically hindered coupling reagents like COMU and OxymaPure, or further increasing the coupling time maybe to 2 hours instead of 1 hour coupling cycle. Additionally, we could do triple coupling instead of double coupling. These changes could also be applied when coupling the 7th amino acid as we observed that it was incomplete.

Peak 4 was a buildup of deletion sequence observed after the 11th amino acid coupling to yield (CVFVKLTTC). Peak 5 was a buildup of deletion sequence observed after the 10th coupling, (CVFVYVKT) to give (CVFVYVKTC) shown in Figure 61. Peak 6 is a result of coupling cysteine to the deletion sequence (CVFVYVKTT) to yield (CVFVYVKTTC). Peak 7 corresponds to (CVFVYVKLTTC) which is the deletion sequence with the highest number of *N*-methylated amino acid. This can be a useful sequence for fragment synthesis of ecumicin highly *N*-methylated derivatives.

13th amino acid coupling

Results for coupling the 13th amino acid, isoleucine are illustrated in Figure 65. Peak 1 showed that the sequence (CVFVYV) was still present and coupled to (*N*MI) to give (CVFVYVI).

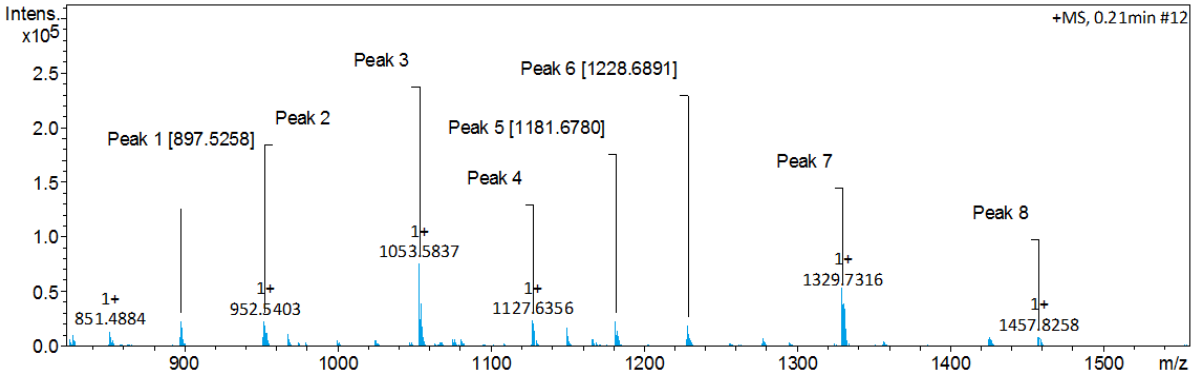


Figure 65: PS21-13 amino acid sequence MS results.

This observation together with the one observed when cysteine was coupled (CVFVYVC), peak 1 in Figure 64 and the 7th amino acid sequence (CVFVYVK), peak 7 in Figure 61 can suggest that the 6th amino acid sequence couples to lysine, cysteine and (*N*MI) preferentially to (*N*ML), (*N*MV) and threonine.

Peak 2 corresponds to (CVFVLTI), peak 3 corresponds to (CVFVLTTCI), peak 4 corresponds to (CVFVYVKCI) and peak 5 corresponds to (CVFVKLTTCI). Peaks 2-5 are secondary deletion sequences which originated primarily from incomplete coupling of tyrosine. Peak 6 corresponds to (CVFVYVKTCI), peak 7 corresponds to (CVFVYVKTTCI) and peak 8 corresponds to (CVFVYVKLTTCI). Peaks 6 and 7 are secondary sequences which originated primarily from incomplete coupling of (*N*ML) and peak 8 is a secondary deletion chain formed as a result of failed coupling of the 9th (*N*MV).

No further coupling was observed when adding the 14 amino acid of the chain to the 18 amino acid. Coupling was only successful at most to the 13th amino acid. However, the desired sequence was successfully synthesized to the 8th amino acid. Incomplete coupling of tyrosine to (*N*MV), lysine to (*N*MV), and (*N*ML) to lysine affected PS20-8 amino acid coupling as several deletion sequences were formed. Unsuccessful coupling of (*N*MV) to (*N*ML) and (*N*MV) to (*N*MI) added more deletion sequences and completely terminated coupling respectively.

An attempt to synthesize PS21 using the fragments method was unsuccessful. The peptide sequence was divided into two fragments, F1 with sequence (INKKVVICTTVL) and F2 with

sequence KVYVFVC. Synthesis of F1 was unsuccessful as (*N*MV) could not couple to (*N*ML) which was attached to the 2-chlorotriyl resin. This could have been as a result of peptide loss due to diketopiperazine formation which was promoted by consecutive N-methylated amino acids.[128] Furthermore it could be that coupling (*N*MV) to (*N*ML) was not favored.

Suggested design of the *N*-methylated ecumicin derivative from the obtained results

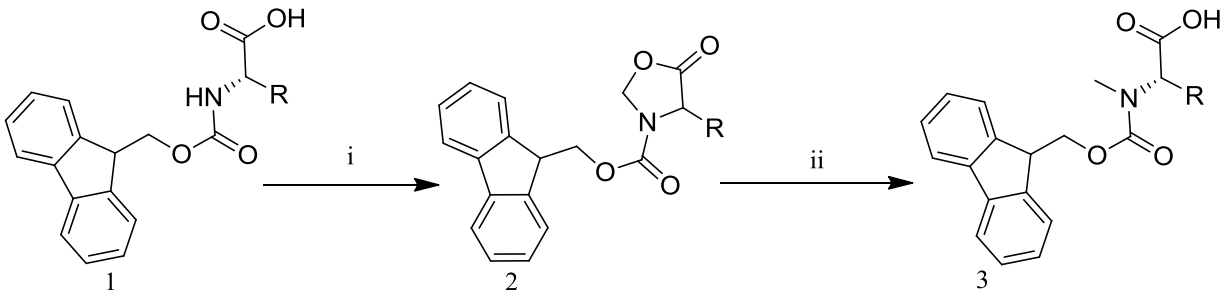
From the results observed for the *N*-methylated peptides, we observed that the first 5 sequence (CVFVY) of PS20 that had two (*N*MV) amino acids coupled successfully without or minimal deletion sequence. Hence we suggested considering it since it has *N*-methylated amino acids that we are interested in for the design of the probable *N*-methylated ecumicin derivative that can be successfully synthesized in very high yield. PS20-8, Figure 52 and PS21 showed that adding (*N*MV) on the 6th position resulted in incomplete coupling and consequently deletion sequences were formed along the way. For this reason we suggested adding valine amino acid giving us (CVFVYV) will be a better option. PS06 results (Figure 25) showed that the 7th amino acid valine was difficult to couple because of possible β sheets formation and solvation challenges that prevent coupling hence we suggested to replace it with lysine which is more cationic building the sequence to (CVFVYVK). PS19-9 and PS19-10 (Figures 45 and 46) showed that coupling of (*N*ML) was incomplete and that the coupling of the subsequent valine amino acid was incomplete as well. We reasoned out that using leucine amino acid instead of (*N*ML) amino acid will possibly improve the coupling efficiency due to reduced steric hindrance leading to sequence (CVFVYVKL). Results obtained from PS20-12 and PS20-13 in Figure 56 and 57 respectively revealed that coupling of two consecutive threonine amino acids to (*N*MV), 9th amino acid was incomplete. Hence for the design of the peptide we proposed to use valine amino acid resulting in sequence (CVFVYVKLV). Possible formation of β sheets when threonine amino acids were coupled consecutively resulted in incomplete coupling of cysteine as observed in Figures 49 and 57 during the synthesis of PS19 and PS20 respectively. Hence to avoid this, we decided to eliminate one threonine amino acid leading to (CVFVYVKLVTC). Since all the *N*-methylated peptides showed that adding *N*-methylated amino acid after cysteine, the 12th amino acid was detrimental to the success synthesis of the peptide; we opted for natural amino acid. However, although the 14th and the 15th amino acids are all valine amino acid which have a propensity of forming β sheets we decided to keep the sequence as they are. From Chapter 3 results, we observed that the addition of cationic lassomcyin derived residue

did not contribute much to the solubility and yield of the peptides hence we did not include it in the designing of the peptide. Therefore, we propose that the sequence; (CVFVYVKLVTCIVV) can be successfully synthesized at very high yield especially when OxymaPure is used as we observed the results from PS01in Chapter 2. However, this sequence is hydrophobic and can present solubility challenges mentioned in Chapter 2 and 3. To solubilize it, we propose to add a pegylation molecule that will drag the molecule into solution.[31,130]

4.2 Synthesis of *N*- methylated amino acids

4.2.1 Results and discussion

Fmoc amino acids were reacted at 110 °C in the Dean-Stark apparatus. The reaction was conducted under dilute conditions with excess of paraformaldehyde. The product was formed as a single spot on TLC, indicating complete consumption. The crude product was washed with sodium carbonate solution and distilled off *in vacuo* to give an a) oily viscous transparent oxazolidinone for valine amino acid, b) a golden oily viscous oxazolidinone for leucine and oily viscous transparent oxazolidinone for isoleucine all in percentage yields of (95-98) %.



Scheme 11: i) Reagents and conditions: Fmoc amino acid, paraformaldehyde, *p*-TSOH, toluene, reflux, 15 hours. ii) Aluminum chloride, triethylsilane (TES), dry DCM, ambient temperature, 4 hours.

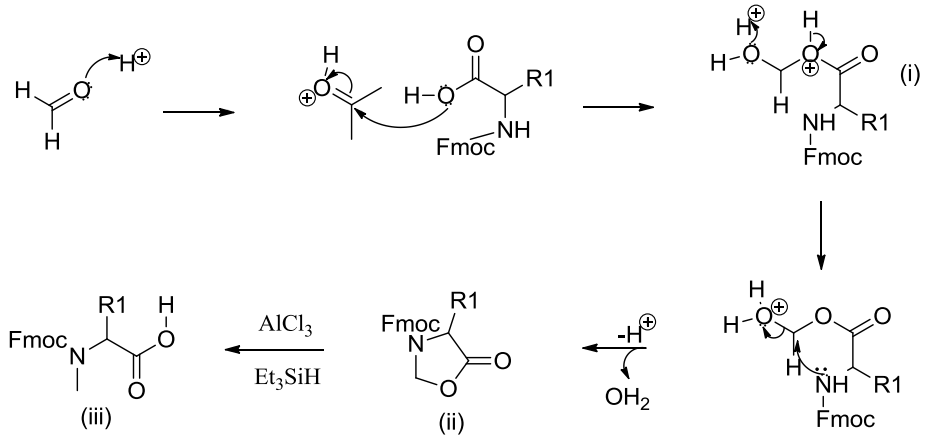
Scheme 11 shows the synthesis of *N*- methylated amino acids. The intermediates were reacted with excess of Lewis acid, aluminum chloride and (TES) at ambient temperature to yield the ring opened Fmoc-*N*-methylated amino acids. The products had more than one spot on TLC indicating impurities; hence they were washed with acidified distilled water followed by purification using flash column chromatography with MeOH: DCM solvent of ratio 1:24. The products were distilled off under *in vacuo* to give white solids in range (88.0-97.2) %

yield (See experimental). Fmoc-*N*-methylated valine, leucine and isoleucine were synthesized as white solid with melting points ranging from 190-191°C, 115-116°C, and 181-182°C respectively.[122,131,132] Melting point ranges were exactly as reported in literature for the compounds. Fmoc-*N*-methylated valine had a relatively high R_f of 0.29 followed by Fmoc-*N*-methylated leucine with 0.28 and then Fmoc-*N*-methylated isoleucine with the lowest value of 0.26 in (1:24, MeOH: DCM).

This shows that Fmoc-*N*-methylated isoleucine is less hydrophobic than Fmoc-*N*-methylated leucine which in turn is less hydrophobic than Fmoc-*N*-methylated valine. The calculated and found mass according to the mass spectrometer were as follows: Fmoc-*N*- methylated valine calculated UHPLC-HRMS (ESI^+) *m/z* for $C_{21}H_{24}NO_4$ is 354.1705 and found mass was 354.1699 $[M+H]^+$. Fmoc-*N* methylated leucine calculated UHPLC-HRMS (ESI^+) *m/z* for $C_{22}H_{26}NO_4$ is 368.1862, and found mass was 368.1855 $[M+H]^+$. Fmoc-*N*-methylated isoleucine calculated UHPLC-HRMS (ESI^+) *m/z* for $C_{22}H_{26}NO_4$ is 368.1862, and found mass was 368.1861 $[M+H]^+$.

4.2.2 Mechanism of *N*-methylation of Fmoc- amino acid

Paraformaldehyde is protonated by the acid PTSA as the catalyst. This protonation activates the carbonyl carbon to be more electrophilic. The oxygen atom of the amino acid hydroxyl group attacks the electrophilic carbon to form an intermediate (i) in Scheme 12. Protonation of the hydroxyl group and loss of proton from the ester oxygen atom occurs simultaneously resulting in turning of the alcohol into water and a better leaving group.



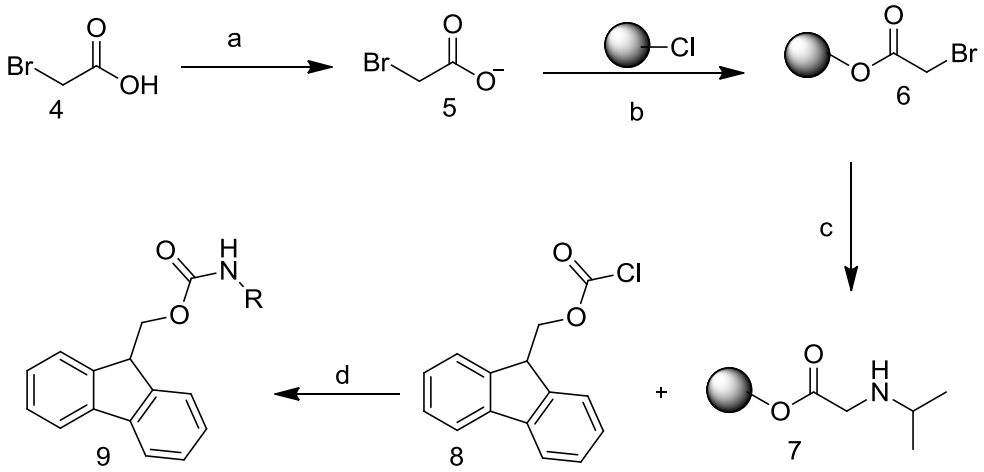
Scheme 12: Proposed mechanism for methylation of Fmoc-amino acid

The electrophilic carbon attached to the water molecule is attacked by the lone pairs from the nucleophilic nitrogen atom resulting in subsequent loss of water to give the oxazolidinone

(ii). The reduction of oxazolidinone with (TES) and Lewis acid, aluminium chloride facilitate ring opening to give the *N*-methylated Fmoc-amino acid (iii).

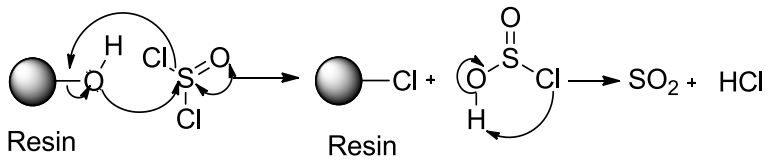
4.3 Synthesis of Valine peptoids

Fmoc valine peptoids were synthesized according to the Scheme 13 below.

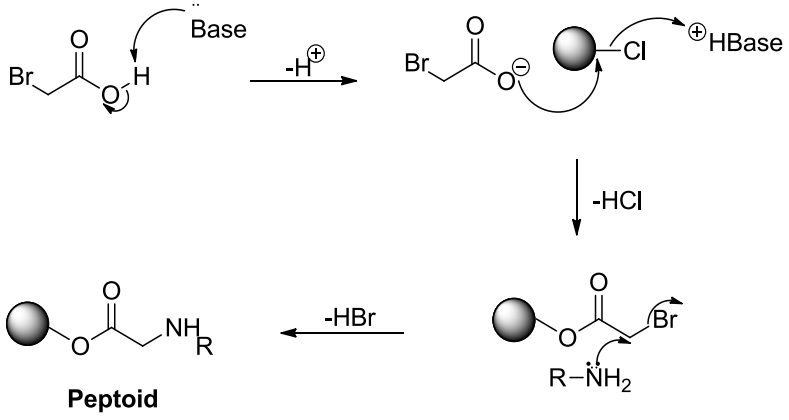


Scheme 13: Peptoids synthesis procedure a) & d): DIPEA, dry DCM; b): Activated 2-chlorotrityl resin; c): Amine, DMF

Schemes 14 and 15 show proposed mechanisms for activation of the resin and peptoid synthesis respectively.

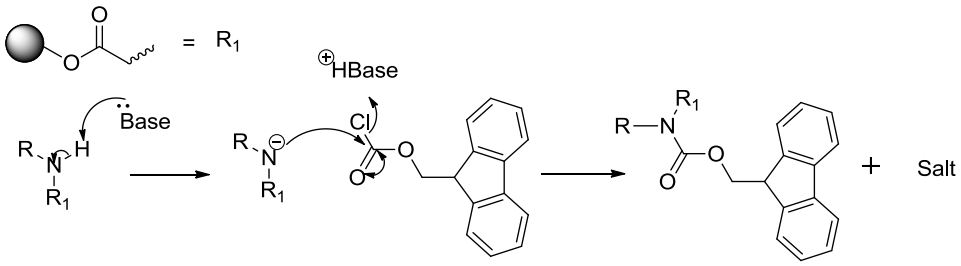


Scheme 14: Proposed resin activation mechanism**.**



Scheme 15: Proposed peptoid synthesis mechanism[133,134]

Bromoacetic acid is activated by extracting a proton from the hydroxyl group using a base giving rise to a strong nucleophile that will displace chloride ion (good leaving group) from the resin. An amine, nucleophile will displace the bromide ion with the loss of a proton from the amine resulting in the formation of the peptoid. For chemo-selectivity during peptide synthesis, the amine group on the peptoid is protected using Fmoc chloride. The mechanism involves the extraction of a proton from the amine to make it a stronger nucleophile which then attacks the electrophile carbonyl carbon of Fmoc followed by displacement of the chloride atom.[84] The reaction proceeds via an addition and elimination mechanism as shown in Scheme 16.



Scheme 16: Proposed mechanism of Peptoid protection by Fmoc-Cl.[84]

The product Fmoc valine peptoid was obtained as an off-white solid (0.5g). UHPLC-HRMS (ESI^+) *m/z* calculated for $C_{20}H_{22}NO_4$ is 340.1549 and found mass was found 340.1539 $[M+H]^+$.

4.4 Synthesis of PS23 peptoid derivative

In this synthesis valine on position 6, was substituted with valine peptoid. The synthetic procedure that was used for *N*-methylated peptide was adopted for PS23 shown in Figure 66 below.

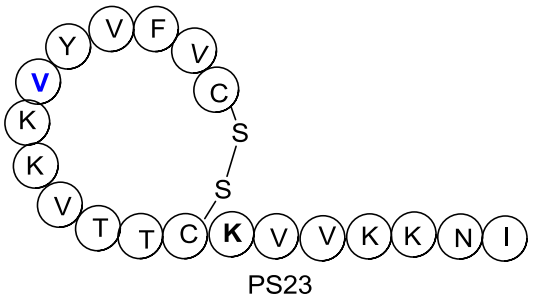


Figure 66: PS23 amino acid sequence.

We believe the peptoid did not couple since the desired mass was not found in the mass spectrometry.

4.5 Conclusion

The synthesis of *N*-methylated peptides was unsuccessful. *N*-methylated amino acids had a huge impact which negatively affected the synthesis of these peptides mainly due to steric hindrance and consequently incomplete coupling. Deletion sequences prevailed especially when coupling *N*-methylated amino acid to another *N*-methylated amino acid. We have also concluded that the suggested sequence, (CVFVYVKLVTCIVV) based on the results of all the peptides synthesized can be successfully achieved in high yields using OxymaPure as the coupling reagent.

CHAPTER 5: Biological activity

5.1 *In-vitro* antimicrobial susceptibility

The common screening methods for the detection of antimicrobial activity for drug candidates are bioautographic, diffusion, and dilution methods. The diffusion method has variants which are agar based (well or disc agar). The dilution method is also categorized into broth micro dilution, broth macro dilution and agar dilution. Two variants of bioautographic method are (direct and indirect).[130,135] Although different methods have their strength and weakness, studies showed that agar dilution, broth dilution and disk diffusion results are consistently reproducible and repeatable when followed correctly.[135]

In order to determine the selectivity of the ecumicin derivatives for only mycobacterium, we tested one of its derivatives and one lassomycin derivative Pep-Lys-NN against four microorganisms. The antimicrobial activities of PS18 and Pep-Lys-NN were tested against gram (+) and gram (-) human pathogenic microbial strains as shown in Table 11 below. PS18 and Pep-Lys-NN were tested since they were obtained in reasonable yield of 41.0 mg and 29.5 mg respectively and high purity.

Table 11: Showing results for peptides antimicrobial activity

		Minimum inhibitory concentration (µg/ml) for different organisms			
Compound	Starting concentration (µg/ml)	E.*coli* ATCC25922	P. *aeruginosa* ATCC 27853	S.*aureus* ATCC29913	B.*subtilis* ATCC 2002
PS18	128	>128	>128	>128	>128
Pep-Lys-NN	256	>256	>256	>256	256

Results showed that PS18 was not active against the four microbial strains at the highest available concentration of 128 µg/ml. Pep-Lys-NN showed selective activity with an MIC value of 256 µg/ml against B. *subtilis* ATCC 2002 and did not show any activity against the other three bacteria.

5.2 Broth dilution assay

The broth dilution assay is used to determine the lowest concentration of the assayed antimicrobial that inhibits the visible growth of the bacterium being tested (MIC). The broth dilution method represents MIC often as a relative value and may be considered to have an inherent variation of one dilution.[135]

Table 12: MIC for PS08 results

Compound	Solubility	MIC_{99} (µM) - 7 days	MIC_{99} (µM) - 14 days
PS08	100% DMSO	>320	320
Controls			
Rif		0.008 µg/ml	
INH		0.05 µg/ml	
Ethambutol		12.5 µg/ml	

PS08 was tested for activity against *Mycobacterium tuberculosis* as shown in Table 12 above. PS08 was tested since it was available in reasonable yield. After 14 days, PS08 had a MIC_{99} value of 320 µM showing that it was inactive. PS17 was tested for *Mycobacterium tuberculosis* activity and it was found to be inactive as shown in Figure 67. After adding Alamar Blue which is a redox dye that is converted by Mycobacterium the blue dye turns into a pink color if there is growth. The wells changed color from blue to pink showing that the peptide was inactive. However, the growth in the higher dilutions was milky and spread out rather than a pellet which was an unusual observation. We suggested that the precipitation of the peptides might have caused this observation.

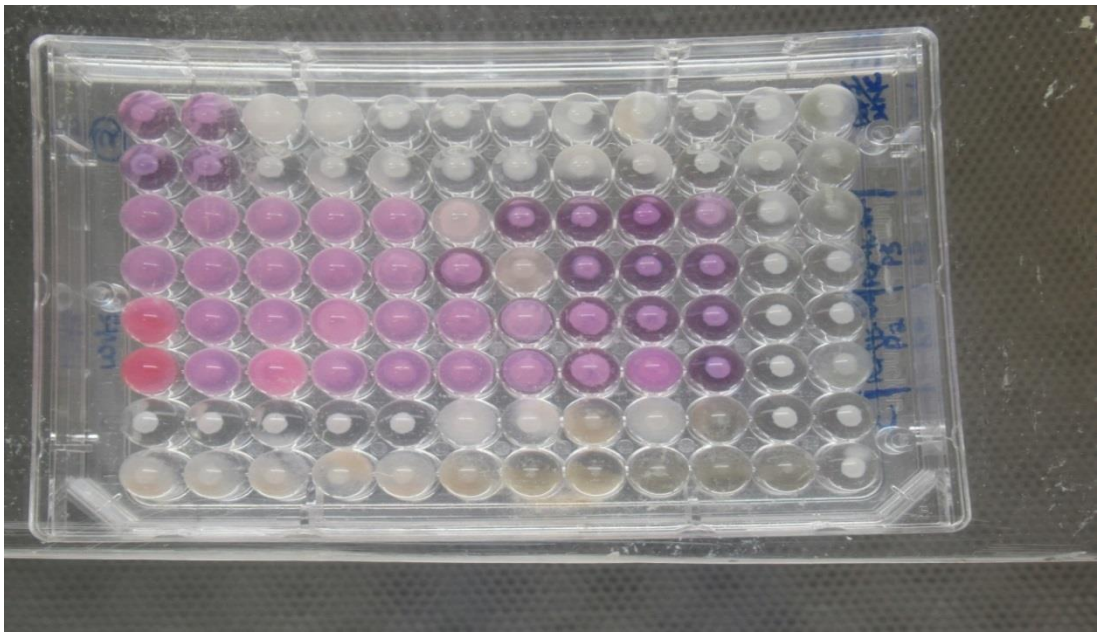


Figure 67: Micro broth dilution results for PS17.

CHAPTER 6: Conclusion

The successful synthesis of ecumicin derivatives depended mainly on coupling reagents, polarity of the peptide and on whether the amino acids were modified (*N*-methylated or peptoid). HBTU was not an effective coupling reagent for tryptophan and subsequent amino acid for the ecumicin natural amino acid derivative PS01. The HATU coupling reagent showed better coupling ability as the peptide PS01, was synthesized up to the 14th amino acid. OxymaPure proved to exceed HATU and HBTU in terms of its performance as the complete synthesis of PS01 was successful but due to a number of side reaction products the peptide was not purified. Substituting tryptophan with tyrosine showed a great improvement in synthesizing the ecumicin derivative PS06. Synthesis was successful using HATU as the coupling reagent but challenges were encountered during the preparation of the sample for purification. The peptide aggregated in DMSO to form a gel texture which could not be further dissolved. Efforts to improve the solubility by adding the arginine amino acids in the sequence were unsuccessful. Replacing two arginines with lysines resulted in the successful synthesis of the cationic ecumicin derivative PS08 in low yield. Synthesis of PS10 with one lysine group was unsuccessful. PS08 had slightly improved solubility as the peptide did not aggregate upon dissolution although 100% DMSO was the only solvent in which the peptide could dissolve. Further modification to improve solubility by replacing the 7th, 8th and 13th amino acid (valine, leucine and isoleucine) with lysine improved solubility. A solvent ratio of (2:3 ACN: DMSO) could dissolve the cationic derivatives. Purification remained a challenge for these peptides due to unwanted side reactions and deletion sequences. Synthesis of *N*-methylated derivatives was successful to the 8th, 13th and 14th amino acid for PS21, PS19 and PS20 respectively. Introduction of the *N*-methylated amino acid mostly caused the termination of the coupling. The synthesis of the peptoid derivative was unsuccessful.

Amongst the successfully synthesized ecumicin peptides derivatives that were tested for biological activity, none of them were active against the *Mycobacterium tuberculosis.*

Replacement of the lactone bond with a disulphide bond did not improve solubility as was observed with PS06. However the structural conformation and activity against *Mycobacterium tuberculosis* could not be addressed because the peptide was not purified due to solubility problems. The effect of arginine on the solubility of ecumicin derivatives could not be deduced because the arginine derivatives were not successfully synthesized. Since

arginine derivatives were not synthesized, comparison of arginine and lysine derivative could not be done. However, increasing the number of lysine groups on the derivatives showed a slight improvement in solubility. This was demonstrated by comparing solvents used to dissolve PS08 and PS17. PS08 with only two lysine groups dissolved in 100% DMSO whilst PS17 with five lysine groups dissolved in 3:2, DMSO: ACN. This could suggest that adding more lysine groups to the derivative could likely facilitate the solubility of the peptide. Although we could not get the binding properties of arginine containing ecumicin derivatives that we could compare to lysine derivative, three lysine containing derivatives (PS08, PS17 and PS18) that were tested were not active. None of the peptides showed an improved activity but rather the activity was lost. The effects of a peptoid moiety on the solubility and binding properties of ecumicin were not determined as the peptoid was not successfully synthesized.

Overly, a total of 14 peptide sequences were attempted. Only 7 ecumicin peptides were successfully synthesized namely PS01, PS06, PS08, PS15, PS16, PS17 and PS18. The other unsuccessfully synthesized peptides were PS07, PS09, PS10, PS19, PS20, PS21 and PS22.

Future work could involve the synthesis of the derivative; (CVFVYVKLVTCIVV) which we propose could be successfully synthesized at a high yield using OxymaPure. Synthesis of these derivatives under microwave assisted conditions will constitute part of the future work.

CHAPTER 7: Experimental

7.1 Materials and Methods

All solvents and reagents were purchased from commercial suppliers. Solvents for *N*-methylation of amino acids, liquid-liquid extraction and TLC development were further purified by distillation. Such solvents were DCM, Hexane, Ethyl acetate, toluene and MeOH. DIPEA, TFA, TIS, EDT, DMSO, bromoacetic acid, *p*-toluene sulphonic acid, aluminium chloride, *para*- formaldehyde, TES, piperidine, DIC, formic acid, thionyl chloride, isopropylamine, HCl, sodium carbonate and magnesium sulphate were supplied by Sigma-Aldrich. OxymaPure was obtained from University of KwaZulu Natal Department of Pharmaceutical Science. Organic solvents such as DMF and HPLC grade isopropanol, diethylether, methanol and acetonitrile were purchased from scientific pyramid. Milli-Q water was used. All amino acids, coupling reagents, Fmoc-Cl, Fmoc-OSu and resins were purchased from DLD scientific. Normal and flash silica chromatography was performed on silica gel 60 Å, 230-400 mesh and 60 Å, 230-400 mesh respectively. Analytical TLC plates (0.2 mm silica gel 60 with fluorescent indicator UV_{254}) were obtained from Sigma-Aldrich. Solvent ratios for chromatography are reported as v/v ratios.

Automated peptide synthesis was done on PS-3TM Peptide Synthesizer. Preparative HPLC was performed on Agilent 1260 Infinity system using Kinetex$^{(R)}$ 5µm B-C18, 100 Å (250 ×230 mm) column with flow rate of 20 ml/min or 15 ml/min and UV detection of 215 nm and 254 nm; buffer A, 0.1% formic acid in H_2O; buffer B, 0.1 formic acid in CH_3CN. LC-MS was performed on Ultra High Performance Liquid Chromatography (Thermo Scientific Ultimate 3000, RS diode array detectors) - High Resolution Mass Spectrometer (Bruker Compact quadruple time of-flight). Structural elucidation, 1D (^1H, ^{13}C) and 2D (COSY, HSQC) NMR spectra were obtained on 400 MHz and 500 MHz Bruker spectrometer as solutions in deuterated solvents. All chemical shifts were reported in δppm. ^1H chemical shifts were internally referenced to tetramethylsilane (δ 0.00) for $CDCl_3$ or to the residual proton resonance in CD_3OD (δ 3.31) and DMSO-d_6 (2.49). Carbon chemical shifts were internally referenced to the solvent resonances in CD_3OD (49.15), DMSO-d_6 (39.51), or $CDCl_3$ (77.16) Peak multiplicity were designated by the following abbreviations: s, singlet; d, doublet; t, triplet; q, quartet; m, multiplet; br, broad; *J*, coupling constant in Hz and rounded to1 decimal place.

Absorbance for loading test was done on Aligent Cary 100 UV/VIS spectrometer. Optical rotation was done on JASCO P-2000 Polarimeter, λ 589 nm.

7.1.1 General procedure A: SPPS for both manual and automation[73]

Approximately 300 mg of Fmoc- rink amide resin was swelled with 5 ml DMF for 10 minutes in a 70 ml glass reaction vessel fitted with fritted filters. The DMF was drained and 5 5 ml aliquot of 20% piperidine was added and mixed for 5 minutes under a flow of inert nitrogen gas. This was repeated after which the resin is washed by bubbling nitrogen gas with 4 ml DMF five times at 30 sec per each wash.

Amino acid (1.20 mmol, 0.2 M) and coupling reagent (1.14 mmol, 0.19 M) HATU/OxymaPure were dissolved in 3ml of 1.0 M DIPEA in DMF and transferred into the reaction vessel where an addition of 3 ml DMF was added. The solution was set to react while bubbling nitrogen gas through for 60 minutes. Coupling was repeated after which the resin was washed with (3×5 ml) DMF, (3×5 ml) dry DCM It was dried for 30 minutes *in vacuo*. Resin loading capacity was determined according to the general procedure B below. The first amino acid was then deprotected with a (2×5 ml) 20% piperidine solution in DMF with nitrogen bubbling for 5 minutes. After deprotection the resin was washed with (5×5 ml) DMF.

The loading capacity was then used to calculate the mole equivalence of the subsequent amino acid which an excess of 4 equivalents to the mmols was attached on the resin. Coupling of subsequence amino acid was conducted at 30 minutes per coupling cycle.

All peptides were synthesized according to general procedure A (Chapter 7.1.1) with variations in scaling up/ coupling reagents and coupling time for *N*-methylated amino acids.

7.1.2 General procedure B: Resin loading capacity determination

After coupling the first amino acid, the resin bound amino acid was washed thoroughly with (5×5 ml) DMF and (3×5 ml) dry DCM. The resin was dried *in vacuo* for 30 min. Duplicates of approximately (5-10) mg of dry resin beads were weighed and transferred into 2 ml plastic Eppendorf tubes. 20% piperidine solution in DMF (1 ml) was added to the resin beads and was shaken in a shaker for 20 minutes at 90 rpm. The samples were centrifuged for 2 minutes and 100µL of each sample was drawn and transferred into DMF (10 ml) in a 15 ml plastic tubes. The samples were then analyzed for absorbance at 301 nm on UV/VIS spectrometer and loading capacity calculated according to the formula below.[136]

$$Loading\ capacity\left(\frac{mmol}{g}\right) of\ resin = \frac{(101 \times Average\ Absorbance)}{(7.8 \times mg\ of\ resin\ beads)}$$

7.1.3 General procedure C: Disulphide peptide cyclization

Iodine, 10 equivalence to the peptide was weighed and dissolved into 1:4 (H_2O: DMF) 10 ml solution to give a 0.2 M solution. The resin bound peptide was transferred to the solution and allowed to shake for 3hrs. The resin was then thoroughly washed with (2×5 ml) DMF, (3×5 ml) 2% ascorbic acid in DMF, (3×5 ml) DMF and (5×5 ml) DCM and dried *in vacuo* for 30 minutes.

7.1.4 General procedure D: Global cleavage

Thoroughly washed resin was cleaved with a cleavage cocktail (94% TFA: 2.5% H_2O: 2.5% EDT: 1% TIS), 10 ml for 3 hrs. The filtrate was divided into two equal portions in 50 ml centrifuge tubes. Cold ether was then added (5-10 times more than the sample volume) to the filtered solution to yield a white precipitate of crude peptide which was centrifuged for 5 minutes at 5000 rpm and the solvent was decanted leaving the crude peptide on the bottom of the centrifuge tube. Washing with cold ether was repeated twice.

7.1.5 General procedure E: Synthesis of Fmoc- oxazolidinone from Fmoc amino acid[89]

The Fmoc amino acid (5 mmol), paraformaldehyde (1 g) and *p*-toluenesulphonic acid (100 mg) were suspended in toluene (100 ml). The mixture was refluxed in a Dean-Stark setup until no more starting material could be detected by TLC (97.5:2:0.2-$CHCl_3$: MeOH: AcOH). The solution was cooled, washed with saturated $NaHCO_3$ and dried over anhydrous $MgSO_4$. Concentration in vacuo gave the crude product which in most cases solidified upon standing

7.1.6 General procedure F: Synthesis of Fmoc-*N*-methylated –*α*- amino acid from Fmoc-oxazolidinone

To a solution of Fmoc- protected oxazolidinone, (1 equiv.) and anhydrous $AlCl_3$ (2 equiv.) in dry DCM (20 ml/ 1 mmol oxazolidinone) was added TES (2 equiv.). The reaction was stirred at ambient temperature until TLC (1:3 ethyl acetate/hexane) showed the absence of starting material. An additional amount of DCM (20 ml) was added, and the organic phase was washed with 1 M HCl. The organic phase was dried over anhydrous magnesium sulphate and concentrated *in vacuo*. The crude product was purified via column chromatography on silica gel with (1:19, MeOH: DCM).

7.1.7 General procedure G: Synthesis of Fmoc-peptoid

To chlorotrityl resin (1 g), in a 50 ml plastic tube, 3 ml of thionylchloride in dry DCM (45 ml) was added and the mixture was shaken overnight. A mixture of bromoacetic acid

(BAA),- (1.60 g, 11.5 mmol, 1 equiv.) and DIPEA (5.88 ml, 34.5 mmol, 3 equiv.) in dry DCM added to yield 1.2 M BAA solution was allowed to shake for an hour. The resin was thoroughly washed with (5×15 ml) dry DCM in a glass reaction vessel fitted with fritted filters by bubbling nitrogen gas. NB This step is done quickly and cautiously to avoid hydration of resin by moisture from the air. Quickly, deprotonated BAA solution was added into the resin and allowed to react for 2 hours under inert nitrogen bubbling. The resin was then washed with (5×15 ml) dry DCM and 24 ml (1 M isopropyl amine solution in DMF) was added and left to react under nitrogen bubbling for 1 hour. To the thoroughly washed resin, Fmoc-Cl (2.44 g, 9.43 mmol) solution dissolved in 8 ml (1 M DIPEA in DMF) and 9.25 ml DMF were added and allowed to react for 4 hours under nitrogen bubbling. The resin bound peptoid was washed with (5×15 ml) DMF and (3×15 ml) DCM. A cleavage solution, 50 ml of 5% TFA in DCM was used to cleave the peptoid from the resin for 30 minutes. TFA was removed from the filtered peptoid solution by adding toluene and evaporating it several times on rotary evaporator. An additional amount of DCM (100 ml) was added, and the organic phase was washed with 1 M HCl (200 ml). The organic phase was dried over anhydrous magnesium sulphate and concentrated *in vacuo*. The crude product (Fmoc-valine peptoid) was purified via column chromatography on silica gel (19:1-DCM: MeOH) to give an off-white solid peptoid : (0.505 g) with R_f 0.26 (24:1-DCM: MeOH); HRMS (ESI^+) *m/z* calculated for $C_{20}H_{22}NO_4$ is 340.1549 and found mass was 340.1539 $[M+H]^+$; ^1H NMR (300 MHz, Chloroform-*d*) δ 7.76 (d, *J* = 7.4 Hz, 2H), 7.56 (t, 2H), 7.46 – 7.27 (m, 4H), 4.59 – 4.36 (m, 3H), 4.23 (d, *J* = 22.1 Hz, 2H), 3.91 (s, 1H), 3.75 (s, 1H), 1.08 (d, *J* = 6.8 Hz, 6H)

7.2 Synthesis of PS12, PS13 and PS14

PS12 intermediate oxazolidinone was synthesized according to general procedure E using Fmoc valine (13.58 g, 40mmol, 1.0 equiv), paraformaldehyde (8 g) and *p*-toluenesulphonic acid (800 mg) were suspended in toluene (800 ml). The mixture was refluxed in a Dean-Stark setup until no more starting material could be detected by TLC (97.5:2:0.2-$CHCl_3$: MeOH: AcOH). The solution was cooled, washed with saturated $NaHCO_3$ and the organic layer was dried over anhydrous $MgSO_4$. Concentration *in vacuo* gave the crude product which in most cases solidified upon standing. Fmoc-*N*-methylated- α-valine was synthesized according to general procedure F using solution of Fmoc- protected oxazolidinone, approximately (12.93 g, 40mmol) and anhydrous $AlCl_3$ (10.67 g, 80mmol, 2.0 equiv) in dry DCM (800ml) was added TES (12.78 ml, 80 mmol, 2 equiv). The reaction was stirred at ambient temperature

until TLC (1:3 ethyl acetate/hexane) showed the absence of starting material. An additional amount of DCM (800 ml) was added, and the organic phase was washed with 1 M HCl (800 ml) NB: The total volume of product solution was divided into three aliquots to accommodate the 2 litre separating funnel which was used. The organic phase was dried over anhydrous magnesium sulphate and concentrated *in vacuo*. The crude product was purified via column chromatography on silica gel (1: 24 - MeOH: DCM) and recrystallized from ACN to give a product as a white solid: mp 190-191 °C (ACN); (13.74 g, 97.2%) with R_f 0.29 (24:1-DCM: MeOH); $[\alpha]^{20}_{D}$ (+)236.0 (*c* 0.33, DMSO); UHPLC-HRMS (ESI^+) *m/z* calculated for $C_{21}H_{24}NO_4$ is 354.1705 and found mass was 354.1699 $[M+H]^+$; Results for ^1H and ^{13}C, are as follows:

^1H NMR (500 MHz, Chloroform-*d*) δ 7.76 (2H, d, *J* = 7.6 Hz, H14; H17), 7.59 (2H, d, *J* = 7.5 Hz, H11; H20), 7.40 (2H, t, *J* = 7.3 Hz, H13; H18), 7.31 (2H, t, *J* = 7.4 Hz, H12; H19), 4.50 (2H, t, H8), 4.26 (1H, t, *J* = 6.6 Hz, H9), 4.20 (1H, d, *J* = 10.6 Hz, H2), 2.90 (3H, s, H6), 2.35 – 2.24 (1H, m, H3), 1.15 – 0.73 (6H, m, H4; H5).

^{13}C NMR (126 MHz, DMSO) δ 172.4: C1, 156.5: C7, 144.3: C10: C21, 141.3: C15; C16, 128.13: C13; C18, 127.6: C14; C17, 125.4: C12; C19, 120.6: C11; C20, 67.2: C2, 64.3: C8, 47.2: C9, 30.6: C6, 27.4, 23.2, 20.2: C4; C5

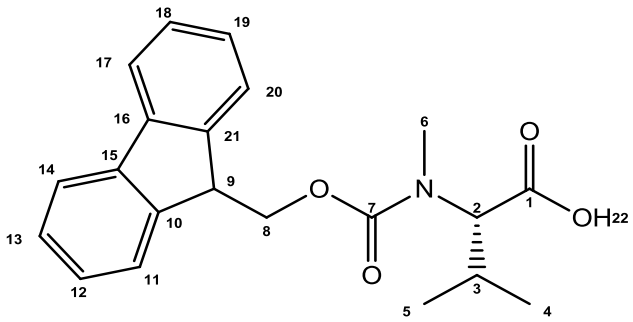


Figure 68: *N*- methylated valine structure

PS13 and ***PS14*** intermediates were synthesised according to general procedure E using (7.349 g, 20 mmol) of each amino acid respectively. General procedure F was then utilised to yield PS13 and PS14 from their respective oxazolidinone intermediates.

The crude ***PS13*** was purified via column chromatography on silica gel (24:1-DCM: methanol) and recrystallized from ACN to give a product as a white solid: mp115-116 °C

(ACN); (6.47 g, 88%) with R_f 0.28 (24:1-DCM: MeOH); $[\alpha]^{20}_D$ (-) 18.9 (*c* 0.56, DMSO); UHPLC-HRMS (ESI^+) *m/z* calculated for $C_{22}H_{26}NO_4$ is 368.1862, and found mass was 368.1855 $[M+H]^+$. Results for ^1H and ^{13}C results are as below:

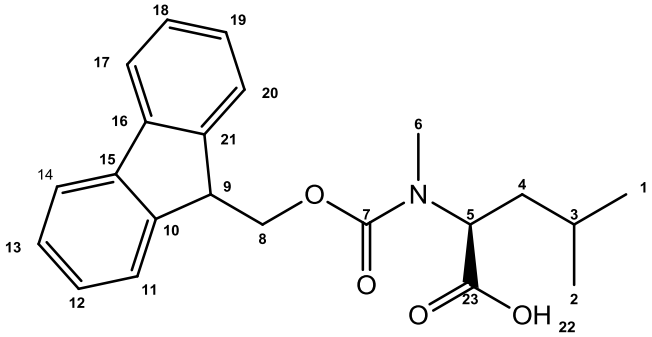


Figure 69: *N*- methylated leucine structure.

^1H NMR (400 MHz, Chloroform-*d*) δ 7.75 (2H, t, *J* = 9.9 Hz, H14; H17), 7.64 – 7.52 (2H, m, H11; H20), 7.40 (2H, t, *J* = 7.9 Hz, H13; H18), 7.31 (2H, t, H12;H19), 4.91 (1H, t, *J* = 8.0 Hz, H9), 4.47 (2H, t, H8), 4.29 (1H, t, *J* = 6.6 Hz, H5), 2.86 (3H, d, *J* = 7.4 Hz, H6), 1.75 (1H, t, *J* = 7.5 Hz, H3), 1.66 – 1.44 (2H, m, H4), 0.95 (6H, q, *J* = 9.3 Hz, H1;H2).
^{13}C NMR (101 MHz, CDCl3) δ 176.5: C23, 157.1: C7, 143.8: C10; C21, 141.4:C15; C16, 127.7: C13; C18, 127.1: C14; C17, 125.0: C12; C19, 120.0: C11; C20, 67.8: C5, 56.8: C8, 47.3: C 9, 37.2: C4, 30.5: C6, 24.9: C3, 23.2: C2, 21.3: C1; C2

The crude ***PS14*** was purified via column chromatography on silica gel (24:1-DCM: methanol) and recrystallized from ACN to give a product as a white solid: mp181-182 °C (ACN); (7.21 g, 95%) with R_f 0.26 (24:1-DCM: MeOH); $[\alpha]^{24}_D$ (-)47.25 (*c* 0.51, DMSO); UHPLC-HRMS (ESI^+) *m/z* calculated for $C_{22}H_{26}NO_4$ is 368.1862**,** found was 368.1861 $[M+H]^+$. Results for ^1H and ^{13}C are as below:

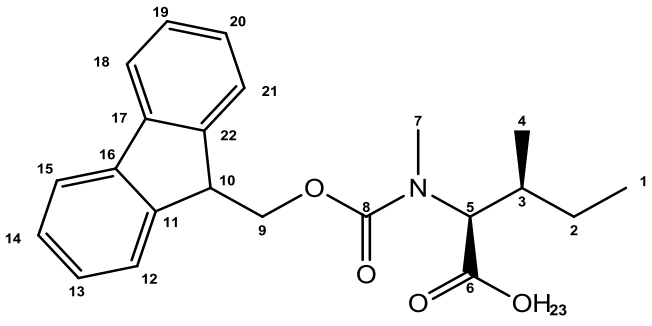


Figure 70: *N*-methylated isoleucine structure

1H NMR (500 MHz, Chloroform-*d*) δ 7.76 (2H, d, *J* = 7.3 Hz, H15; H19), 7.63 – 7.55 (2H, m, H12; H21), 7.39 (2H, q, *J* = 7.5 Hz, H14; H19), 7.30 (2H, q, *J* = 7.2 Hz, H13; H20), 4.48 (2H, t, H9), 4.38 (1H, d, *J* = 10.5 Hz, H5), 4.25 (1H, q, *J* = 10.3, 8.6 Hz, H10), 2.89 (3H, s,H7), 2.13 – 1.98 (1H, m, H3), 1.46 – 1.29 (1H, m, H2), 1.14 – 1.02 (1H, m, H2), 1.02 – 0.85 (6H, m, H1;H4). 13C NMR (126 MHz, CDCl3) δ 174.3:C6, 157.4:C8, 143.8: C11, 143.7: C22, 141.4: C16; C17, 127.8: C14, 127.7: C19, 127.1:C15; C18, 124.9: C13, 124.4:C20, 120.0:C12; C21, 67.9**:** C5, 62.7: C9, 47.3: C10, 33.3: C3, 31.8: C7, 25.1: C2, 15.7: C4, 10.7: C1.

7.3 Synthesis of PS01

PS01 was synthesized using general procedure A with the following coupling amounts. Cysteine (0.70 g, 1.20 mmol, 0.2M) and coupling reagent HBTU (0.43 g, 1.14 mmol, 0.19 M) of was dissolved in 3 ml (1.0 M DIPEA solution in DMF) and transferred into the reaction vessel where an additional 3 ml of DMF was added. The solution was mixed by bubbling nitrogen gas for 40 minutes. The solution was drained and the resin washed with (2×4 ml) DMF. Same equivalents of cysteine, HBTU and DIPEA were used again for double coupling with the same coupling time. After coupling of the first amino acid, the loading capacity was determined according to general procedure B. Resin bound cysteine was deprotected by adding (2×5 ml) 20% piperidine solution for 5 minutes and thoroughly washed with (5×4 ml) DMF. The cycle of coupling and deprotection was repeated until the final amino acid. Washing was done before deprotection was done using (3×5ml) 20% piperidine solution in DMF. PS01 was cleaved using general procedure C. Sample was dissolved in 100% DMSO (1 mg/ml) and analyzed on HRMS-direct infusion before cyclization; *m/z* (ESI^+), calculated for $C_{81}H_{131}N_{17}O_{17}S_2$ is 1678.9350 and found mass was 652.9003 $[M+H]^+$.

7.3.1 Synthesis of PS01a and PS01b

PS01a and PS01b were synthesized using the general procedure A with the following. Cysteine (0.70 g, 20 mmol, 0.2 M) and coupling reagent HATU (0.43 g, 1.14 mmol, 0.19 M) was dissolved in 3 ml (1.0 M DIPEA solution in DMF) and transferred into the reaction vessel where an additional 3 ml of DMF was added. The solution was mixed by bubbling nitrogen gas for 30 minutes. The solution was drained and the resin washed with (2×4 ml) DMF. Same equivalents of cysteine, HATU and DIPEA were used again for double coupling with the same coupling time. After coupling of the first amino acid, the loading capacity was determined according to general procedure B and found to be 0.4122 mmol/g of resin. Resin

bound cysteine was deprotected by adding (2×5 ml) 20% piperidine solution for 5 minutes and thoroughly washed with (5×4 ml) DMF. The cycle of coupling and deprotection was repeated until the 4th amino acid. Peptide bound resin was washed with (5×4 ml) DMF and (3×4ml) dry DCM and dried for 15 minutes *in vacuo*. The peptide bound resin was weighted and divided into two portions PS01a (165.1 mg) and PS01b (165.7 mg) Coupling and deprotection cycles continued parallel for both portions to the final amino acid.

For PS01a, (1.20 mmol, 0.2 M) amino acid and coupling reagent HATU (0.23 g) was dissolved in 1.5 ml (1.0M DIPEA solution in DMF) and transferred into the reaction vessel where an additional 1.5 ml DMF was added. For PS01b, (81.2 mg, 1.14 mmol, 0.19 M) OxymaPure/DIC (89 µL) was used instead of HATU and the rest of the conditions were treated as PS01a.

Final Fmoc removal was done using (2×2.5 ml) piperidine solution for 5 minutes. Iodine, 10 equivalents (0.621 mmol, 78.7 mg) was weighed and dissolved into 1:4 (H_2O: DMF) 5 ml solution to give a 0.124 M solution. The resin bound peptide was transferred to the solution and allowed to shake for 3hrs. The resin was then thoroughly washed with (4×3 ml) DMF, (3×3 ml) 2% ascorbic acid in DMF, (2×3 ml) DMF and (5×5 ml) dry DCM and dried *in vacuo* for 30 minutes. Peptides were cleaved with a 5 ml cleavage cocktail according to general procedure C. Samples for PS01a and PS01b which were sampled the final coupling and were dissolved in 100% DMSO (1 mg/ml) and analyzed on UHPLC-HRMS. The calculated (ESI^+) *m/z* for $C_{81}H_{129}N_{17}O_{17}S_2$ is 1675.9194 and found for PS01a**,** $C_{79}H_{122}N_{16}O_{16}S_2$ was 1579.6676 $[M+H]^+$ and found for PS01b**,** 1677.7456 $[M+H]^{1+}$. Analytical HPLC (C_{18} column, 2.6 µm, 4.6×150 mm) gradient elution method employing water and acetonitrile with flow rate 0.3ml/min, column temp 20 °C and detector λ 215 nm were used. Acetonitrile was allowed to increase from 30% to 60% in 20 minutes.

7.4 Synthesis of PS06, PS07, PS08, PS09 and PS10

These peptides were synthesized using the peptide synthesizer according to general method A.

7.5 Synthesis of PS15 and PS16

Since the sequence of *PS15* and *PS16* peptides were the same for the first 15 amino acids from the C-terminus, one batch of resin was used to synthesize the peptides to the 15th amino acid. We then spilt the resin bound peptide into two portions and further synthesize separately. 1.50 g of rink amide (MBHA) resin was swelled overnight in 50 ml of DMF with

gentle shaking. 4.80 mmol cysteine (2.81 g) and 0.19 M HATU (4.56 mmol, 1.73 g) were dissolved in 12 ml (1.0 M) DIPEA and transferred into the reaction vessel where an additional 12 ml of DMF was added. For the first amino acid, coupling was done for (2×1 hour) (double coupling) and washed with (3×20 ml) DMF and (3×20 ml) DCM. Loading capacity was determined according to general procedure B and found to be 0.57 mmol/g of resin. Fmoc removal was done using (2×25 ml) 20% piperidine for 5 min. After deprotection, the resin was washed with (3×20 ml) DMF and (3×20 ml) DCM. Amino acid (4.28 mmol), HATU (3.48 mmol) was dissolved in (12.5 ml, 10.70 mmol, 1.0 M DIPEA) and transferred into the reaction vessel where an additional 12.5 ml DMF was added to make a 0.2 M amino acid and 0.19 M coupling reagent concentration. Double coupling was done with each coupling taking 30 minutes. The cycle for coupling and deprotection was repeated until the 15th amino acid. Resin bound peptide was washed with (3×20 ml) DMF and (3×20 ml) DCM, dried *in vacuo* and splitted into two portion: PS15 (1.32 g) and PS16 (1.32 g). The equivalence of amino acid, DIPEA, coupling reagents and volume of DMF were reduced by a faction of 0.5 since the equivalence of the peptide was halved.

Coupling PS16 continued to the final amino acid. Iodine (0.54 g, 10 equiv) was dissolved in minimum (1:4; H_2O: DMF) and made up to 15 ml (0.29 M) and the peptide bound resin was added. The mixture was reacted for 3 hours with gentle shaking (60 rpm). The resin was thoroughly washed with (4×10 ml) DMF, (3×10 ml) 2% ascorbic acid in DMF, (2×10 ml) DMF and (5×10 ml) DCM and dried *in vacuo* for 30 minutes. Peptides were cleaved with 10ml of cleavage cocktail according to general procedure C. PS15 (3 mg) for UHPLC-HRMS analysis was dissolved in 1 ml (1:1; DMSO: ACN). DMSO was added first. Preparative HPLC, Kinetex$^{(R)}$ 5 µm B-C18, 100Å (250 ×230 mm) column gradient elution with flow rate of 15 ml/min and UV detection of 215 nm and 254 nm; buffer A, 0.1% formic acid in H_2O; buffer B, 0.1 formic acid in CH_3CN and column temp 20 °C. (90.1 mg, 12.48 % crude yield), HRMS (ESI^+) *m/z* calculated for $C_{79}H_{130}N_{18}O_{18}S_2$ is 1682.9252 and cyclic found *m/z* was 841.6746 $[M]^{2+}$ and uncyclic found *m/z was* 843.4248$[M]^{2+}$ at t_R 8.99. Analytical HPLC (C_{18} column, 2.6 µm, 4.6×150 mm) gradient elution method employing, water and acetonitrile in 10 minutes were used in the UHPLC, buffer A, 0.1% formic acid in H_2O; buffer B, 0.1 formic acid in CH_3CN and the column temperature was set to 20 °C. Acetonitrile was allowed to increase from 5 % to 70 % in 10 minutes

PS16 (2.5 mg) for UHPLC-HRMS analysis was dissolved in 1.5 ml (1:1; ACN: H2O). For the preparative HPLC, Kinetex$^{(R)}$ 5 µm B-C18, 100Å (250 ×230 mm) column gradient

elution with flow rate of 15 ml/min and UV detection of 215 nm and 254 nm; buffer A, 0.1% formic acid in H_2O; buffer B, 0.1 formic acid in CH_3CN and column temp 20 °C was used. (239.0 mg, 25.70% crude yield), HRMS (ESI^+) *m/z* calculated for $C_{101}H_{171}N_{25}O_{23}S_2$ 1084.1211 and found *m/z* was 1084.0861 $[M+2H]^{2+}$ at t_R 7.57. A gradient elution method employing water and acetonitrile in 10 minutes was used in the UHPLC, buffer A, 0.1% formic acid in H_2O; buffer B, 0.1 formic acid in CH_3CN and the column temperature was set to 20 °C. Acetonitrile was allowed to increase from 5% to 95% in 10 minutes.

7.6 Synthesis of PS17 and PS18

PS17 and PS18 were synthesized using the general procedure A the same way PS15 and PS 16 were synthesized. Rink amide (MBHA) resin (1.50 g) was used and the loading capacity was determined to be 0.5242 mmol/g of resin. After the first 15 amino acid the sample was split in two portions PS17 (1.20 g) and PS18 (1.20 g).

PS17 (1.0mg) for UHPLC-HRMS analysis was dissolved in 1.5 ml (1:1; ACN: H2O). For the preparative HPLC, Kinetex$^{(R)}$ 5 µm B-C18, 100 Å (250 ×230 mm) column gradient elution method employing water and acetonitrile in 11 minutes was used. Acetonitrile was allowed to increase with a stepped gradient from 15% to 95% in 11 minutes with flow rate of 15 ml/min and UV detection of 215 nm and 254 nm; buffer A, 0.1% formic acid in H_2O; buffer B, 0.1 formic acid in CH_3CN and the column temperature was set to 20 °C. Crude yield of 5.75% was obtained. HRMS (ESI^+) *m/z* calculated for $C_{102}H_{174}N_{26}O_{23}S_2$ is 1098.6344, found was 1099.1447 $[M+2H]^{2+}$ at t_R5.50. Analytical HPLC (C_{18} column, 2.6 µm, 4.6×150 mm) gradient elution method employing water and acetonitrile in 9 minutes was used in the UHPLC instrument with flow rate of 0.3 ml/min and UV detection of 215 nm and 254 nm; buffer A, 0.1% formic acid in H_2O; buffer B, 0.1 formic acid in CH_3CN and the column temperature was set to 20 °C. Acetonitrile was allowed to increase from 15% to 95% in 9 minutes.

PS18 (1.0 mg) for UHPLC-HRMS analysis was dissolved in 1.5 ml (1:1; ACN: H2O). Preparative HPLC, Kinetex$^{(R)}$ 5 µm B-C18, 100 Å (250 ×230 mm) column gradient elution method employing water and acetonitrile in 12 minutes was used. Acetonitrile was allowed to increase with a stepped gradient from 15% to 95% in 12 minutes with flow rate of 15 ml/min and UV detection of 215 nm and 254 nm; buffer A, 0.1% formic acid in H_2O; buffer B, 0.1% formic acid in CH_3CN and column temp 20 °C. Crude yield of (41.0 mg, 6.05%), HRMS (ESI^+) *m/z* calculated for $C_{80}H_{133}N_{19}O_{18}S_2$ is 855.9759 and *m/z* found was 857.8445

$[M+2H]^{2+}$ at t_R7.61. UHPLC (C_{18} column, 2.6 µm, 4.6×150 mm) gradient elution method employing water and acetonitrile in 10 minutes was used in the UHPLC, buffer A, 0.1% formic acid in H_2O; buffer B, 0.1 formic acid in CH_3CN and the column temperature was set to 20 °C. Acetonitrile was allowed to increase from 5% to 95% in 10 minutes.

7.7 Synthesis of PS19, PS20, PS21 and PS22

Rink amide (MBHA) resin (750.0 mg) was weighed and swelled overnight in 30 ml of DMF with gentle shaking. Cysteine (1.41 g, 2.40 mmol) and HATU (0.87 g, 2.28 mmol, 0.19 M) were dissolved in 6ml (1.0 M) DIPEA and transferred into the reaction vessel where an additional 6 ml of DMF was added. For the first amino acid, coupling was done for (2×1 hour), (double coupling) and washed with (3×10 ml DMF) and (3×10 ml DCM). Loading capacity was determined according to general procedure B and found to be 0.5578 mmol/g of resin. Fmoc protecting group was removed by (2×10ml) 20% piperidine for 5 min. After deprotection, the resin was washed with (3×10 ml) DMF and (3×10 ml) DCM. Amino acid (1.68 mmol) and (1.60 mmol, 0.61 g) of HATU was dissolved in (4.2 mmol, 4.2 ml) 1.0 M DIPEA and transferred into the reaction vessel where an additional 4.2 ml DMF was added to make a 0.2 M amino acid and 0.19M coupling reagent concentration. Double coupling was done with each coupling cycle taking 30 min. Deprotection was done after complete coupling of every amino acid with (2×7 ml) 20% piperidine in DMF for 5 minutes and washed with (5×10 ml) DMF. Coupling time for *N*-methylated amino was increased by a factor of 2 (60 minutes) per each coupling. After the 5th amino acid, HOBt (1.60 mmol, 0.2162 g) coupling reagent was added except for the coupling of *N*-methylated amino acid. The cycle of coupling and deprotection was repeated until the final amino acid. Resin bound peptide was washed with (3×10 ml DMF) and (3×10 ml DCM), dried *in vacuo* for 15 minutes. Iodine (0.53 g, 10equiv) was dissolved in minimum (1:4; H_2O: DMF) and made up to 15 ml (0.28 M) and the peptide bound resin was added. The mixture was reacted for 3hrs with gentle shaking (90 rpm). The resin was thoroughly washed with (4×10 ml) DMF, (3× 10ml) 2% ascorbic acid in DMF, (2×10 ml) DMF and (5×10 ml) DCM and dried *in vacuo* for 30 minutes. Peptide was cleaved with 15ml of cleavage cocktail according to general procedure C. Peptide (≈1 mg) for UHPLC-HRMS analysis was dissolved in 1ml (1:1; DMSO: ACN). HRMS (ESI^+) *m/z* calculated for $C_{104}H_{175}N_{23}O_{23}S_2$ is 2178.2673 and found *m/z* for 13 amino acid was 1483.7344 $[M+H]^+$.

PS20, PS21 and PS22 were synthesized using the general procedure A the same way PS19 was synthesized. Rink amide (MBHA) resin (0.750 g) was used for each, PS20 and PS21 and

the loading capacities were 0.5771 mmol/g of resin and 0.5244 mmol/g of resin respectively. HRMS (ESI^+) *m/z* calculated for PS20, $C_{108}H_{184}N_{24}O_{23}S_2$ is 2249.3408 and found for 14 amino acid was 1653.8767 $[M+H]^+$. HRMS (ESI^+) *m/z* calculated for PS21 $C_{111}H_{190}N_{24}O_{23}S_2$ is 2292.3877 found *m/z* for 8 amino acid $C_{52}H_{84}N_{10}O_9S_2$ was 1025.6215$[M+H]^+$.

REFERENCES

(1) Lee, H.; Suh, J.-W. *Journal of Industrial Microbiology & Biotechnology* **2016**, *43*, 205.

(2) Ramón-García, S.; Mikut, R.; Ng, C.; Ruden, S.; Volkmer, R.; Reischl, M.; Hilpert, K.; Thompson, C. J. *Antimicrobial Agents and Chemotherapy* **2013**, *57*, 2295.

(3) "Global tuberculosis report 2017," World Health Organization, 2018.

(4) Ozeki, Y.; Igarashi, M.; Doe, M.; Tamaru, A.; Kinoshita, N.; Ogura, Y.; Iwamoto, T.; Sawa, R.; Umekita, M.; Enany, S.; Nishiuchi, Y.; Osada-Oka, M.; Hayashi, T.; Niki, M.; Tateishi, Y.; Hatano, M.; Matsumoto, S. *Plos One* **2015**, *10*, 2

(5) Quan, D.; Nagalingam, G.; Payne, R.; Triccas, J. A. *International Journal of Infectious Diseases* **2017**, *56*, 212.

(6) Zumla, A.; Raviglione, M.; Hafner, R.; von Reyn, C. F. *The New England Journal of Medicine* **2013**, *368*, 745.

(7) Banuls, A.-L.; Sanou, A.; Van Anh, N. T.; Godreuil, S. *Journal of Medical Microbiology* **2015**, *64*, 1261.

(8) Fosgerau, K.; Hoffmann, T. *Drug Discovery Today* **2015**, *20*, 122.

(9) Ramírez-Lapausa, M.; Menéndez-Saldaña, A.; Noguerado-Asensio, A. *Rev Esp Sanid Penit* **2015**, *17*, 3.

(10) Akopian, T.; Kandror, O.; Raju, R. M.; Unni Krishnan, M.; Rubin, E. J.; Goldberg, A. L. *The EMBO Journal* **2012**, *31*, 1529.

(11) Jung, I.-P.; Ha, N.-R.; Kim, A.-R.; Kim, S.-H.; Yoon, M.-Y. *International Journal of Biological Macromolecules* **2017,** *101*, 348.

(12) Kolyva, A. S.; Karakousis, P. C. *Old and New TB Drugs: Mechanisms of Action and Resistance*, **2012**, 209

(13) Lear, S.; Munshi, T.; Hudson, A.; Hatton, C.; Clardy, J.; Mosely, J.; Bull, T.; Sit, C.; Cobb, S. *Organic & Biomolecular Chemistry* **2016**, *14*, 4534.

(14) Famulla, K.; Sass, P.; Malik, I.; Akopian, T.; Kandror, O.; Alber, M.; Hinzen, B.; Ruebsamen-Schaeff, H.; Kalscheuer, R.; Goldberg, A. L. *Molecular Microbiology* **2016,** *101(2)*, 194.

(15) Luis M. Deleon Rodriguez, H. K. a. M. A. B. *Royal Society of Chemistry* **2015**, *14*, 1177.

(16) Arbex, M. A.; Varella, M. d. C. L.; Siqueira, H. R. d.; Mello, F. A. F. d. *Journal of Brazil Pneumol* **2010**, *36*, 626.

(17) Medicine, E. J. C. a. M. D. A. P. o. "TB and CoMorbidities Challenges and Opportunities," Brown University Providence, Rhodes Island **2012**, 1

(18) https://www.niaid.nih.gov/diseases-conditions/tbdrugs accessed on 30/03/2018.

(19) Gao, W.; Kim, J.-Y.; Chen, S.-N.; Cho, S.-H.; Choi, J.; Jaki, B. U.; Jin, Y.-Y.; Lankin, D. C.; Lee, J.-E.; Lee, S.-Y. *Organic Letters* **2014**, *16*, 6044.

(20) Parish, T. *Chemistry & Biology* **2014**, *21*, 437.

(21) Gao, W.; Kim, J.-Y.; Anderson, J. R.; Akopian, T.; Hong, S.; Jin, Y.-Y.; Kandror, O.; Kim, J.-W.; Lee, I.-A.; Lee, S.-Y. *Antimicrobial Agents and Chemotherapy* **2015**, *59*, 880.

(22) Conlon, B. P.; Nakayasu, E. S.; Fleck, L. E.; LaFleur, M. D.; Isabella, V. M.; Coleman, K.; Leonard, S. N.; Smith, R. D.; Adkins, J. N.; Lewis, K. *Nature (London, U. K.)* **2013**, *503*, 365.

(23) Ingvarsson, H.; Maté, M. J.; Högbom, M.; Portnoï, D.; Benaroudj, N.; Alzari, P. M.; Ortiz-Lombardía, M.; Unge, T. *Acta Crystallographica Section D: Biological Crystallography* **2007**, *63*, 249.

(24) Schmitz, K. R.; Carney, D. W.; Sello, J. K.; Sauer, R. T. *Proceedings of the National Academy of Sciences* **2014**, *111*, E4587.

(25) Vasudevan, D.; Rao, S. P.; Noble, C. G. *Journal of Biological Chemistry* **2013**, *288*, 30883.

(26) Moreira, W.; Ngan, G. J. Y.; Low, J. L.; Poulsen, A.; Chia, B. C. S.; Ang, M. J. Y.; Yap, A.; Fulwood, J.; Lakshmanan, U.; Lim, J.; Khoo, A. Y. T.; Flotow, H.; Hill, J.; Raju, R. M.; Rubin, E. J.; Dick, T. *Microbiology* **2015**, *6*.

(27) Schmitt, E. K.; Riwanto, M.; Sambandamurthy, V.; Roggo, S.; Miault, C.; Zwingelstein, C.; Krastel, P.; Noble, C.; Beer, D.; Rao, S. P. S.; Au, M.; Niyomrattanakit, P.; Lim, V.; Zheng, J.; Jeffery, D.; Pethe, K.; Camacho, L. R. *Angewandte Chemie International Edition* **2011**, *50*, 5889.

(28) Kang, S.-J.; Kim, D.-H.; Mishig-Ochir, T.; Lee, B.-J. *Archives of Pharmacal Research* **2012**, *35*, 409.

(29) Seo, M.-D.; Won, H.-S.; Kim, J.-H.; Mishig-Ochir, T.; Lee, B.-J. *Molecules* **2012**, *17*, 12276.

(30) Tam, J.; Wang, S.; Wong, K.; Tan, W. *Pharmaceuticals* **2015**, *8*, 711.

(31) Kumar, P.; Kizhakkedathu, J.; Straus, S. *Biomolecules* **2018**, *8*, 4.

(32) Le, C.-F.; Fang, C.-M.; Sekaran, S. D. *Antimicrobial Agents and Chemotherapy* **2017**, AAC. 02340.

(33) Pushpanathan, M.; Gunasekaran, P.; Rajendhran, J. *International Journal of Peptides* **2013**, 1.

(34) Lee, T.-H.; N Hall, K.; Aguilar, M.-I. *Current Topics in Medicinal Chemistry* **2016**, *16*, 25.

(35) Ageitos, J.; Sánchez-Pérez, A.; Calo-Mata, P.; Villa, T. *Biochemical Pharmacology* **2017**, *133*, 117.

(36) Shai, Y. *Peptide Science: Original Research on Biomolecules* **2002**, *66*, 236.

(37) Petrou, C.; Sarigiannis, Y. In *Peptide Applications in Biomedicine, Biotechnology and Bioengineering*; Elsevier: 2018, 1.

(38) Zhao, H., MSc Dessertation, University of Helsinki, 2003.

(39) Bechinger, B.; Gorr, S.-U. *Journal of Dental Research* **2017**, *96*, 254.

(40) Khusro, A.; Aarti, C.; Agastian, P. *Asian Pacific Journal of Tropical Medicine* **2016**, *9*, 1023.

(41) Zhao, N.; Pan, Y.; Cheng, Z.; Liu, H. *Amino Acids* **2016**, *48*, 1347.

(42) Maksimov, M. O.; Pan, S. J.; Link, A. J. *Natural Product Reports* **2012**, *29*, 996.

(43) Dong, M.; Pfeiffer, B.; Altmann, K.-H. *Drug Discovery Today* **2017**, *22*, 585.

(44) Harris, P. W.; Cook, G. M.; Leung, I. K.; Brimble, M. A. *Australian Journal of Chemistry* **2017**, *70*, 172.

(45) Martin-Gómez, H.; Tulla-Puche, J. *Organic & Biomolecular Chemistry* **2018**, *16*, 5065.

(46) Gavrish, E.; Sit, C. S.; Cao, S.; Kandror, O.; Spoering, A.; Peoples, A.; Ling, L.; Fetterman, A.; Hughes, D.; Bissell, A. *Chemistry & Biology* **2014**, *21*, 509.

(47) Barbie, P.; Kazmaier, U. *Organic Letters* **2015**, *18*, 204.

(48) Montalbetti, C. A.; Falque, V. *Tetrahedron* **2005**, *61*, 10827.

(49) Valeur, E.; Bradley, M. *Chemical Society Reviews* **2009**, *38*, 606.

(50) KVSRG, P.; Bharathi, K.; Haseena Banu, B. *International Journal of Pharmaceutical Sciences Review and Research* **2011**, *8*, 108.

(51) El-Faham, A.; Albericio, F. *Chemical Reviews* **2011**, *111*, 6557.

(52) Marder, O.; Albericio, F. *Chimica Oggi* **2003**, *21*, 35.

(53) Al-Warhi, T. I.; Al-Hazimi, H. M.; El-Faham, A. *Journal of Saudi Chemical Society* **2012**, *16*, 97.

(54) Subirós-Funosas, R.; Khattab, S. N.; Nieto-Rodriguez, L.; El-Faham, A.; Albericio, F. *Aldrichim Acta* **2013**, *46*, 21.

(55) Han, S.-Y.; Kim, Y.-A. *Tetrahedron* **2004**, *60*, 2447.

(56) Takahashi, D.; Yamamoto, T. *Tetrahedron Letters* **2012**, *53*, 1936.

(57) Okada, Y. *Current Organic Chemistry* **2001**, *5*, 1.

(58) Chandrudu, S.; Simerska, P.; Toth, I. *Molecules* **2013**, *18*, 4373.

(59) Agyei, D.; Ahmed, I.; Akram, Z.; MN Iqbal, H.; K Danquah, M. *Protein and Peptide Letters* **2017**, *24*, 94.

(60) Jebara, K. B.; Cáceres, P.; Berlingieri, F.; Weber-Vintzel, L. *Preventive Veterinary Medicine* **2012**, *107*, 149.

(61) Palasek, S. A.; Cox, Z. J.; Collins, J. M. *Journal of Peptide Science: An Official Publication of The European Peptide Society* **2007**, *13*, 143.

(62) Pedersen, S. L.; Tofteng, A. P.; Malik, L.; Jensen, K. J. *Chemical Society Reviews* **2012**, *41*, 1826.

(63) Abu-Baker, S.; Garber, P.; Hina, B.; Reed, T.; Shahrokh, G.; Al-Saghir, M.; Lorigan, G. *Open Journal of Synthesis Theory and Applications* **2013**, *3*, 1.

(64) Kumar, A.; Jad, Y. E.; Collins, J. M.; Albericio, F.; de la Torre, B. G. *ACS Sustainable Chemistry & Engineering* **2018**, *6*, 8034.

(65) Coantic, S.; Subra, G.; Martinez, J. *International Journal of Peptide Research and Therapeutics* **2008**, *14*, 143.

(66) Collins, J. M.; Singh, S. K.; Vanier, G. S. *Chemicca Oggi/Chemistry Today* **2012**, *30*.

(67) Erdelyi, M.; Gogoll, A. *Synthesis* **2002**, *2002*, 1592.

(68) Luna, O. F.; Gomez, J.; Cárdenas, C.; Albericio, F.; Marshall, S. H.; Guzmán, F. *Molecules* **2016**, *21*, 1542.

(69) Mitchell, A. R. *Peptide Science* **2008**, *90*, 175.

(70) Fields, G. B. *Current Protocols in Protein Science* **2001**, *26*, 18.1. 1.

(71) Ralhan, K.; KrishnaKumar, V. G.; Gupta, S. *RSC Advances* **2015**, *5*, 104417.

(72) Lopez, J.; Pletscher, S.; Aemissegger, A.; Bucher, C.; Gallou, F. *Organic Process Research & Development* **2018**, *22*, 494.

(73) Shelton, P. T.; Jensen, K. J. *Peptide Synthesis and Applications* **2013**, 23.

(74) https://www.purolite.com/dam/jcr:6c02cac8-fd4a-41e6-a839-ee27651b6628/(UC238)%20PuroSynth%20Brochure%20250518%20HW%20WEB.pdf. accessed on 02/05/2019.

(75) https://www.peptide.com/resins-solid-phase-peptide-synthesis-core-resins-i-250.html. accessed on 02/05/2019.

(76) King, D. S.; FIELDS, C. G.; FIELDS, G. B. *International Journal of Peptide and Protein Research* **1990**, *36*, 255.

(77) Fields, C. G.; Fields, G. B. *Tetrahedron Letters* **1993**, *34*, 6661.

(78) Pearson, D. A.; Blanchette, M.; Baker, M. L.; Guindon, C. A. *Tetrahedron Letters* **1989**, *30*, 2739.

(79) Eritja, R.; Ziehler-Martin, J. P.; Walker, P. A.; Lee, T. D.; Legesse, K.; Albericio, F.; Kaplan, B. E. *Tetrahedron* **1987**, *43*, 2675.

(80) Akaji, K.; Yoshida, M.; Tatsumi, T.; Kimura, T.; Fujiwara, Y.; Kiso, Y. *Journal of the Chemical Society, Chemical Communications* **1990**, 288.

(81) Hughes, J.; Leopold, E. *Peptide Research* **1995**, *8*, 298.

(82) Atherton, E. *A Practical Approach* **1989**.

(83) Yang, Y. *Side reactions in peptide synthesis*; Academic Press, 2015.

(84) Isidro-Llobet, A.; Alvarez, M.; Albericio, F. *Chemical Reviews* **2009**, *109*, 2455.

(85) Mahajan, A.; Rawat, A. S.; Bhatt, N.; Chauhan, M. K. *Indian Journal of Pharmaceutical Education and Research* **2014**, *48*, 34.

(86) Adessi, C.; Soto, C. *Current Medicinal Chemistry* **2002**, *9*, 963.

(87) Di, L. *The American Association of Pharmaceutical Scientists Journal* **2015**, *17*, 134.

(88) Hruby, V. J.; Balse, P. *Current Medicinal Chemistry* **2000**, *7*, 945.

(89) Zhang, S.; Govender, T.; Norström, T.; Arvidsson, P. I. *The Journal of Organic Chemistry* **2005**, *70*, 6918.

(90) Davies, J. S. *Journal of Peptide Science: An Official Publication of the European Peptide Society* **2003**, *9*, 471.

(91) Kale, S. S.; Villequey, C.; Kong, X.-D.; Zorzi, A.; Deyle, K.; Heinis, C. *Nature Chemistry* **2018,** *10*,715.

(92) White, C. J.; Yudin, A. K. *Nature Chemistry* **2011**, *3*, 509.

(93) Malesevic, M.; Strijowski, U.; Bächle, D.; Sewald, N. *Journal of biotechnology* **2004**, *112*, 73.

(94) Mazur, S.; Jayalekshmy, P. *Journal of the American Chemical Society* **1979**, *101*, 677.

(95) Werle, M.; Bernkop-Schnürch, A. *Amino Acids* **2006**, *30*, 351.

(96) Yin, N.; Brimble, M. A.; Harris, P. W.; Wen, J. *Journal of Medicinal Chemistry* **2014**, *764,765*.

(97) Mojsoska, B.; Carretero, G.; Larsen, S.; Mateiu, R. V.; Jenssen, H. *Scientific Reports* **2017**, *7*, 42332.

(98) Webster, A. M.; Cobb, S. L. *Chemistry–A European Journal* **2018**, *24*, 7560.

(99) Miller, S. M.; Simon, R. J.; Ng, S.; Zuckermann, R. N.; Kerr, J. M.; Moos, W. H. *Bioorganic & Medicinal Chemistry Letters* **1994**, *4*, 2657.

(100) Antosova, Z.; Mackova, M.; Kral, V.; Macek, T. *Trends in Biotechnology* **2009**, *27*, 628.

(101) Bray, B. L. *Nature Reviews Drug Discovery* **2003**, *2*, 587.

(102) Singh, R.; Singh, S.; Lillard, J. W. *Journal of Pharmaceutical Sciences* **2008**, *97*, 2497.

(103) Hawkins, P. M.; Giltrap, A. M.; Nagalingam, G.; Britton, W. J.; Payne, R. J. *Organic Letters* **2018**, *20*, 1019.

(104) Sax, P. E.; Losina, E.; Weinstein, M. C.; Paltiel, A. D.; Goldie, S. J.; Muccio, T. M.; Kimmel, A. D.; Zhang, H.; Freedberg, K. A.; Walensky, R. P. *JAIDS Journal of Acquired Immune Deficiency Syndromes* **2005**, *39*, 69.

(105) Steinbrook, R. *New England Journal of Medicine* **2003**, *348*, 2171.

(106) Henninot, A.; Collins, J. C.; Nuss, J. M. *Journal of Medicinal Chemistry* **2017**,*61*, 1384.

(107) Witt, K. A.; Gillespie, T. J.; Huber, J. D.; Egleton, R. D.; Davis, T. P. *Peptides* **2001**, *22*, 2329.

(108) Li, P.; Roller, P. P. *Current Topics in Medicinal Chemistry* **2002**,*2*, 325-341.

(109) Andreu, D.; Albericio, F.; Solé, N. A.; Munson, M. C.; Ferrer, M.; Barany, G. *Peptide Synthesis Protocols* **1995**, *35*, 91.

(110) Guzmán, F.; Barberis, S.; Illanes, A. *Electronic Journal of Biotechnology* **2007**, *10*, 279.

(111) Jou, G.; González, I.; Albericio, F.; Lloyd-Williams, P.; Giralt, E. *The Journal of Organic Chemistry* **1997**, *62*, 354.

(112) Giralt, E.; Rizo, J.; Pedroso, E. *Tetrahedron* **1984**, *40*, 4141.

(113) Meister, S.; Kent, S. In *Proceedings of the 8th American Peptide Symposium*

1983, 103.

(114) El-Faham, A.; Al Marhoon, Z.; Abdel-Megeed, A.; Albericio, F. *Molecules* **2013**, *18*, 14747.

(115) Gleason, N. J.; Vostrikov, V. V.; Greathouse, D. V.; Grant, C. V.; Opella, S. J.; Koeppe, R. E. *Biochemistry* **2012**, *51*, 2044.

(116) Levin, S.; Nowick, J. S. *Journal of the American Chemical Society* **2007**, *129*, 13043.

(117) Nowick, J. S. *Accounts of Chemical Research* **2008**, *41*, 1319.

(118) Jäkel, C. E.; Meschenmoser, K.; Kim, Y.; Weiher, H.; Schmidt-Wolf, I. G. *In Vivo* **2012**, *26*, 419.

(119) Ko, Y. T.; Falcao, C.; Torchilin, V. P. *Molecular Pharmaceutics* **2009**, *6*, 971.

(120) Rana, N.; Huang, S.; Patel, P.; Samuni, U.; Sabatino, D. *Bioorganic & Medicinal Chemistry Letters* **2016**, *26*, 3567.

(121) Onuchic, J. N.; Jennings, P. A.; Ben-Jacob, E. *Proceedings of the National Academy of Sciences* **2013**, *110*, 3212.

(122) https://www.chemicalbook.com/ProductList_En.aspx?kwd=Fmoc-N-methyl-L-isoleucine acccessed on 02/05/2019.

(123) Trent, A.; Marullo, R.; Lin, B.; Black, M.; Tirrell, M. *Soft Matter* **2011**, *7*, 9572.

(124) https://www.thermofisher.com/za/en/home/life-science/protein-biology/protein-biology-learning-center/protein-biology-resource-library/pierce-protein-methods/peptide-design.html acccesed on 29/01/2019.

(125) Milton, R. d. L.; Milton, S. C.; Adams, P. A. *Journal of the American Chemical Society* **1990**, *112*, 6039.

(126) Bruno, B. J.; Miller, G. D.; Lim, C. S. *Therapeutic Delivery* **2013**, *4*, 1443.

(127) Coste, J.; Frerot, E.; Jouin, P. *The Journal of Organic Chemistry* **1994**, *59*, 2437.

(128) Marcucci, E.; Tulla-Puche, J.; Albericio, F. *Organic Letters* **2011**, *14*, 612.

(129) Kopple, K. D. *Journal of Pharmaceutical Sciences* **1972**, *61*, 1345.

(130) Zarai, Z.; Kadri, A.; Chobba, I. B.; Mansour, R. B.; Bekir, A.; Mejdoub, H.; Gharsallah, N. *Lipids in Health and Disease* **2011**, *10*, 161.

(131)https://www.chemicalbook.com/ChemicalProductProperty_EN_CB5663927.htm accessed on 02/05/2019.

(132) https://www.chemicalbook.com/ProductList_en.aspx?kwd=Fmoc-N-methyl-L-leucine accesed on 02/05/2019.

(133) Zuckermann, R. N. *Peptide Science* **2011**, *96*, 545.

(134) Gangloff, N.; Ulbricht, J.; Lorson, T.; Schlaad, H.; Luxenhofer, R. *Chemical Reviews* **2015**, *116*, 1753.

(135) Jenkins, S. G.; Schuetz, A. N. In *Mayo Clinic Proceedings*; Elsevier: 2012; *87*, 290-301.

(136) https://www.anaspec.com/html/peptide_tips.html. accesed on 02/05/2019.

APPENDIX

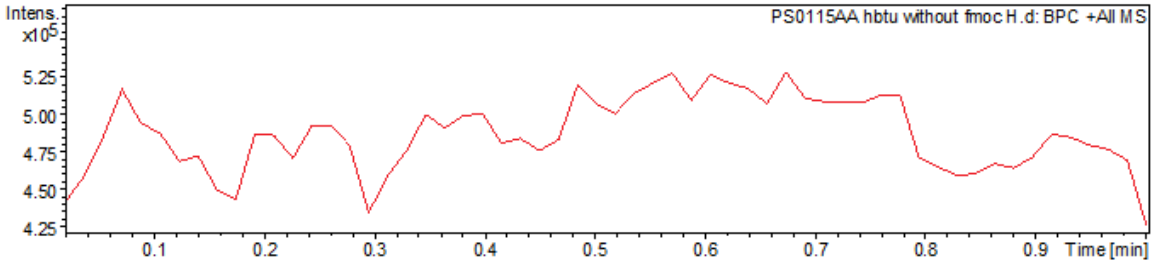
Display Report

Analysis Info

AnalysisName	D:\Data\Maya\Runs\PS0115AA hbtu without fmoc H.d	Acquisition Date	12/9/2016 11:41:14 AM
Method	Tune_pos_High.m	Operator	BDAL@DE
SampleName	PS0115AA hbtu without fmoc H	Instrument	compact 8255754.20116
Comment			

Acquisition Parameter

Source Type	ESI	Ion Polarity	Positive	Set Nebulizer	0.3 Bar
Focus	Active	Set Capillary	3200 V	Set Dry Heater	200 °C
Scan Begin	50 m/z	Set End Plate Offset	-500 V	Set Dry Gas	3.0 l/min
Scan End	3000 m/z	Set Charging Voltage	2000 V	Set Divert Valve	Source
		Set Corona	0 nA	Set APCI Heater	0 °C



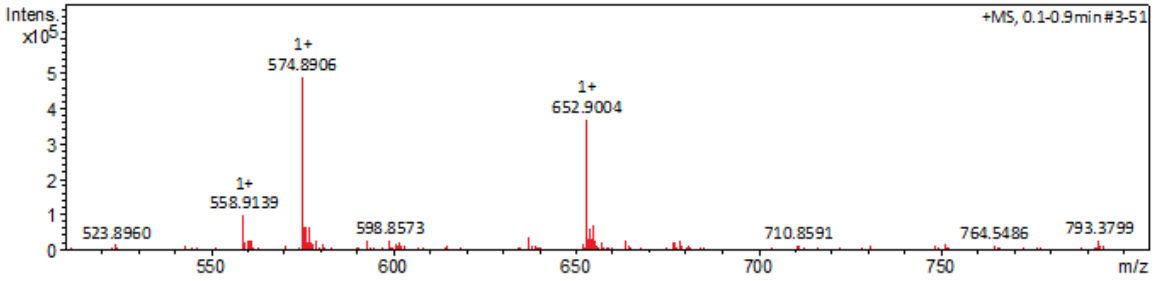


Figure 71: MS results for PS01 using HBTU coupling reagent.

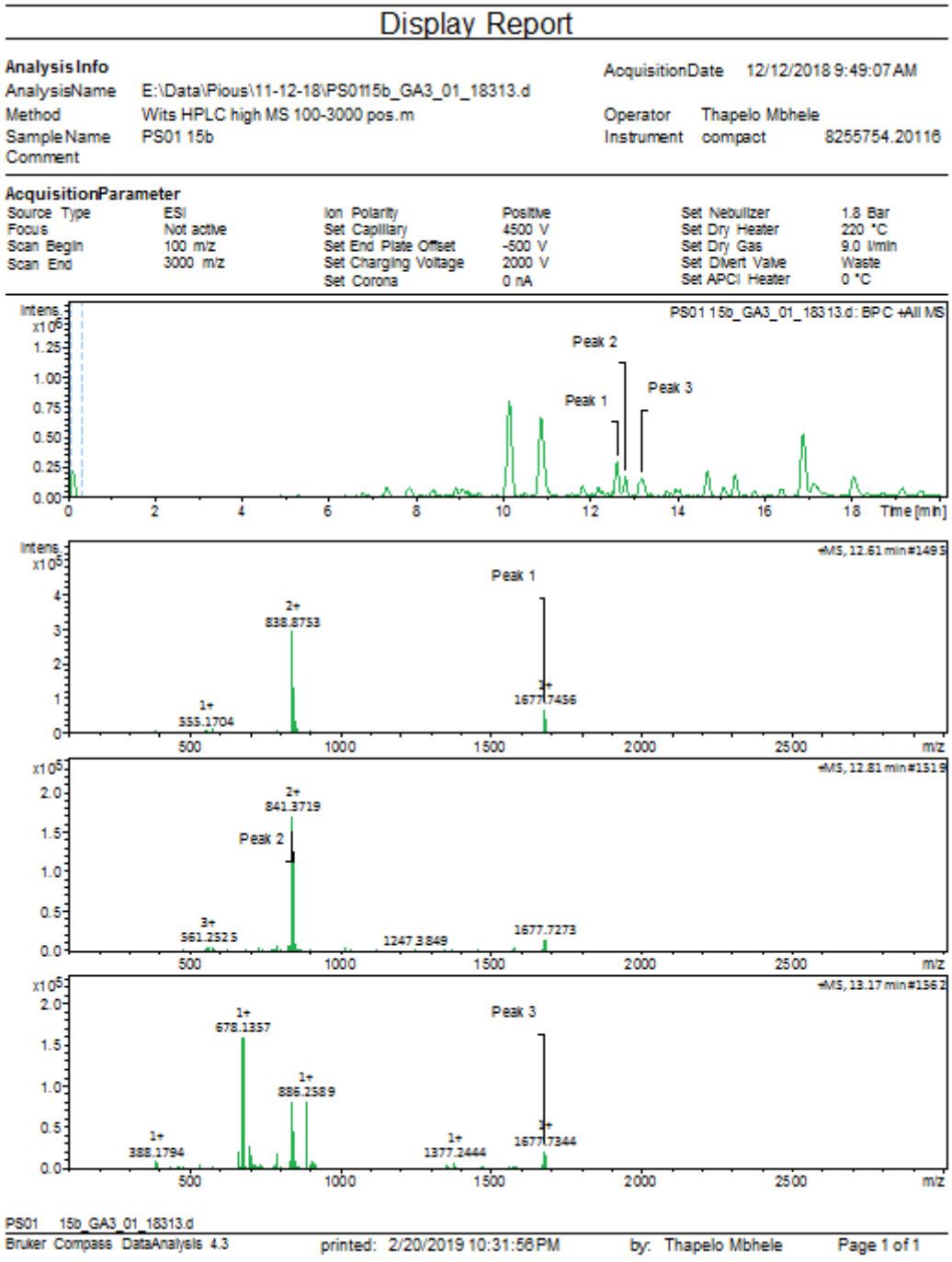


Figure 72: LC-MS results for PS01 sing OxymaPure coupling reagent.

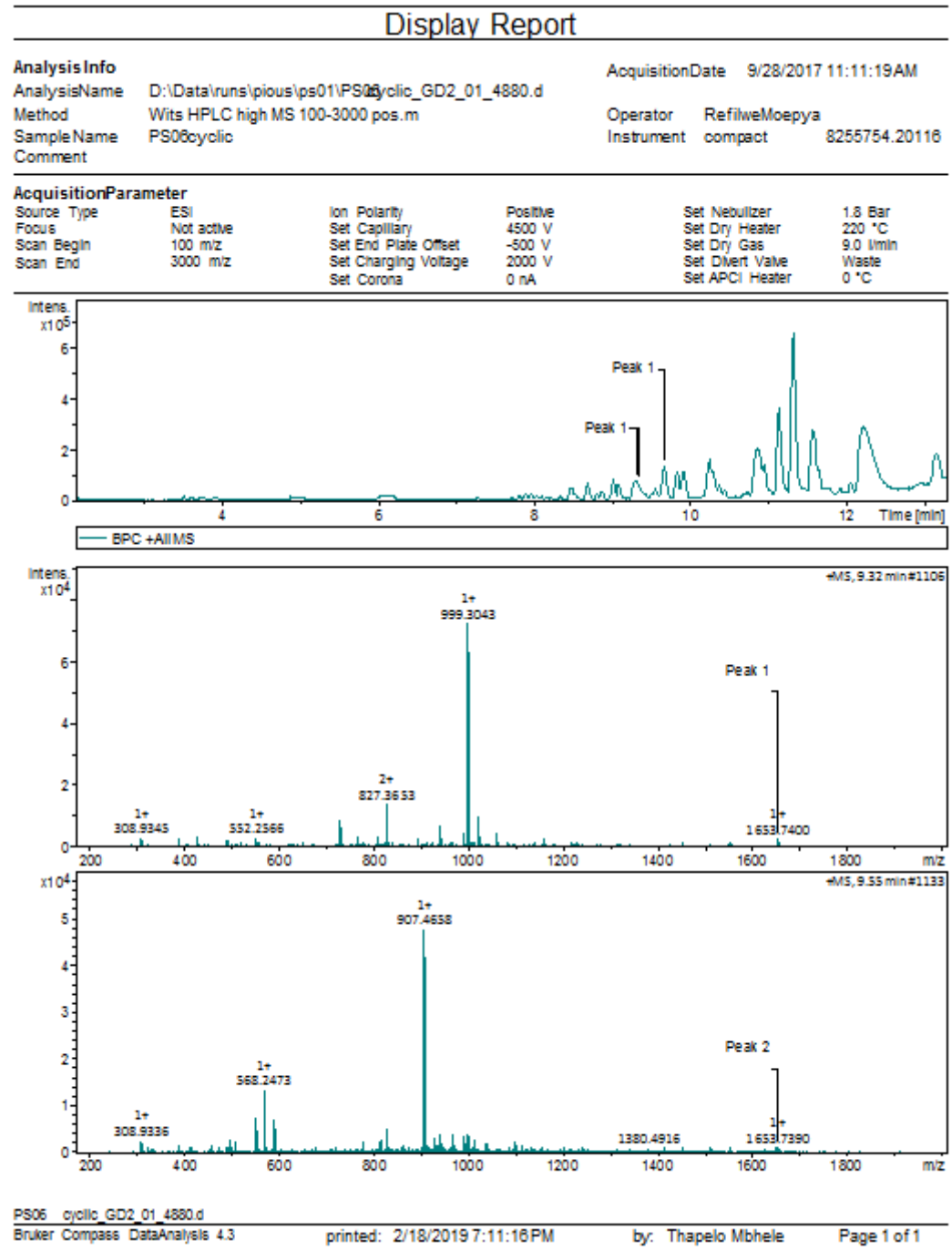


Figure 73: LC-MS results for PS06.

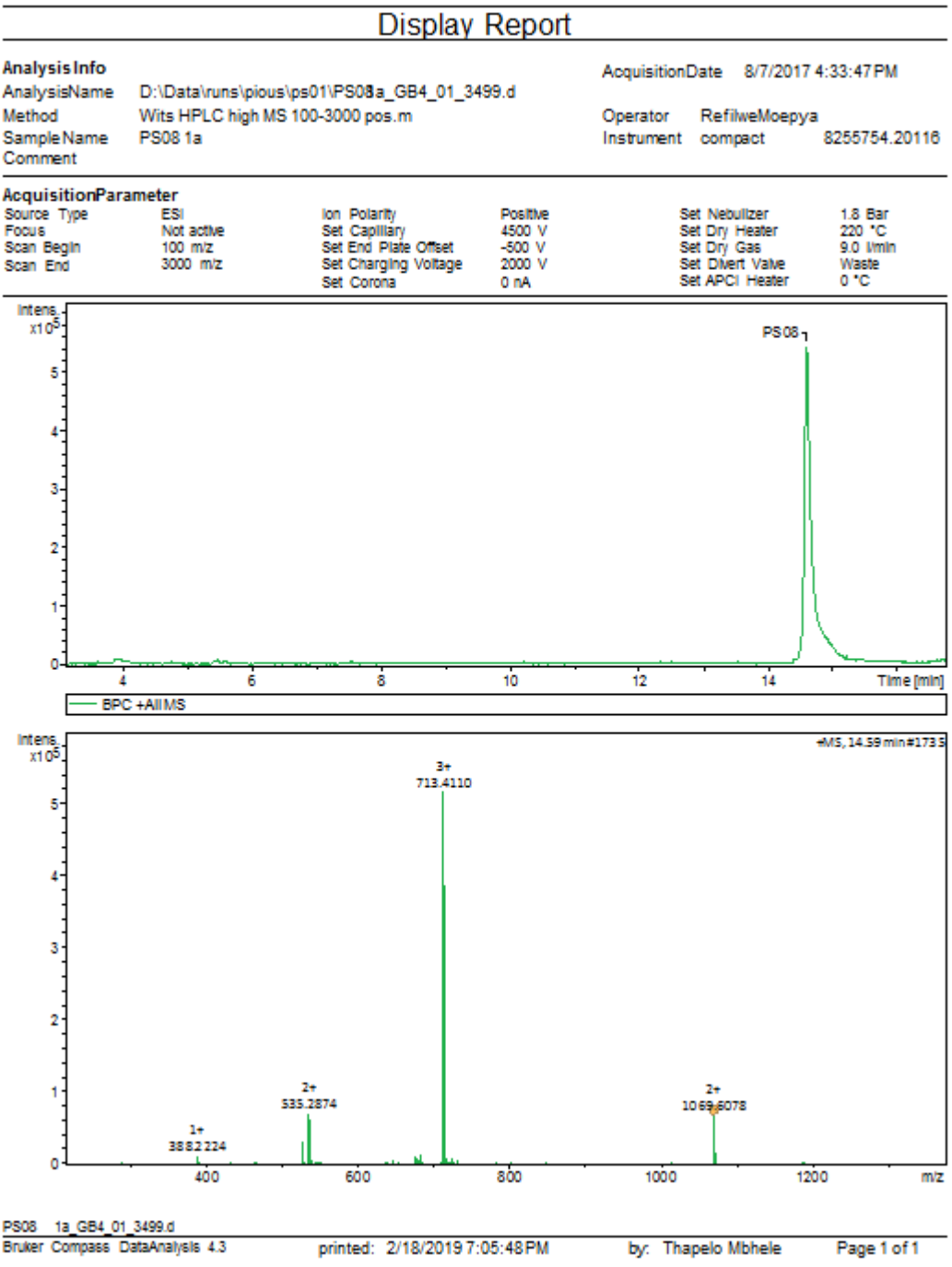


Figure 74: LC-MS for PS08.

Display Report

Analysis Info

Analysis Name	D:\Data\Runs\Pious\11-09-2018\PS19 14 nfm_GC5_01_13711.d	Acquisition Date	9/11/2018 9:19:26 PM
Method	Loop Mid 100-3000.m	Operator	Thapelo Mbhele
Sample Name	PS19 14 nfm	Instrument	compact 8255754.20116
Comment			

Acquisition Parameter

Source Type	ESI	Ion Polarity	Positive	Set Nebulizer	1.8 Bar
Focus	Not active	Set Capillary	4500 V	Set Dry Heater	220 °C
Scan Begin	100 m/z	Set End Plate Offset	-500 V	Set Dry Gas	9.0 l/min
Scan End	3000 m/z	Set Charging Voltage	2000 V	Set Divert Valve	Waste
		Set Corona	0 nA	Set APCI Heater	0 °C

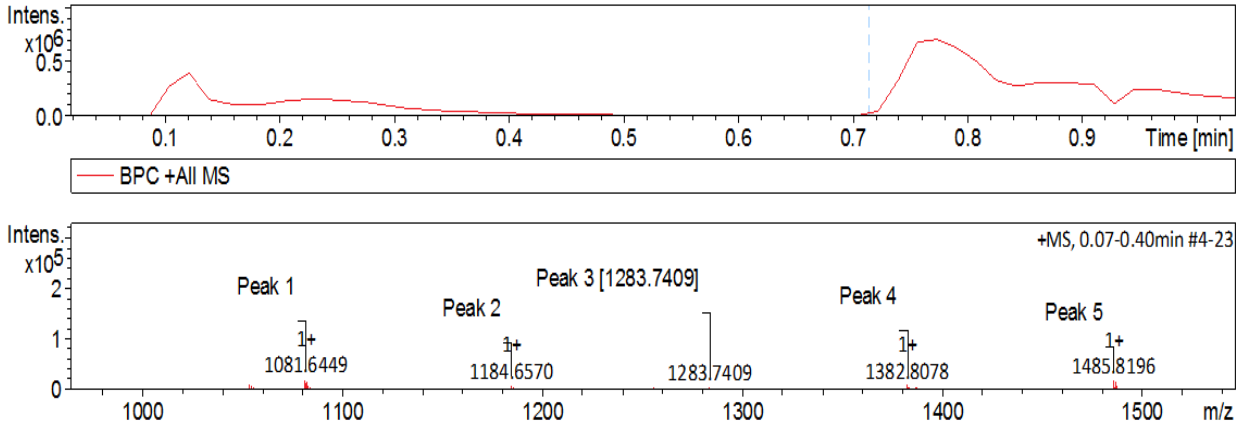


Figure 75: MS results for PS19-14 amino acid sequence.

Display Report

Analysis Info

Analysis Name	E:\Data\Pious\12-09-2018\PS20 14nfm_GC6_01_13727.d	Acquisition Date	9/12/2018 12:31:42 PM
Method	Loop Mid 100-3000.m	Operator	Thapelo Mbhele
Sample Name	PS20 14nfm	Instrument	compact 8255754.20116
Comment			

Acquisition Parameter

Source Type	ESI	Ion Polarity	Positive	Set Nebulizer	1.8 Bar
Focus	Not active	Set Capillary	4500 V	Set Dry Heater	220 °C
Scan Begin	100 m/z	Set End Plate Offset	-500 V	Set Dry Gas	9.0 l/min
Scan End	3000 m/z	Set Charging Voltage	2000 V	Set Divert Valve	Waste
		Set Corona	0 nA	Set APCI Heater	0 °C

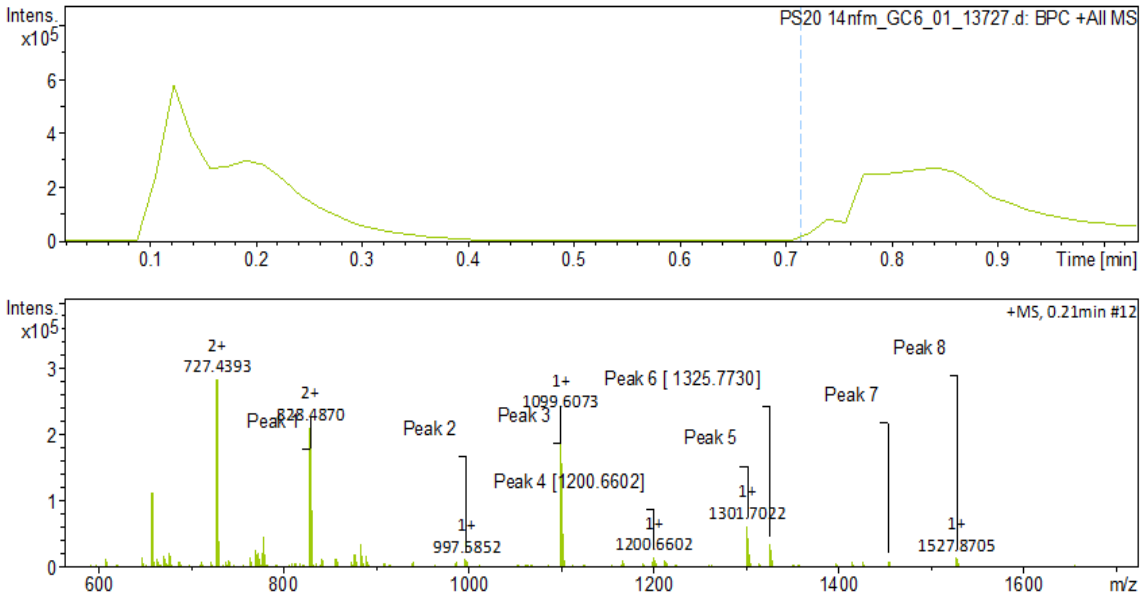


Figure 76: MS results for PS20-14 amino acid sequence.

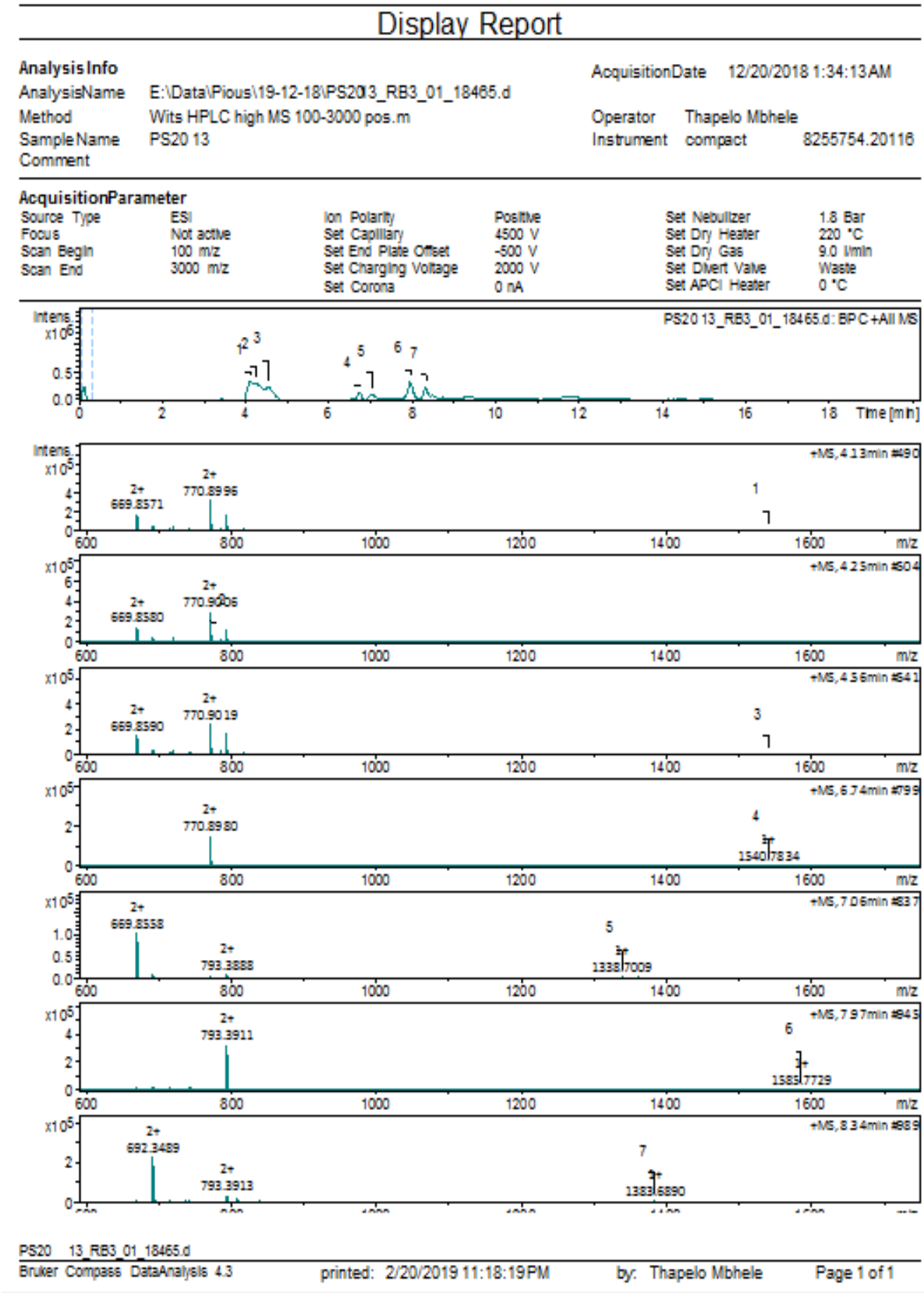


Figure 77: LCMS results for PS20-13 amino acid sequence.

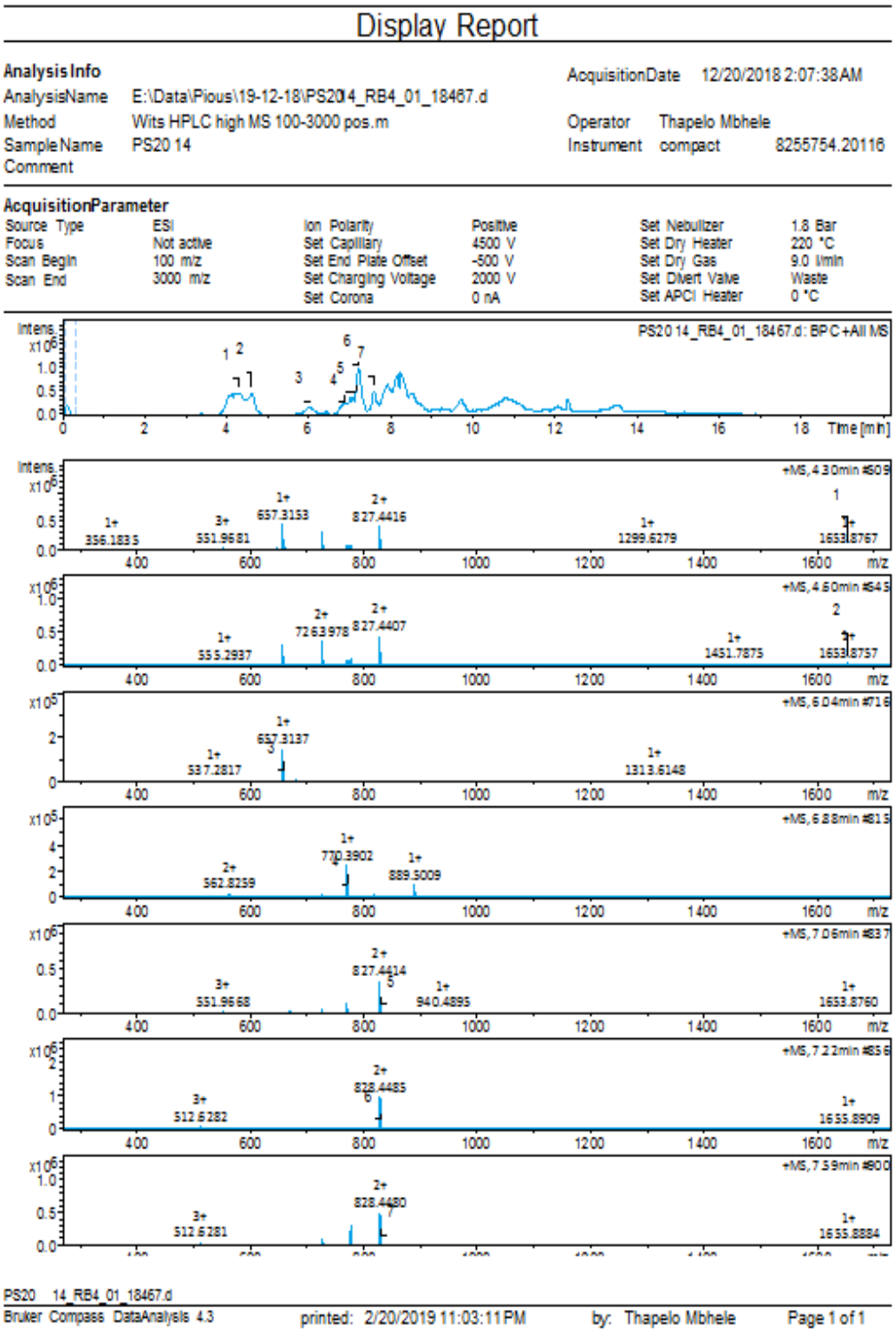


Figure 78: LCMS for PS20-14 amino acid sequence 1.

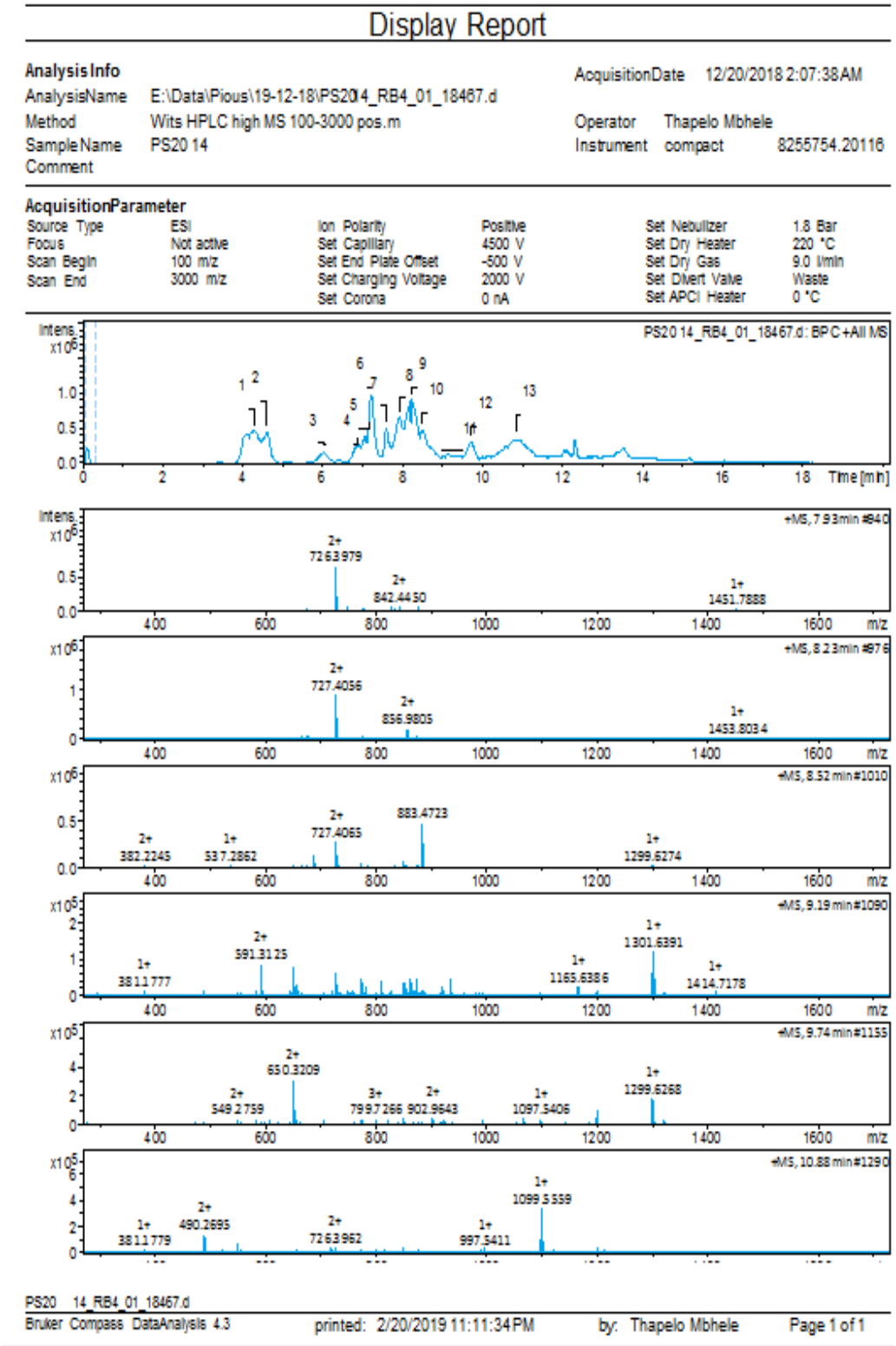


Figure 79: PS20- LCMS PS20-14 amino acid sequence results 2.

Display Report

Analysis Info

Analysis Name	E:\Data\Pious\12-09-2018\PS21 13nfm_GC6_01_13749.d	Acquisition Date	9/12/2018 5:50:47 PM
Method	Loop Mid 100-3000.m	Operator	Thapelo Mbhele
Sample Name	PS21 13nfm	Instrument	compact 8255754.20116
Comment			

Acquisition Parameter

Source Type	ESI	Ion Polarity	Positive	Set Nebulizer	1.8 Bar
Focus	Not active	Set Capillary	4500 V	Set Dry Heater	220 °C
Scan Begin	100 m/z	Set End Plate Offset	-500 V	Set Dry Gas	9.0 l/min
Scan End	3000 m/z	Set Charging Voltage	2000 V	Set Divert Valve	Waste
		Set Corona	0 nA	Set APCI Heater	0 °C

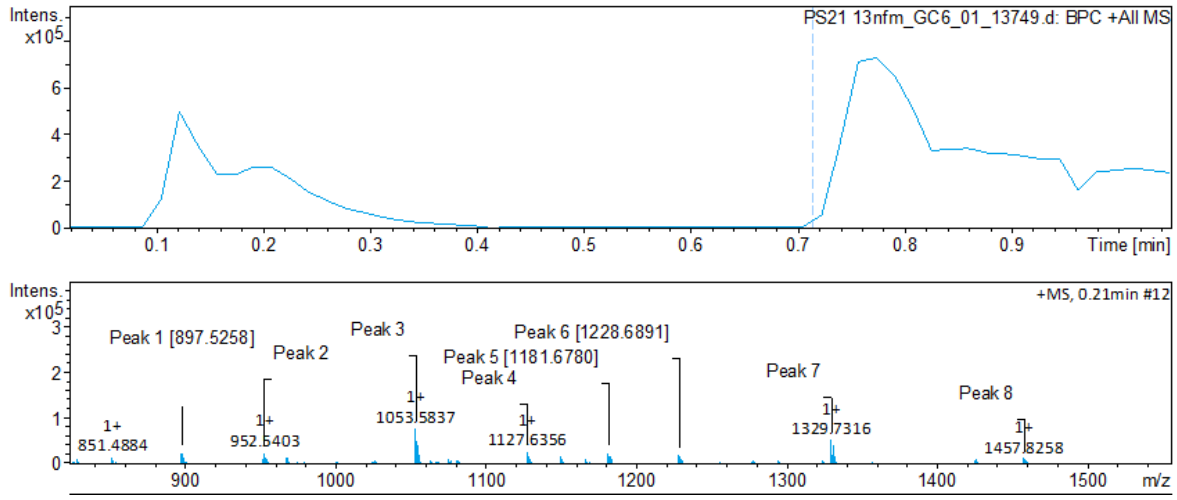


Figure 80: MS results for PS21-13 amino acid sequence.

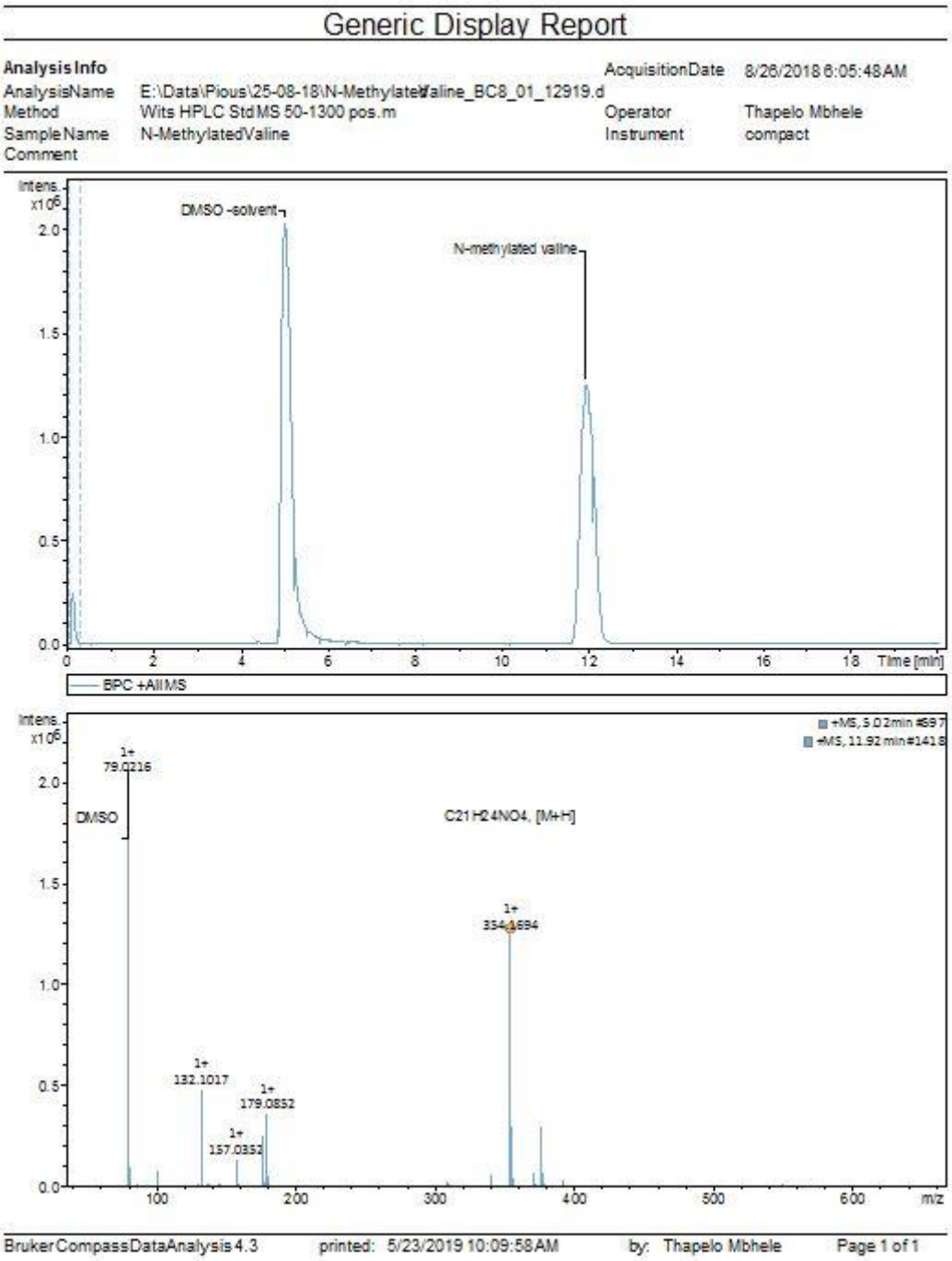


Figure 81: *N*-methylated valine LC-MS results.

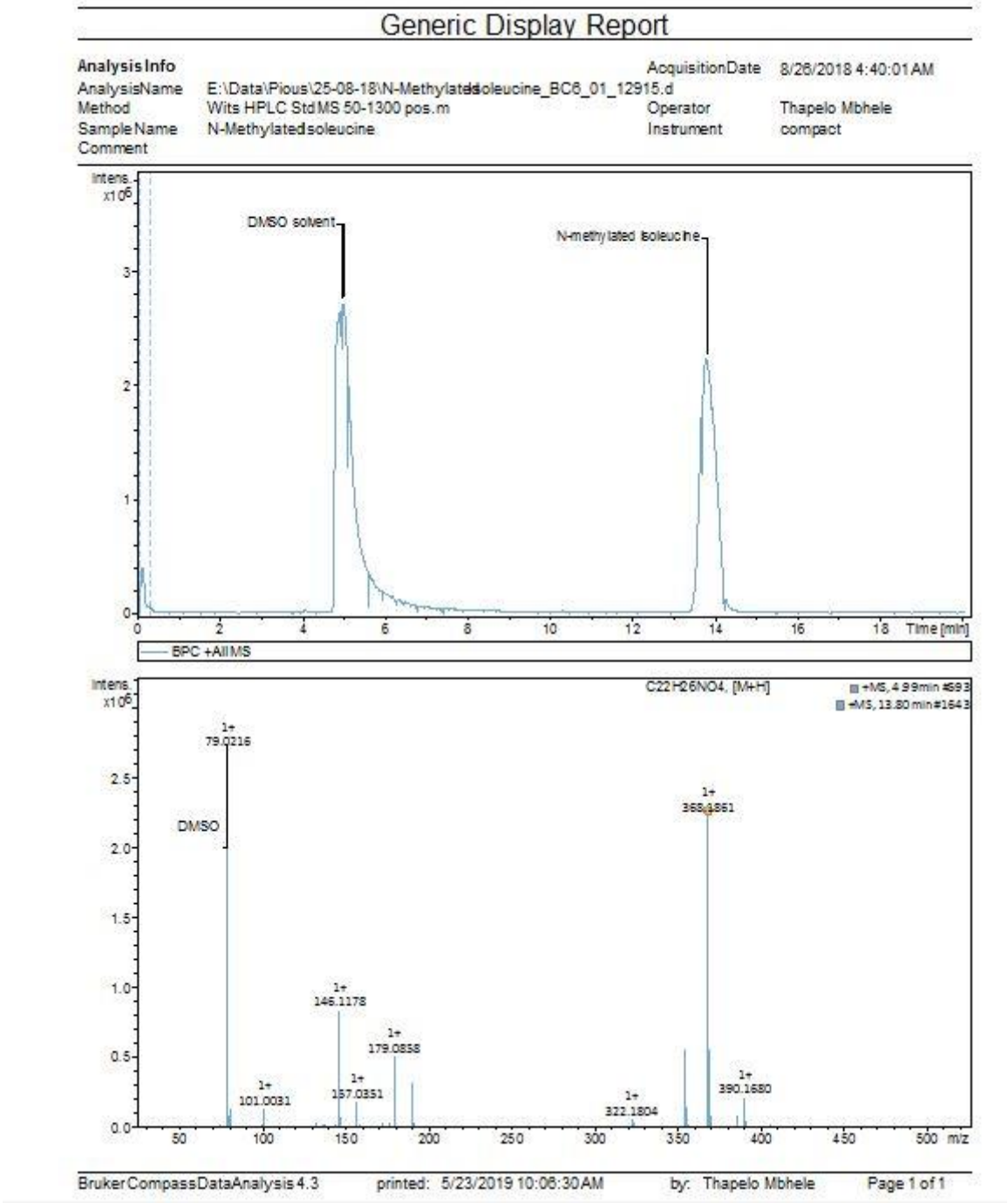


Figure 82: *N*-methylated isoleucine LC-MS results.

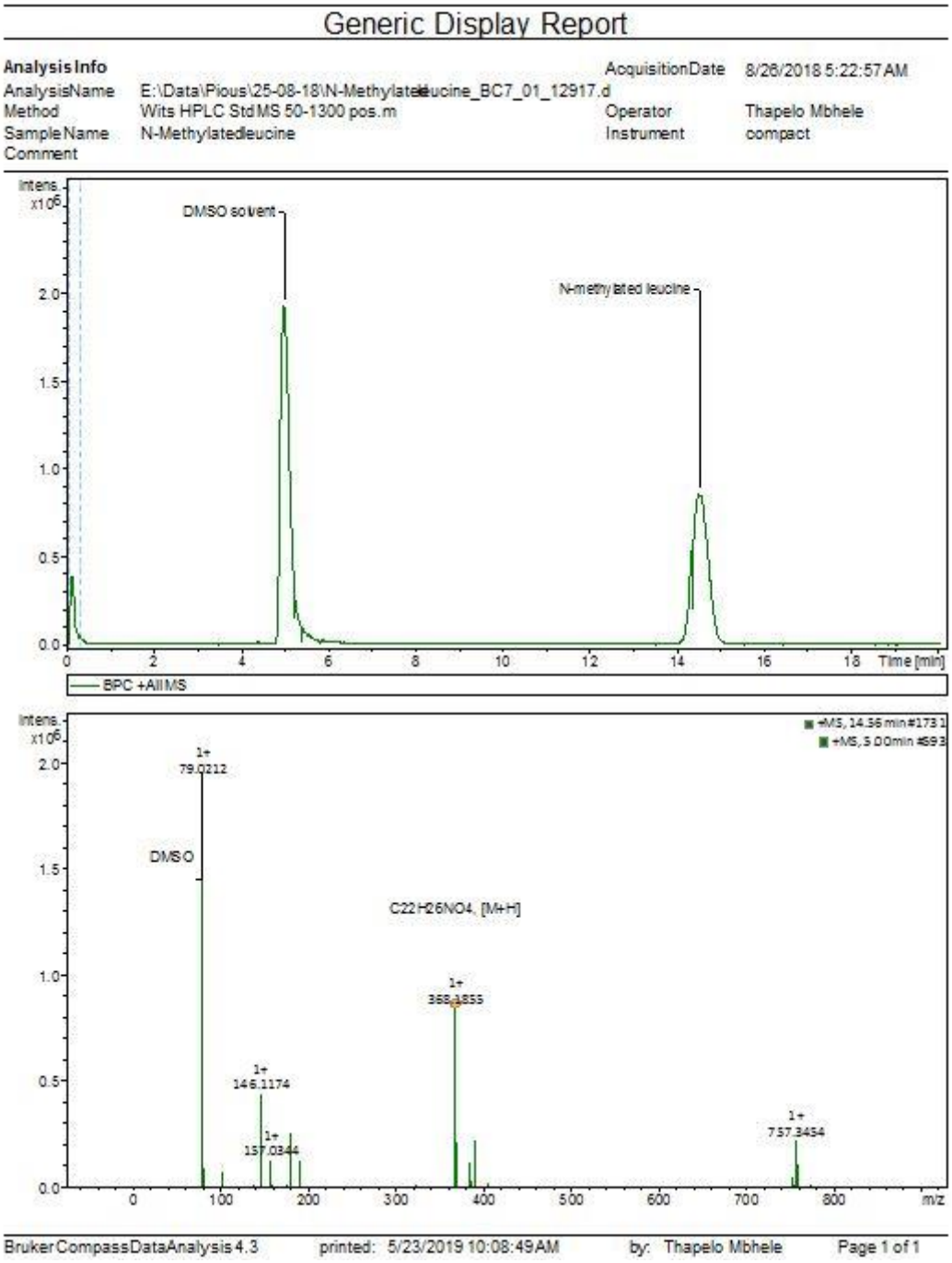


Figure 83: *N*-methylated leucine LC-MS results.

Display Report

Analysis Info

Analysis Name	E:\Data\Pious\16-07-18\frmoc-valine peptoid_GD1_01_10500.d	Acquisition Date	7/16/2018 4:32:32 PM
Method	Wits HPLC Mid MS 100-3000 pos.m	Operator	Thapelo Mbhele
Sample Name	frmoc-valine peptoid	Instrument	compact 8255754.20116
Comment			

Acquisition Parameter

Source Type	ESI	Ion Polarity	Positive	Set Nebulizer	1.8 Bar
Focus	Not active	Set Capillary	4500 V	Set Dry Heater	220 °C
Scan Begin	100 m/z	Set End Plate Offset	-500 V	Set Dry Gas	9.0 l/min
Scan End	3000 m/z	Set Charging Voltage	2000 V	Set Divert Valve	Waste
		Set Corona	0 nA	Set APCI Heater	0 °C

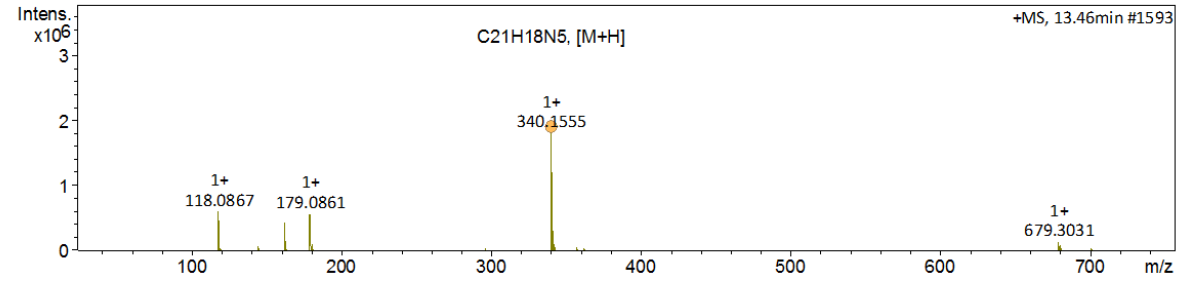


Figure 84: MS results of Fmoc valine peptoid.

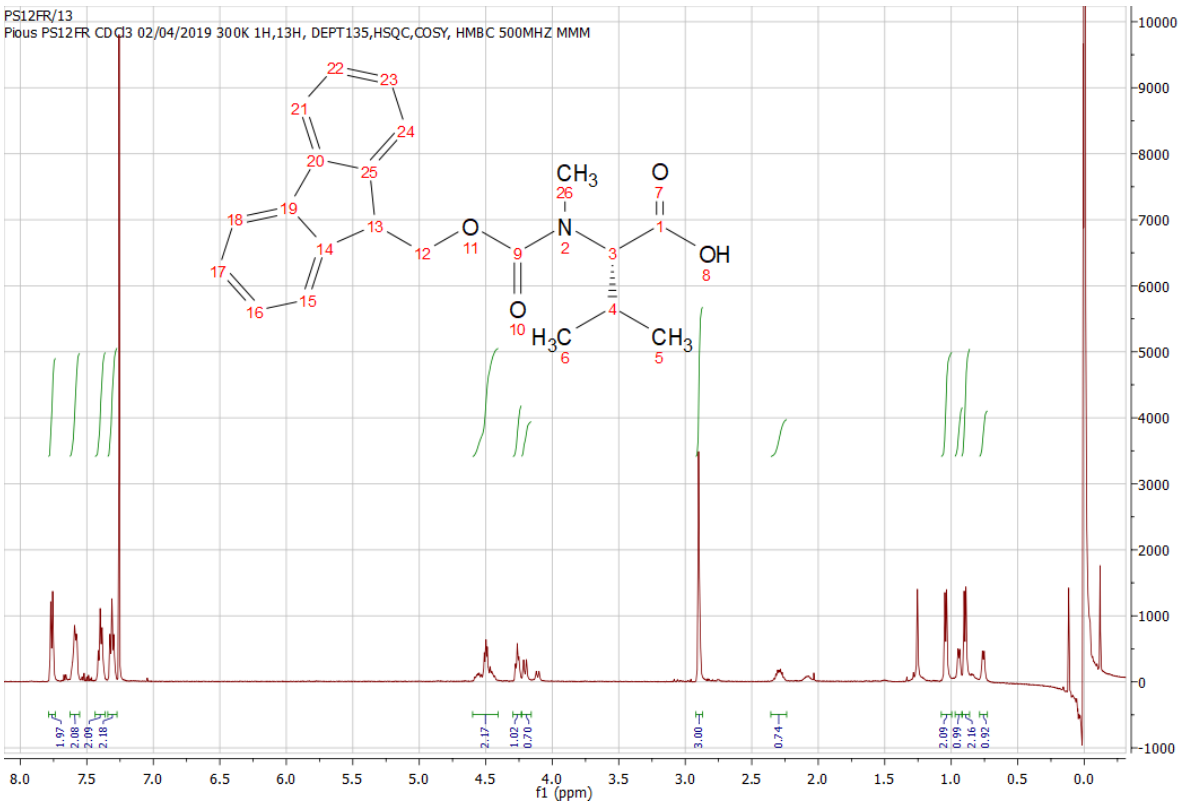


Figure 85: PS12 [1] H NMR Spectrum.

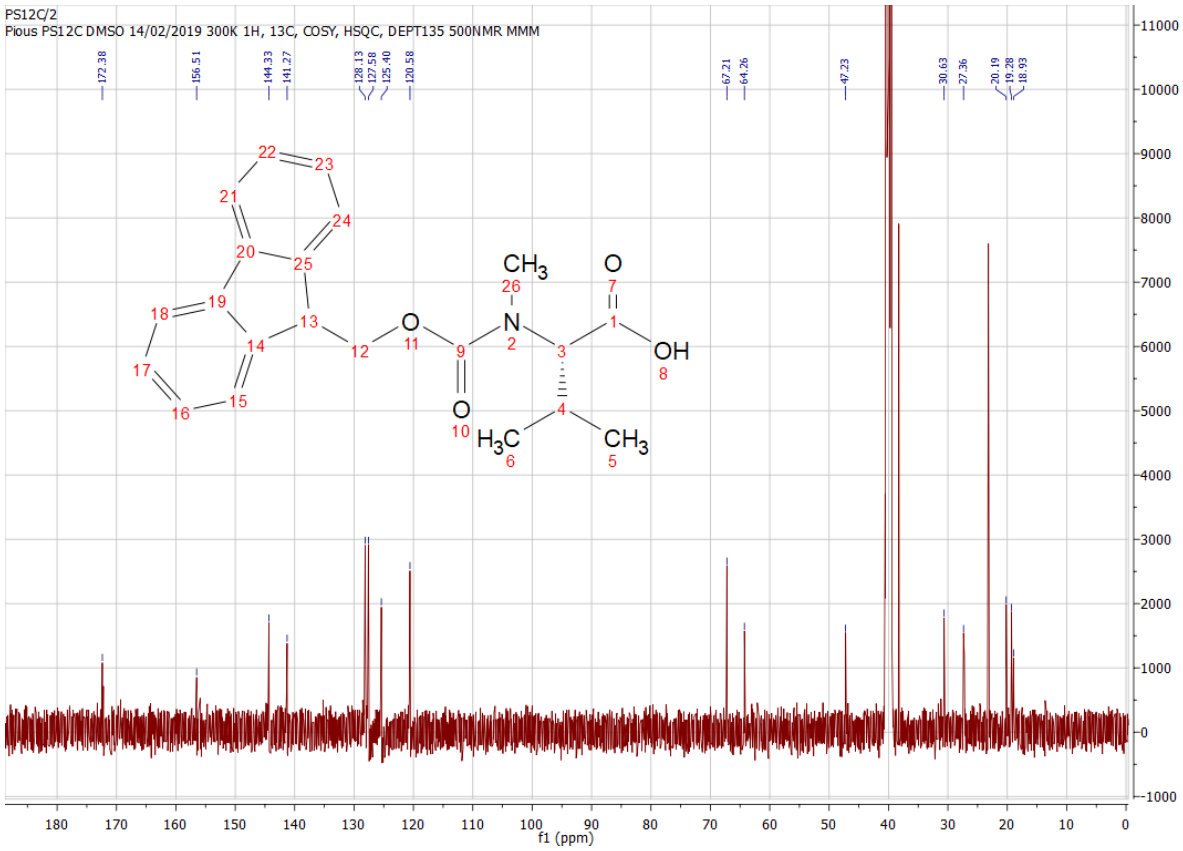


Figure 86: PS12 ^{13}C NMR Spectrum.

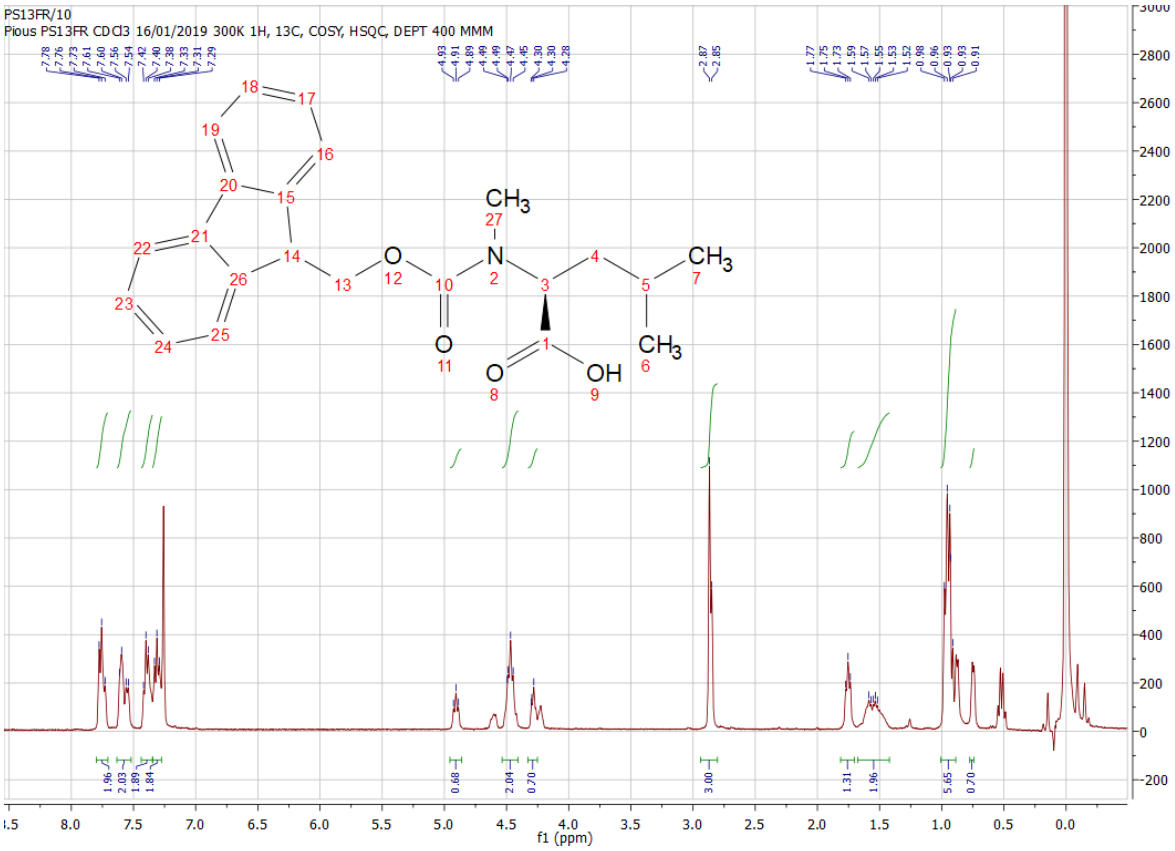


Figure 87: PS13 ^{1}H NMR Spectrum.

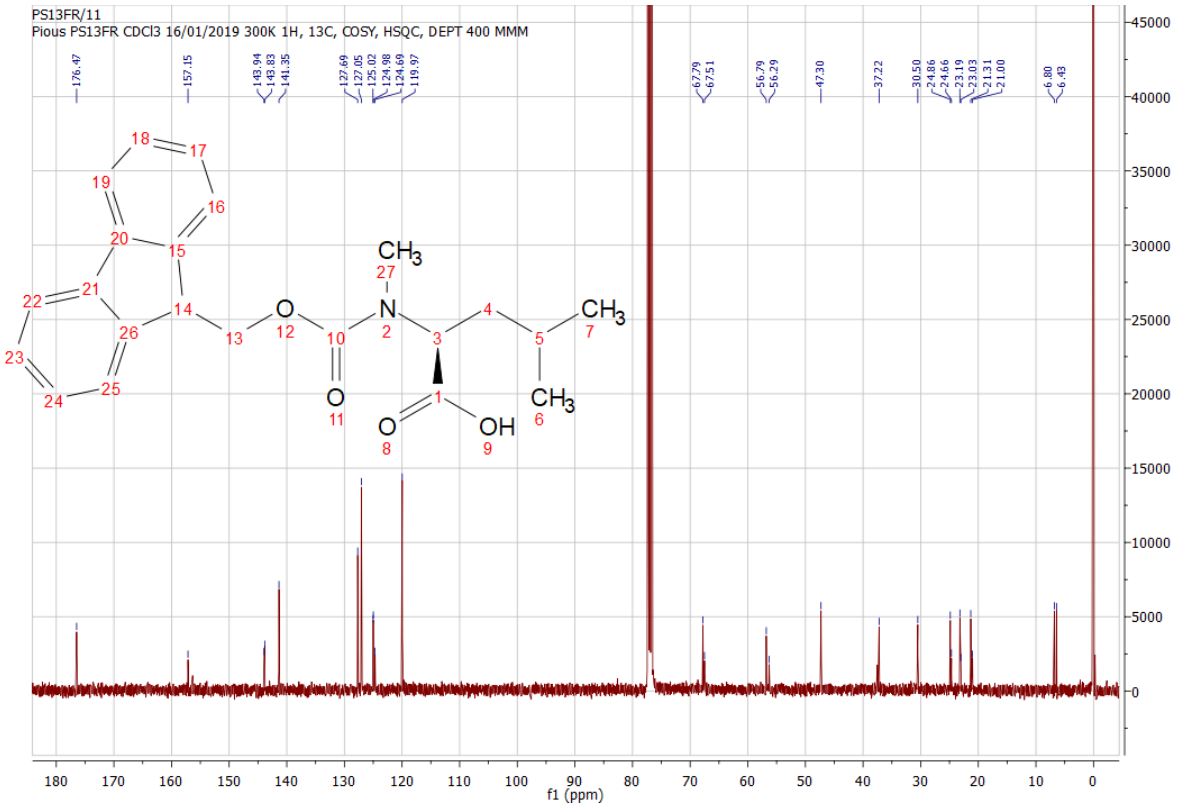


Figure 88: PS13 ^{13}C NMR Spectrum.

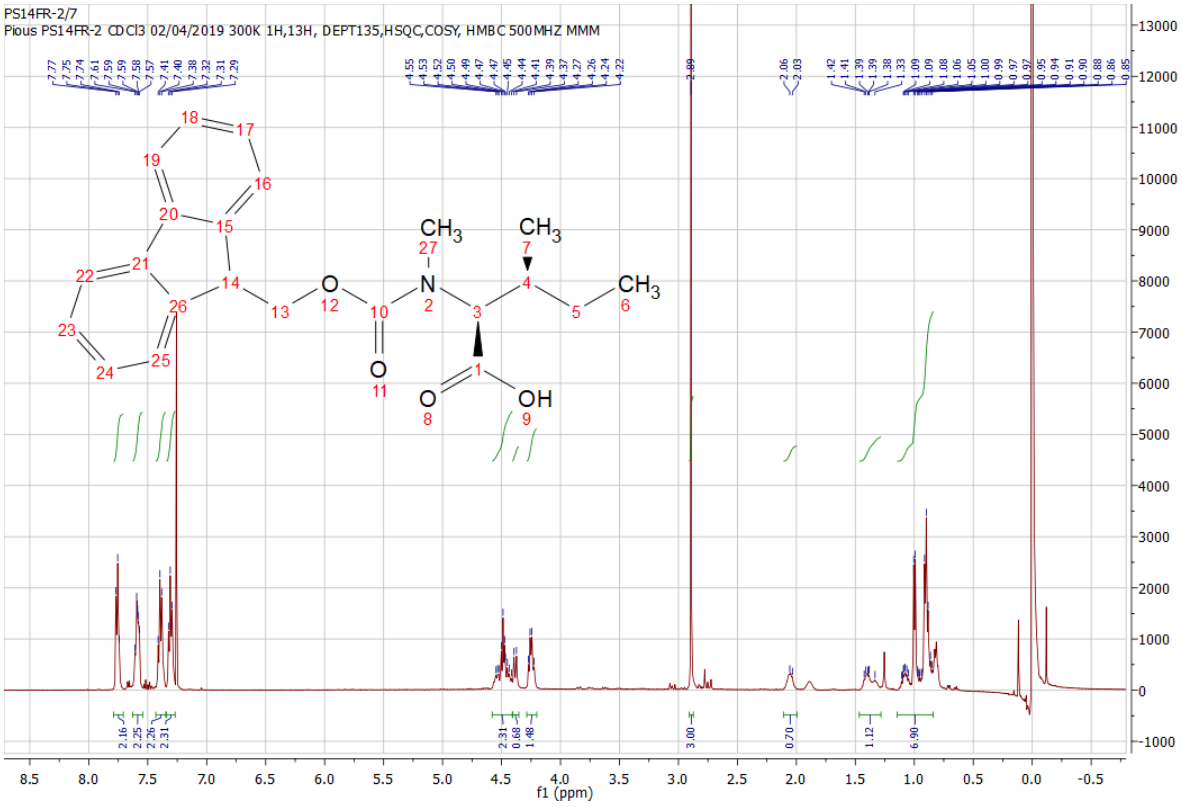


Figure 89: PS 14 ^{1}H NMR Spectrum.

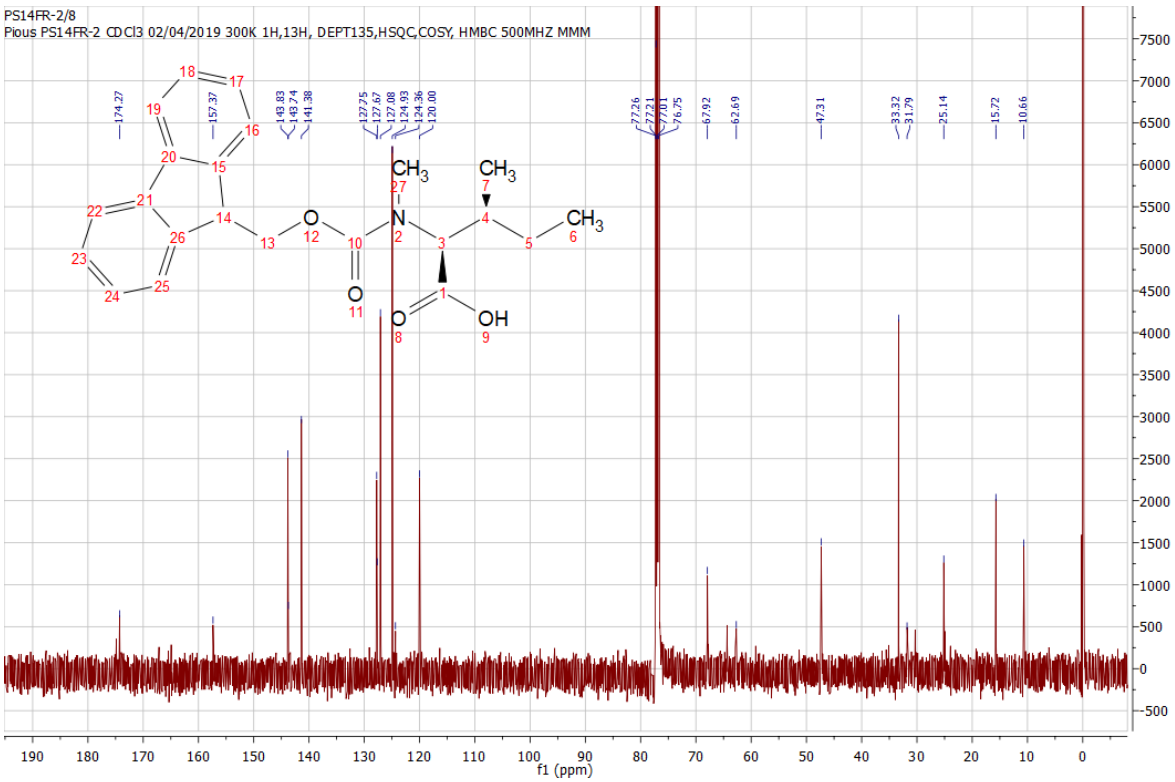


Figure 90: PS14 ^{13}C NMR Spectrum.

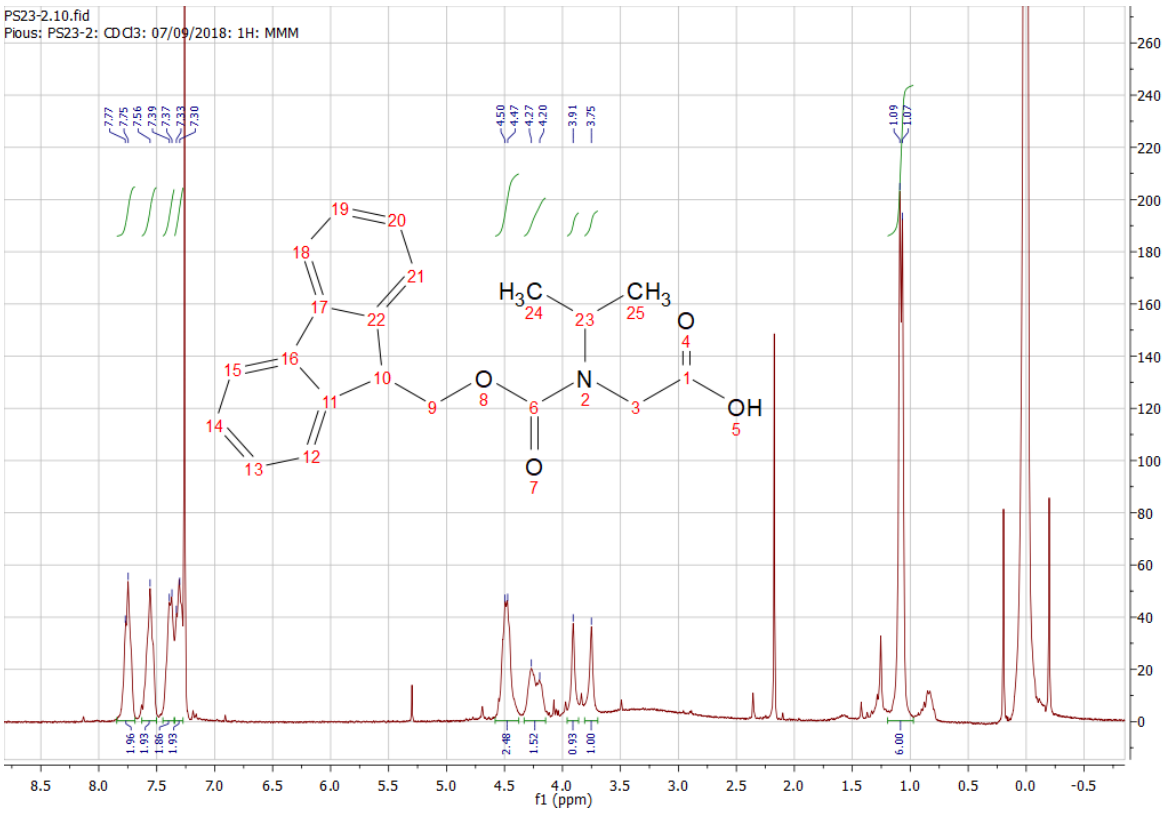


Figure 91: PS22 ^{1}H NMR Spectrum.